The switching of chemical properties by photo-stimulation

A Doctoral Thesis
by
Takashi Matsuhira

Submitted to
The Graduate School of Science
Osaka University

May, 2008

Contents

Acknowledgement

This work has been performed under the direction of Professor Norikazu Ueyama, Professor Hitoshi Yamamoto, and Professor Akira Harada at the Department of Macromolecular Science, Graduate School of Science, Osaka University. The author is greatly indebted to Professor Hitoshi Yamamoto for his continuous guidance, helpful suggestions, and fruitful discussions. The author also wishes to express his sincere gratitude to Assistant Professore Taka-aki Okamura for his numerous helpful suggestions. Acknowledgements are also made to Assistant Professor Akira Onoda for his helpful suggestions in the experiments.

The author wishes to thank Sumio Kaizaki, for the measurement of UV-vis spectrum at low temperature. The author would like to express great gratitude to Mr. Seiji Adachi for the measurement of solution NMR spectra. The author wishes to thank Mr. Tetsuo Yamamoto for the X-ray measurement. The author also wishes to thank Mr. Mitsuo Ohama for the measurement of IR spectra. The author shows gratitude to Ms. Kazuyo Hayashi and Ms Tomomi Hirai for Elemental analysis. The author thanks Mr. Hiroshi Adachi for the measurement of mass spectra. The author thanks Mr. Kazuki Tsuchihashi for the synthesis and measurement of the *ortho*-coumaric acid derivatives.

The author thanks greatly all the members of Ueyama laboratory for their heartfelt friendship and helpful discussions.

The author expresses his special thanks for the 21st Centry Center of Excellence (21COE) program “Creation of Integrated EcoChemistry of Osaka University”, and for the Global Education and Research Center for Bio-Environmental Chemistry (GCOE) program of Osaka University.

Finally, the author thanks his parents, Toshimasa and Youko, for their incessant encouragement.

May, 2008

Takashi Matsuhira

Chapter 1

General Introduction

Hydrogen bond plays an important role in expressing the function of protein like native enzymes. It is thought that reactivity regulation is affected by the switching of hydrogen bond network around the active site.[1-4] There are many enzymes, which have hydrogen bond acceptors in reaction center as the side chain of aspartic acid, serine, and cystein. For example, aspartic protease has an aspartic acid in the reaction center, and hydroxylate generated by the carboxylate catalyze the hydroxylation of the amide conjugation of peptide. Pepsin is one of the most famous enzymes of this family. The X-ray crystallography of pepsin shows that there are NH···O and OH···O hydrogen bonds around the reaction center Asp 31, from proximate Gly 33 and Ser 34 (Figure 1).[5-10] These hydrogen bonds around the active site are interrupted to activate enzyme when substance was approached. And the switching of hydrogen bonds triggered by approximation of substance is thought to control the electron density of carboxylate oxygen and constructs the enzymatic reaction cycle of resting and activated state. The same trend are found in cystein protease and in serine protease, whose hydrogen bond toward sulfur atom and that toward oxygen atom.[11-20] There are some examples of switching such a hydrogen bond network with the light stimulus. That is rhodopsin

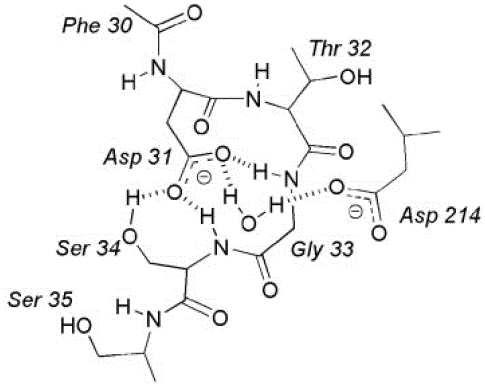

Figure 1. The structure of pepsin around the active site, obtained from X-ray crystallography.

family, photoreceptor of optical sensation, and photoactive yellow protein (PYP), one of the photo-acceptable proteins.[1, 2, 22-39] For example, around the chromophore of PYP, hydrogen bond toward phenolate from Glu 46 and Tyr 42 formed in ground state was interrupted by *trans*/*cis* (*E*/*Z*) photoisomerization of C=C double bond (Scheme 1). The switching of hydrogen bond network toward phenolate oxygen is thought to control the protonation and deprotonation process and to play an important role to express the function of PYP.

The character of hydrogen bond has been investigated for one century. There are many events dominated by hydrogen bond, such as secondary structure formation, reactivity control, and expressing the function of native enzyme. The discipline, which contains hydrogen bond, was versatile, not only biological chemistry, but also materials, inorganic, organic, supramolecular, and biomedicinal chemistry. Hydrogen bond is a weak interaction comparing with covalent bond, but its strength is flexible from 0.2 to 40 kcal mol^{-1}.[40-47] This fact indicates that hydrogen bond regulates the strength depending on the environment, and hydrogen bond is useful for the switching the reaction activity. In a previous study, we investigated the effect of the intramolecular NH···O hydrogen bond toward the oxy anion, such as carboxylate and phenolate.[48-64] We have proposed that the proximity of the amide NH group and the carboxylic oxygen atoms lowers the pK_a value of the corresponding acid by stabilizing the carboxylate with forming the intramolecular NH···O hydrogen bond (Figure 2). This effect was also found in phenol and thiol compounds. Therefore, the switching of the intramolecular NH···O hydrogen bond by external stimulation is expected to realize the control of the pK_a value.

In this thesis, the author designed the novel carboxylic acid or phenol derivatives, which allow the switching of an intramolecular NH···O distance stimulated by light irradiation (Figure 3). According to this strategy, photoirradiation stimulates the proximity of the amide NH and carboxyl oxygen according to *E*/*Z* photoisomerization of photoinduced framework, which allowed forming intramolecular NH···O hydrogen bond in carboxylate, and lowers the pK_a value of carboxylic acid. The author detected the intramolecular NH···O hydrogen bond by using various spectroscopic analyses such as ^{1}H NMR spectroscopy, FT-IR spectroscopy, and X-ray crystallography.

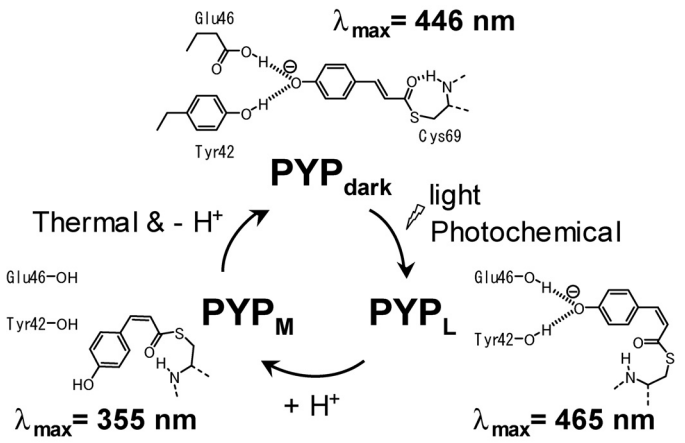

Scheme 1. Photocycle of Photoactive Yellow Protein (PYP), around the chromophore

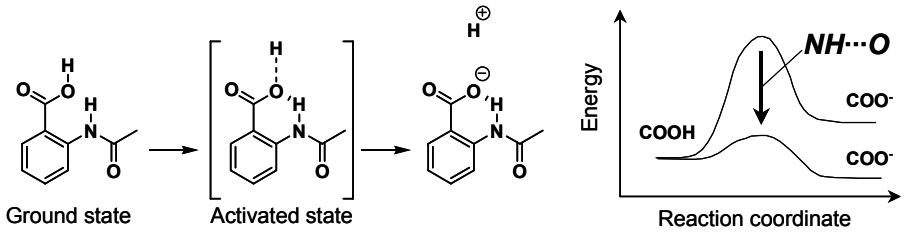

Figure 2. Deprotonation process of carboxylic acid derivative, whose carboxylate and transition state is stabilized by intramolecular NH···O hydrogen bond toward carboxylic oxygen from proximate amide NH.

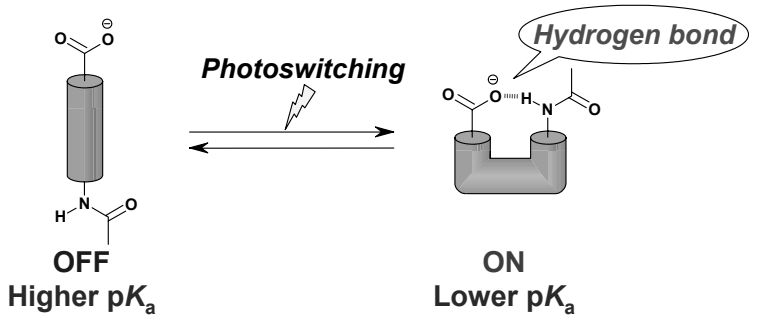

Figure 3. Schematic illustration of the photoswitching of intramolecular NH···O hydrogen bond toward carboxylic oxygen.

Photoswitching devices

Photoisomerization is considered to be one of the most promising strategies for stimulating the switching devices, which effectively facilitates the control of molecular structures. There are many investigations about photoisomerization.[65-87, 93, 94] For example, as shown in Figure 4, they uses these photochromic compounds as a functional photoswitching devices to change their characters such as colors, a)dendrimer structure[67-69], b)chirality[94], c)trapping efficiency of metal ion[93], macrosize crystal shape[74], and so on. Effects of intramolecular OH···O, NH···N, or NH···O hydrogen bonds on the photo reactivity (4d, 4e),[66, 75-79] as well as the pK_a change of phenol or carboxylic acid derivatives by switching the conjugation through photoisomerization (4f),[80-84] have also been investigated. However, to the best of our knowledge, no previous studies have attempted to control the character of carboxylates, such as pK_a values, by switching an intramolecular hydrogen bond. The author approached the photoswitching of NH···O hydrogen bond toward carboxylate or phenolate. To design the photoswitching of intramolecular NH···O hydrogen bond, the author introduced the photoisomerization of π-conjugated C=C or C=N double bond to carboxylic acid and phenol derivatives. There are many compounds known to take *E*/*Z* photoisomerization. The author chose the benzylideneaniline, cinnamic acid, and coumaric acid framework to switch the intramolecular NH···O hydrogen bond (Figure 5). Benzylideneaniline framework has a very similar structure to azobenzene or stilbene, which are very famous photodevices (Figure 5a). Benzylideneaniline derivative photoisomerizes from *E* to *Z* conformation by UV light irradiation, and thermally isomerizes from *Z* to *E* conformation up to *ca.* 203 K. [85-87] Cinnamic acid framework is rather small comparing with benzylideneaniline derivative, and progresses one-way photoisomerization from *E* to *Z* conformation by UV-light irradiation (Figure 5b).[84] Coumaric acid framework has a characteristic nature, that absorption maximum of phenolate derivative was red-shifted because of their extended π-conjugation (Figure 5c).[3, 31-39] That means the phenolate could be isomerized by longer wavelength light irradiation.

The author used these photoinduced frameworks to switch an intramolecular NH···O hydrogen bond. The benzylideneaniline derivative is expected to progress a reversible switching of intramolecular NH···O hydrogen bond by *E*/*Z* photoisomrization and *Z*/*E* thermal isomerization (Figure 5d). The cinnamic acid derivatives are expected to progress the OFF→ON switching and ON→OFF switching of intramolecular NH···O hydrogen bond respectively, according to the one-way photoisomerization of cinnamate

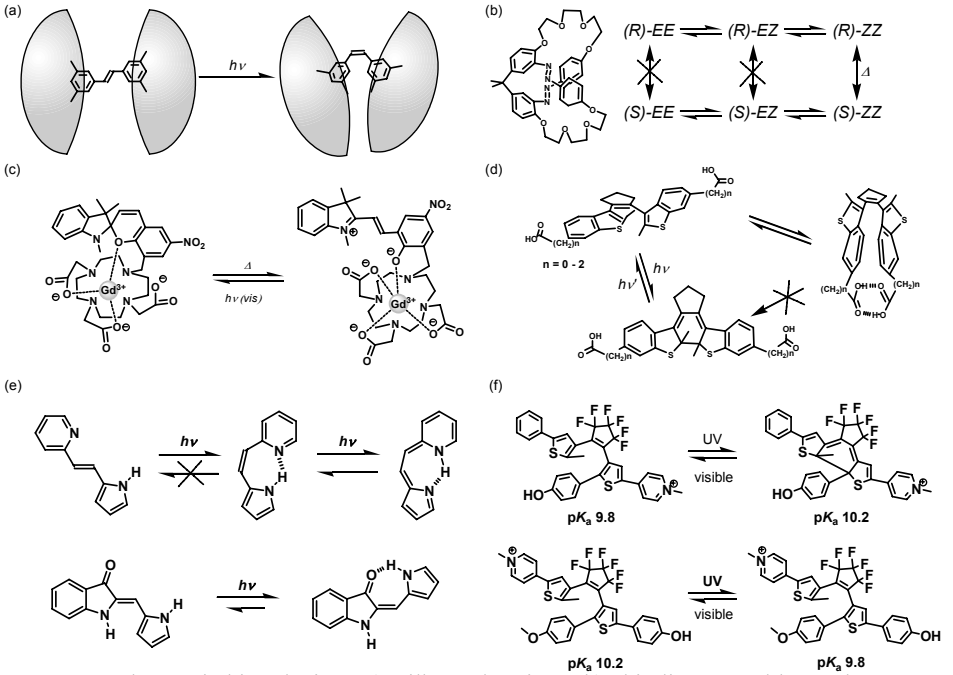

Figure 4. Photoswitching devices. a) stilbene dentrimer, b) chirality control by azobenzene, c) chapturing Gd ion by spiropyran, d) photoreactivity control by OH···O hydrogen bond, e) photoreaction control by NH···O and NH···O hydrogen bond, f) acidity control by diarylethene.

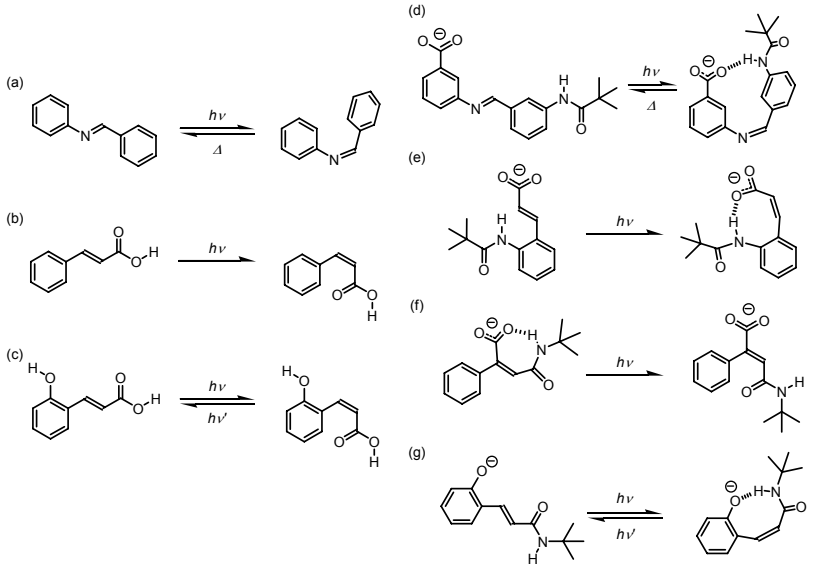

Figure 5. Photoswitching frameworks a) benzylideneaniline, b) cinnamic acid, c) *ortho*-coumaric acid, and molecular design of the switching of intramolecular NH···O hydrogen bond d) benzylideneaniline derivative, e) OFF→ON type cinnamic acid derivative, f) ON→OFF type cinnamic acid derivative, and g) *ortho*-coumaric acid derivative.

frame (Figure 5e, 5f). The former forms an intramolecular NH···O hydrogen bond according to photoisomerization, and conversely the latter interrupts the hydrogen bond. The coumaric acid derivative is expected to switch the intramolecular NH···O hydrogen bond toward phenolate oxygen, and control the *E*/*Z* ratio by deprotonation of phenol moiety using different wavelength light irradiation (5g).

pK_a control by switching of intramolecular NH···O hydrogen bond

In our laboratory, pK_a values of various thiol[88], phenol[89], and carboxylic acid[48] derivatives with amide groups at *ortho*-positions have been estimated. As shown in our results, the prelocated amide groups nearby the deprotonating group (mercapt, hydroxyl, or carboxyl groups) lower the pK_a values of these groups (Figure 6). The hydrogen bonds promote deprotonation process by stabilizing the transition state in this reaction. In this thesis, the author designed to switch the intramolecular distance between deprotonating group and amide group by using photoisomerization. When the amide group exists near a hydroxyl group, the pK_a value is expected to be lowered. There are investigations which photocontrol the acidity by switching the conjugations accompanying with photoisomerization,[80-81] however, there is no investigation having the concept to control pK_a value by photoswitching of hydrogen bonding.

Figure 7 shows the pK_a values of OFF→ON type photoisomers in aqueous micellar solution. Their amide group proximate the carboxylic acid or phenol in *Z* compound, and the formation of the intramolecular NH···O hydrogen bond from the neighboring amide NH toward carboxylate or phenolate oxygen lowers the pK_a value of corresponding acid, respectively. According to the decrease of pK_a value, pH value was also decreased by photoisomerization in OFF→ON type cinnamic acid derivative. The pK_a value of ON→OFF type compound was compaired with OFF→ON type compound in organic solvent (dimethylsulfoxide; DMSO) by tracing the deprotonation ratio obtained from ^{1}H NMR spectrum in ion exchange reaction (Figure 8). According to the photoisomerization, pK_a value of ON→OFF type compound was increased whereas that of OFF→ON type was decreased. It is thought that the interruption of intramolecular NH···O hydrogen bond after photoisomerization in ON→OFF type compound destabilizes the carboxylate and increases the pK_a value of the corresponding acid. The pK_a value of OFF→ON and ON→OFF type compound in DMSO solution was reversed after photoisomerization.

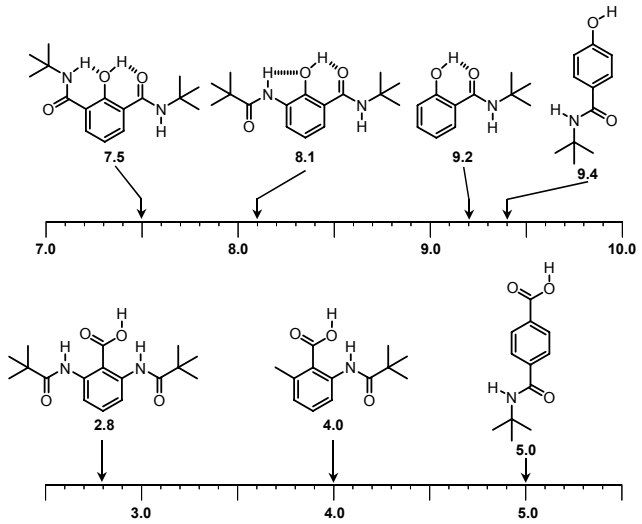

Figure 6. pK_a values of phenol (upside) and carboxylic acid (downside) derivatives; the effect of proximity of amide groups. The pK_a values were obtained by potentiometric titration in 10% aqueous micellar solution of Triton® X-100.

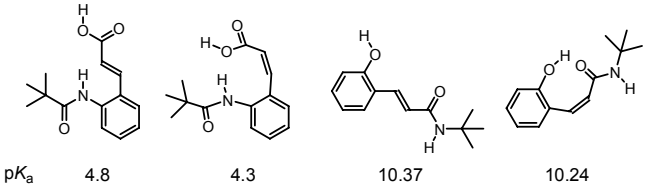

Figure 7. pK_a values of carboxylic acid and phenol derivatives. The pK_a value of carboxylic acid was obtained by potentiometric titration 10 mM in 10% aqueous micellar solution of Triton® X-100 at 278 K, and that of phenol was obtained from UV titration 5 mM in 10% aqueous micellar solution of laurylether at 303 K.

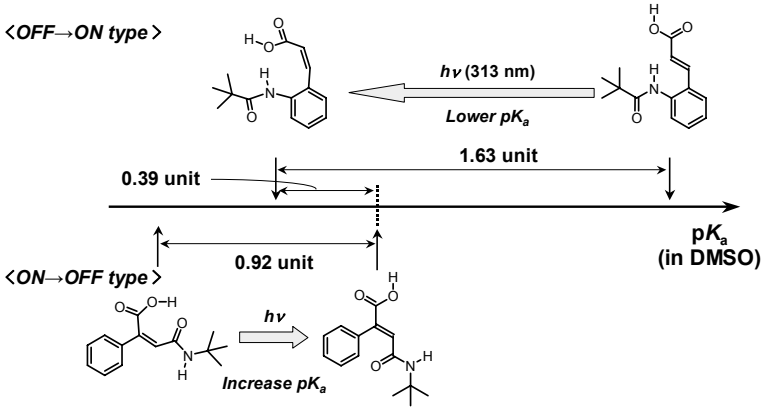

Figure 8. pK_a differences of OFF→ON and ON→OFF type carboxylic acids in DMSO solution obtained from ^{1}H NMR analysis of ion exchange reaction.

Artificial photocycle of phenol and phenolate, derived by the switching of an intramolecular NH···O hydrogen bond

Photoactive Yellow Protein (PYP) is one of the photo-acceptable proteins that switches the intramolecular hydrogen bond network around the phenolate oxygen of the *para*-coumaric acid chromophore.[1-4] The photocycle of PYP indicate that hydrogen bond between phenolate oxygen and hydroxyl moiety of Glu 46 or Tyr 42 formed in ground state were interrupted by *E*/*Z* photoisomerization of coumaric acid framework, accompanying with the protonation and deprotonation process of phenol moiety (Scheme 1).[31-39] The author designed an artificial photocycle of small molecule, which models the PYP photocycle (Figure 9). In this photocycle, *E* phenol derivative photoisomerizes toward *Z* phenol by UV-light irradiation. Then, deprotonation process progressed because of the decrease of pK_a value in *Z* phenol. *Z* phenolate takes photoisomerization toward *E* isomer by the same UV-light irradiation, and *E* phenolate turns back to the initial state by protonation process.

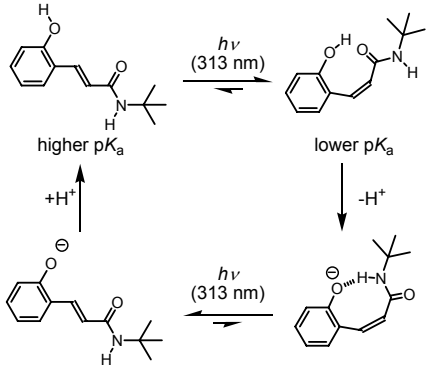

Figure 9. Artificial photocycle of *ortho*-coumaric acid derivative, which involves protonation and deprotonation process derived by pK_a change owing to photoswitching of an intramolecular NH···O hydrogen bond.

Intramolecular hydrogen bond switching of oligopeptide

The switching of intramolecular hydrogen bond network in peptides or native proteins plays an important role to construct their characteristic second dimension structure such as α-helix, β-strand, and β-turn. *Onoda et al.* investigated the conformation change of the tripeptide (Asp-Val-Gly), which have similar residues around the active site of pepsin (Figure 10).[90, 91] According to the deprotonation of aspartic acid, the conformation of peptide changes the conformation from linear structure toward turn structure with forming multiple NH···O hydrogen bonds between amide NH of peptide and carboxylic oxygen. The conformation change by intramolecular NH···O hydrogen bond switching was also investigated in artificial compound. The conformation of cyclohexyl skeleton was transformed from chair structure to boat structure, by forming two strong intramolecular NH···O hydrogen bond accompanying with the deprotonation of Kemp's acid (Figure 10).[92]

The author introduced the photoswitchable cinnamic acid framework toward the C-terminal of oligopeptide (Figure 11). The structure in solution was obtained from ^{1}H NMR spectrum. The designed compounds are expected to switch the conformation of peptide not only deprotonation but also photoisomerization process. All the amide NH of the *E* and *Z* carboxylic acid was free from intramolecular hydrogen bond. According to the deprotonation, *E* carboxylate forms an intramolecular NH···O hydrogen bond between Leu-NH and carboxylic oxygen. And the hydrogen bond network was switched by photoisomerization, the *Z* carboxylate forms three intramolecular NH···O hydrogen bond from Leu-NH, Ala-NH, and aryl-NH.

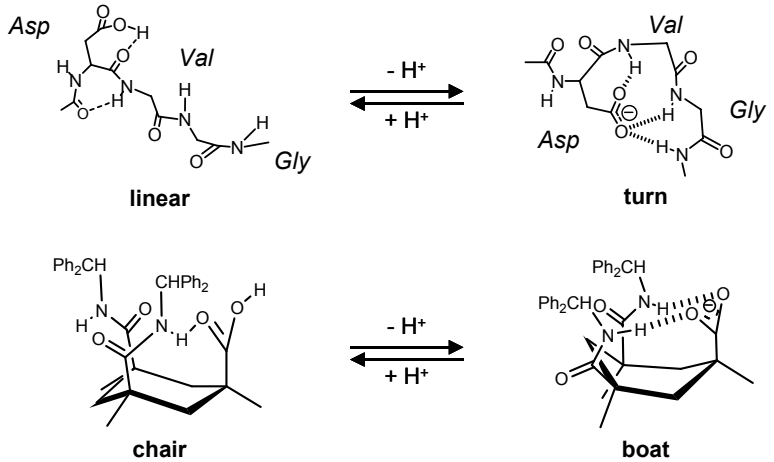

Figure 10. Conformation changes of tripeptide (upside) and cyclohexane skeleton (downside) accompanying with the deprotonation and protonation process of carboxylic acids.

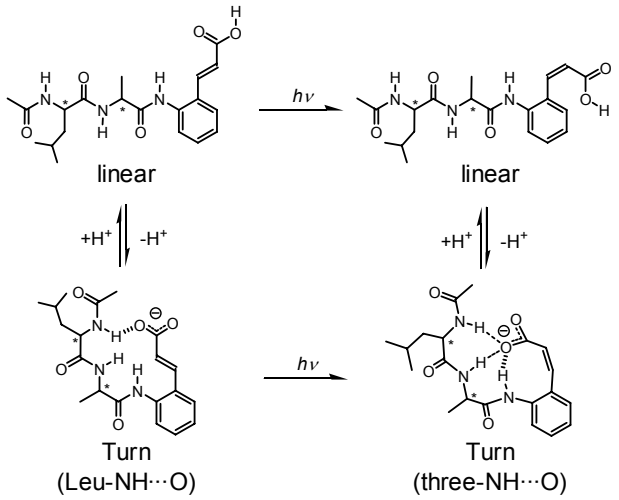

Figure 11. Expected conformation changes and photoswitching of intramolecular NH···O hydrogen bond network of Ac-Leu-Ala-NH-C_6H_4-CH=CH-COOH.

Outline of this thesis

Chapter 2

In this chapter, carboxylic acid and carboxylate, which both have an amide group linked to an azomethine moiety that switches the intramolecular NH···O hydrogen bond through photoirradiation, were synthesized and characterized. *E* carboxylate compound was determined to form intermolecular, rather than intramolecular, NH···O hydrogen bonds in solid state and in the THF solution. Using UV light irradiation, the generation of a *Z* isomer was observed by UV–visible and ^{1}H NMR spectra. The temperature coefficient for the chemical shift of amide NH signals and *Z* to *E* thermal reversion rates of their compounds show that the intramolecular NH···O hydrogen bond of *Z* carboxylate is stronger than that of *Z* carboxylic acid. The reversible switching of an intramolecular NH···O hydrogen bond toward the carboxylate group was achieved by *E*

to *Z* photoisomerization and by *Z* to *E* thermal isomerization of the azomethine double bond.

Chapter 3

OFF→ON one-way photoswitching of the intramolecular NH···O hydrogen bond by using *E* to *Z* photoisomerization of cinnamate framework was achieved. The author synthesize the carboxylic acid and carboxylate derivatives, which have a photoinduced cinnamate frame so as to switch the intramolecular distance between amide NH and carboxylic oxygen atoms by using phohtoisomerization. According to the 313 nm UV light irradiation, *E* to *Z* photoisomerization was progressed. Since *Z* cinnamate compound is thermally stable, *Z* compounds are isolated from the mixture of photoisomers. *Z* carboxylate forms an intramolecular NH···O hydrogen bond both in DMSO-d_6 solution and in solid state. The pK_a value of *Z* carboxylic acid was lower than that of *E* compound, not only in an aqueous micellar solution but also in DMSO solution. The author propose that the intramolecular NH···O hydrogen bond formed in *Z* carboxylate encourages the deprotonation process and lowers the pK_a value of the corresponding carboxylic acid. The pH value was also decreased by photoisomerization accompaning with the decrease of pK_a value.

Chapter 4

As well as chapter 3, ON→OFF one-way photoswitching of the intramolecular NH···O hydrogen bond by using *E* to *Z* photoisomerization of cinnamate framework was achieved. According to the photoisomerization by 313 nm UV light irradiation, the distance between amide NH and carboxylic oxygen was disgregated. And an intramolecular NH···O hydrogen bond formed in *E* carboxylate was interrupted in *Z* compound in DMSO-d_6 solution. The pK_a value of *Z* carboxylic acid was increased in *E* compound in DMSO solution. And the author found that the pK_a value of ON→OFF and OFF→ON type compound was reversed after photoisomerization in DMSO solution.

Chapter 5

An intramolecular NH···O hydrogen bond between the amide NH and phenolate oxygen was switched by photoisomerization of *ortho*-coumaric acid framework. *Ortho*-coumaric acid moiety has an extended π-conjugation in phenolate, thus the red shift of the absorption maximum was observed. Because of the difference of the absorption wavelength, phenol and phenolate have different *E*/*Z* ratio whereas same

wavelength light irradiation. 313 nm UV light irradiation preferentially generates *Z* form in phenol and generates *E* form in phenolate. The pK_a value of the phenol compound was lowered in *Z* compound by stabilizing the *Z* phenolate with formation of an intramolecular NH···O hydrogen bond. The change of *E*/*Z* ratio in phenol and phenolate, and the decrease of pK_a value in *Z* phenol compound, indicate that the artificial photocycle was constructed like PYP photocycle containing protonation and deprotonation process.

Chapter 6

Multiple hydrogen bonds between the amide NH of oligopeptide and carboxylate oxygen were photoswitched by *E*/*Z* photoisomerization of cinnamate framework. The author introduced the *ortho*-amino cinnamic acid framework toward the C-terminal of the monopeptide (Ac-Ala-) and dipeptide (Ac-Leu-Ala-). Monopeptide derivative (Ac-Ala-NH-C_6H_4-CH=CH-COOH) forms one intramolecular NH···O hydrogen bond in *Z* carboxylate between aryl NH and carboxyl oxygen; the amide NH of Ala moiety was free from interaction. Dipeptide derivative (Ac-Leu-Ala-NH-C_6H_4-CH=CH-COOH) forms one intramolecular NH···O hydrogen bond in *E* carboxylate between Leu NH and carboxyl oxygen, and forms three intramolecular NH···O hydrogen bonds in *Z* carboxylate. Elongation of peptide moiety may stabilize the *Z* carboxylate by forming multiple intramolecular NH···O hydrogen bonds.

References

[1] G. O. Borgstahl, D. R. Williams, E. D. Getzoff, *Biochemistry* **1995**, *34*, 6278-6287.

[2] A. Warshel, *Biochemistry* **1981**, *20*, 3167-3177.

[3] Y. Imamoto, M. Kataoka, F. Tokunaga, T. Asahi, H. Masuhara, *Biochemistry* **2001**, *40*, 6047-6052.

[4] Y. Imamoto, Y. Shirahige, F. Tokunaga, T. Kinoshita, K. Yoshihara, M. Kataoka, *Biochemistry* **2001**, *40*, 8997-9004.

[5] D. P. H. Cruikahank, K. W., and D. J. Tholen, *Nature*, **1985**, *315*, 122-124.

[6] M. C. Fujinaga, M. M., N. I. Tarosova, S. C. Morimann, and M. N. G. James, *Protein Science*, **1995**, 960-972.

[7] M. J. Millar, R. J. K. Mohano, J. Leis and A. Wlodawer, *Nature*, **1989**, *337*, 576-579.

[8] A. M. C. Silva, E. R., H. L. Cham, and J. W. Erickson, *J. Mol. Biol.*, **1996**, *255*, 324-346.

[9] K. B. Suguna, R. R., E. A. Padlan, E. Subramanian, S. Scheriff, G.. H. Cohen, D. R. Davis, *J. Mol. Biol.*, **1987**, *196*, 877-900.

[10] A. M. Wlodawer, M. Jaskolski, and B. K. Sathyanarayama, *Science*, **1989**, *245*, 616-621.

[11] B. V. A. Cheesman, and D. L. Rabenstein, *J. Am. Chem. Soc.*, **1988**, *110*, 6359-6364.

[12] Z. R. W. Gan, and W. W., *J. Biol. Chem.*, **1987**, *262*, 6704-6707.

[13] H. C. F. Hawkins, *Biochem. J.*, **1991**, 335-339.

[14] S. D. R. Katti, *Protein Sci.*, **1995**, *4*, 1998-2005.

[15] S. D. J. Lewis, F. A., and J. A. Shafer, *Biochemistry*, **1976**, *15*, 5009-5017.

[16] S. D. J. Lewis, F. A., and J. A. Shafer, *Biochemistry*, **1981**, *20*, 48-51.

[17] S. Z. P. J. Liu, W. W. Johnson, G. L. Gilliland, and R. N. Armstrong, *J. Biol. Chem.*, **1992**, *267*, 4296-4299.

[18] J. L. B. Martin, J. C. A., J. Kuriyan, *Nature*, **1993**, *365*, 464-468.

[19] J. W. C. Nerson, T. E., *Biochemistry*, **1994**, *33*, 5974-5983.

[20] U. M. Srinivasan, J.J., *Biochemistry*, **1997**, *36*, 3199-3206.

[21] C. Mattos, D. A. Giammona, G. A. Petsko, D. Ringe, *Biochemistry*, **1995**, *34*, 3193-3203.

[22] Christophe Dugave, L. D. *Chem. Rev.* **2003**, *103*, 2475-2532.

[23] Krzsztof Palczewski, T. K., Tetsuya Hori, Craig A. Behnke, Hiroyuki Motoshima, Barian A. Fox, Isolde Le Trong, David C. Teller, Tetsuji Okada, Ronald E. Stenkamp, Masaki Yamamoto, Masashi Miyano *Science* **2000**, *289*, 739-745.

[24] Tetsuji Okada, Y. F., Maria Silow, Javier Navarro, Ehud M. Landau, Yoshinori Shichida *Proc. Natl. Acad. Sci. USA* **2002**, *99*, 5982-5987.

[25] Babak Borhan, M. L. S., Hiroo Imai, Yoshinori Shichida, Koji Nakanishi *Science* **2000**, *288*, 2209-2212.

[26] Santosh T. Menon, M. H., Thomas P. Sakmar *Phys. Rev.* **2001**, *81*, 1659-1688.

[27] James B. Hurley, T. G. E., Barry Honig, Michael Ottolenghi *Nature* **1977**, *270*, 540-542.

[28] Tchiya Rosenfeld, A. A., Michael Ottolenghi *J. Phys. Chem.* **1974**, *78*, 336-341.

[29] Istvan Szundi, J. W. L., David S. Kliger. *Biochem.* **2003**, *42*, 5091-5098.

[30] Gregory Choi, J. L., Jhenny Flor Galan, Robert R. Birge, Arlene D. Albert, and Philip L. Yeagle *Biochemistry* **2002**, *41*, 7318-7324.

[31] U. K. Genick, S. M. Soltis, P. Kuhn, I. L. Canestrelli, E. D. Getzoff, *Nature*, **1998**, *392*, 206-209.

[32] M. Baca, G. E. Borgstahl, M. Boissinot, P. M. Burke, D. R. Williams, K. A. Slater, E. D. Getzoff, *Biochemistry*, **1994**, *33*, 14369-14377.

[33] M. Kim, R. A. Mathiesm W. D. Hoff, K. J. Hellingwerf, *Biochemistry*, **1995**, *34*,

12669-12672.

[34] B. Perman, V. Srajer, Z. Ren, T. Teng, C. Pradervand, T. Ursby, D. Bourgeois, F. Schotte, M. Wulff, R. Kort, K. Hellingwerf, K. Moffat, *Science*, **1998**, *279*, 1946-1950.

[35] U. K. Genick, G. E. O. Borgstahl, Z. R. Kingham Ng, C. Pradervand, P. M. Burke, V. Srajer, T. Y. Teng, W. Schildkamp, D. E. McRee, K. Moffat, E. D, Getzoff, *Science*, **1997**, *275*, 1471-1475.

[36] A. Xie, W. D. Hoff, A. R. Kroon, K. J. Hellingwerf, *Biochemistry*, **1996**, *35*, 14671-14678.

[37] A. Xie, L. Kelemen, J. Hendriks, B. J. White, K. J. Hellingwerf, W. D. Hoff, *Biochemistry*, **2001**, *40*,1510-1517.

[38] Y. Imamoto, K. Mihara, O. Hisatomi, M. Kataoka, F. Tokunaga, N. Bojkova, K. Yoshihara, *J. Biol. Chem.*, **1997**, *272*, 12905-12908.

[39] G. Rubinstenn, G.. W. Vuister, F. A. Mulder, P. E. Dux, R. Boelens, K. J. Hellingwerf, R. Kaptein, *Struct. Biol.*, **1998**, 568-570.

[40] P. F. V. Gilli, V. Bertolasi, G. Gilli, *J. Am. Chem. Soc.*, **1994**, *116*, 909-915.

[41] Z. R. Malarski, L. Sobczyk, E. Grech, *J. Phys. Chem.*, **1982**, *86*, 401-406.

[42] T. S. Steiner, A. M. M., M. Luts, J. Kroon, *Acta. Cryst.*, **2000**, *C56*, 577-579.

[43] T. Steiner, *Angew. Chem. Int. Ed.*, **2002**, *41*, 48-76.

[44] B. P. C. Hay, G. Sandrone, D. A. Dixton, *Inrog. Chem.*, **1998**, *37*, 5887-5894.

[45] G. D. Sandrone, D. A. P., *J. Phys. Chem. A*, **1999**, *103*, 3554-3561.

[46] G. K. Sandrone, *J. Mol. Biol.*, **2000**, *305*, 535-557.

[47] R. G. Vargas, D. A. Dixton, B. P. Hay, *J. Am. Chem. Soc.*, **2000**, *122*, 4750-4755.

[48] A. Onoda, Y. Yamada, J. Takeda, Y. Nakayama, T. Okamura, M. Doi, H. Yamamoto, N. Ueyama, *Bull. Chem. Soc. Jpn.* **2004**, *77*, 321-329.

[49] A. Onoda, Y. Yamada, Y. Nakayama, K. Takahashi, H. Adachi, T. Okamura, A. Nakamura, H. Yamamoto, N. Ueyama, D, Vyprachticky, Y. Okamoto, *Inorg. Chem.* **2004**, *43*, 4447-4455.

[50] N. Ueyama, K. Takahashi, A. Onoda, T. Okamura, H. Yamamoto, *Macromol. Symp.* **2003**, *204*, 287-294.

[51] D. Kanamori, T. Okamura, H. Yamamoto, N. Ueyama, *Angew. Chem. Int. Ed.* **2005**, *44*, 969-972.

[52] D. Kanamori, A. Furukawa, T. Okamura, H. Yamamoto, N. Ueyama, *Otg. Biomol. Chem.* **2005**, *3*, 1453-1459.

[53] D. Kanamori, Y. Yamada, A. Onoda, T. Okamura, S. Adachi, H. Yamamoto, N. Ueyama, *Inorg. Chim. Acta.* **2005**, *358*, 331-338.

[54] K. Takahashi, M. Doi, A. Kobayashi, T. Taguchi, A. Onoda, T. Okamura, H. Yamamoto, N. Ueyama, *J. Cryst. Growth* **2004**, *263*, 552-563.

[55] N. Ueyama, K. Takahashi, A. Onoda, T. Okamura, H. Yamamoto, *Macromol. Symp.* **2002**, *186*, 129-134.

[56] N. Ueyama, H. Kozuki, M. Doi, Y. Yamada, K. Takahashi, A. Onoda, T. Okamura, H. Yamamoto, *Macromolecules* **2001**, *34*, 2607-2614.

[57] A. Onoda, Y. Yamada, M. Doi, T. Okamura, N. Ueyama, *Inorg. Chem.* **2001**, *40*, 516-521.

[58] T. Okamura, S. Takamizawa, N. Ueyama, and A. Nakamura, *Inorg. Chem.*, **1998**, *37*, 18-28.

[59] T. Okamura, N. Ueyama, A. Nakamura, E. Ainscough, A. M. Brodiem and J. M. Waters, *J. Chem. Soc. Chem. Comun.*, **1993**, *21*, 1658-1660.

[60] W. Y. Sun, N. Ueyama, A. Nakamura, *Inorg. Chem.*, **1991**, *30*, 4026-4031

[61] N. Ueyama, T. Okamura, and A. Nakamura, *J. Chem. Soc. Chem. Comun.*, **1992**, *14*, 1019-1020.

[62] N. Ueyama, T. Okamura, and A. Nakamura, *J. Am. Chem. Soc.*, **1992**, *114*, 8129-8137.

[63] N. Ueyama, Y. yamada, T. Okamura, S. Kimura, and A. Nakamura, *Inorg. Chem.*, **1996**, *35*, 6473-6484.

[64] N. Ueyama, T. Terakawa, M. Nakata, and A. Nakamura, *J. Am. Chem. Soc.*, **1983**, *105*, 7098-7102.

[65] M. Irie, T. Fukaminato, T. Sasaki, N. Tamai, T. Kawai, *Nature* **2002**, *420*, 759-760.

[66] M. Irie, O. Miyatake, K. Uchida, T. Eriguchi, *J. Am. Chem. Soc.* **1994**, *116*, 9894-9900.

[67] J. Hayakawa, A. Momotake, T. Arai, *Chem. Commun.* **2003**, 94-95.

[68] J. Hayakawa, A. Momotake, R. Nagahata, T. Arai, *Chem. Lett.* **2003**, *32*, 1008-1009.

[69] H. Tatewaki, T. Mizutani, J. Hayakawa, T. Arai, M. Tarazima, *J. Phys. Chem. A* **2003**, *107*, 6515-6521.

[70] J. H. Yoo, I. Cho, S. Y. Kim, *J. Polym. Sci. part A: Polym. Chem.* **2004**, *42*, 5401-5406.

[71] O. Ohtani, R. Sasai, T. Adachi, I. Hatta, K. Takagi, *Langmuir* **2002**, *18*, 1165-1170.

[72] R. Behrendt, C. Renner, M. Schenk, F. Wang, J. Wachtveitl, D. Oesterhelt, L. Moroder, *Angew. Chem. Int. Ed.* **1999**, *38*, 2771-2774.

[73] R. Behrendt, M. Schenk, H. J. Musiol, L. Moroder, *J. Peptide Sci.* **1999**, *5*, 519-529.

[74] S. Kobatake, S. Takami, H. Muto, T. Ishikawa, M. Irie, *Nature* **2007**, *446*, 778-781.

[75] F. D. Lewis, B. A. Yoon, T. Arai, T. Iwasaki, K. Tokumaru, *J. Am. Chem. Soc.* **1995**, *117*, 3029-3036.

[76] T. Arai, M. Moriyama, K. Tokumaru, *J. Am. Chem. Soc.* **1994**, *116*, 3171-3172.

[77] A. Masumoto, K. Maeda, T. Arai, *J. Phys. Chem. A* **2003**, *107*, 10039-10045.

[78] M. Ikegami, T. Arai, *Bull. Chem. Soc. Jpn.* **2003**, *76*, 1783-1792.

[79] M. Ikegami, T. Arai, *Chem. Lett.* **2005**, *34*, 492-493.

[80] Y. Odo, K. Matsuda, M. Irie, *Chem. Eur. J.* **2006**, *12*, 4283-4288.

[81] S. H. Kawai, S. L. Gilat, J. M. Lehn, *Eur. J. Org. Chem.* **1999**, 2359-2366.

[82] M Irie, Y Hirano, S Hashimoto, K Hayashi, *Macromolecules* **1981**, *14*, 262-267.

[83] K Ishihara, T Matsuo, K Tsunemitsu, I Shinohara, *Journal of Polymer Science: Polymer Chemistry Ed.* 1984, *22*, 3687-3695.

[84] Richard Fuchs, Jordan J. Bloomfield *J. Org. Chem.* **1966**, *31*, 3423-3425.

[85] T. Asano, H. Furuta, H. J. Hofmann, R. Cimaraglia, Y. Tsuno, M. Fujino, *J. Org. Chem.* **1993**, *58*, 4418-4423.

[86] K. Maeda, K. A. Muszkat, S. S. Ozeri, *J. Chem. Soc., Perkin Trans 2* **1980**, *9*, 1282-1287.

[87] K. Maeda, E. Fischer, *Israel J. Chem.* **1977**, *16*, 294-298.

[88] N. Ueyama, M. Inohara, A. Onoda, T. Ueno, T. Okamura, A. Nakamura, *Inorganic Chem.* **1999**, *38*, 4028-4031.

[89] D. Kanamori, Y. Yamada, A. Onoda, T. Okamura, S. Adachi, H. Yamamoto, N. Ueyama, *Inorganic Chim. Acta* **2005**, *358*, 85-92.

[90] A. Onoda, H. Yamamoto, Y. Yamada, K. Lee, S. Adachi, T. Okamura, K. Yoshizawa-Kumagaye, K. Nakajima, T. Kawakami, S. Aimoto, N. Ueyama, *Biopolymers*, **2005**, *80* (2 and 3), 233-248.

[91] N. Ueyama, K. Takahashi, A. Onoda, T. Okamura, H. Yamamoto, *Macromol. Symp.*, **2003**, *204*, 287-294.

[92] A. Onoda, H. Haruna, H. Yamamoto, K. Takahashi, H. Kozuki, T. Okamura, N. Ueyama, *Eur. J. Org. Chem.* **2005**, 641-645.

[93] C. Tu, A. Y. Louie, *Chem. Commun.* **2007**, 1331-1333.

[94] N. Tamaoki, N. Wada, *J. Am. Chem. Soc.* **2006**, *128*, 6284-6285.

Chapter 2

The reversible switching of an intramolecular NH···O hydrogen bond by photo and thermal isomerization of benzylideneaniline framework

Introduction

Benzylideneaniline is the photochromic compound, which is known to progress *E* to *Z* photoisomerization and *Z* to *E* thermal isomerization.[1-3, 16-18] The behavior of this framework is similar to the azobenzene,[4-6, 19-29] which is the typical photochromic compound, but *Z* isomer of benzylideneaniline is unstable than that of azobenzene (Scheme 1). The *Z* isomer of benzilideneaniline turned to the *E* isomer immediately, whereas that of azobenzene keeps the conformation for an hour order, at room temperature. The destabilization of *Z* benzylideneaniline is caused by the low rotation energy barrier of an azomethine (C=N) moiety. The fast isomerization of azomethine double bond is useful to signal transduction of light stimulation, and adopted in the chromophor of Rhodopsin or Bacteriorhodopsin as Shiff base conjugated between rethinal and an amine moiety of lysine side chain (Chart 1).[7-15, 30, 31] In this chapter, the author designed two novel compounds: carboxylic acid *E*-1/*Z*-1 and carboxylate *E*-2/*Z*-2, both of which have an amide group linked with a photoinduced azomethine moiety. These compounds are expected to switch the intramolecular NH···O hydrogen bond, accompanied by *trans*-to-*cis* photoisomerization and by *cis*-to-*trans* thermal isomerization of the azomethine double bond (Scheme 2).

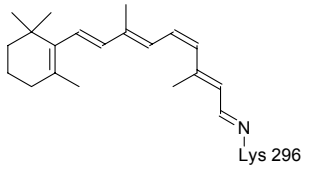

Chart 1.

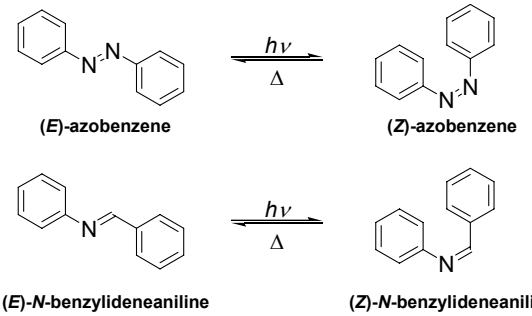

Scheme 1. Photoisomerization and thermal reversion of azobenzene and benzylideneaniline.

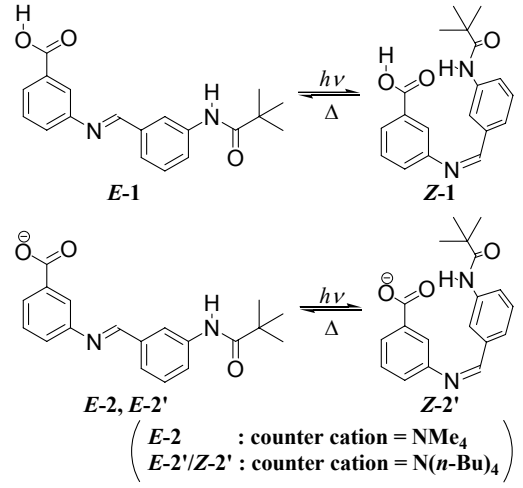

Scheme 2. Photoisomerization and thermal reversion of diarylazomethines ***E*-1**, ***E*-2** and ***E*-2'**.

Results and Discussion

Synthesis

Synthetic pathway was shown in Scheme 3.[32, 33] Benzylideneaniline framework was obtained by condensation from the corresponding aniline and benzaldehyde. Carboxylate was obtained by the counter cation exchange reaction.

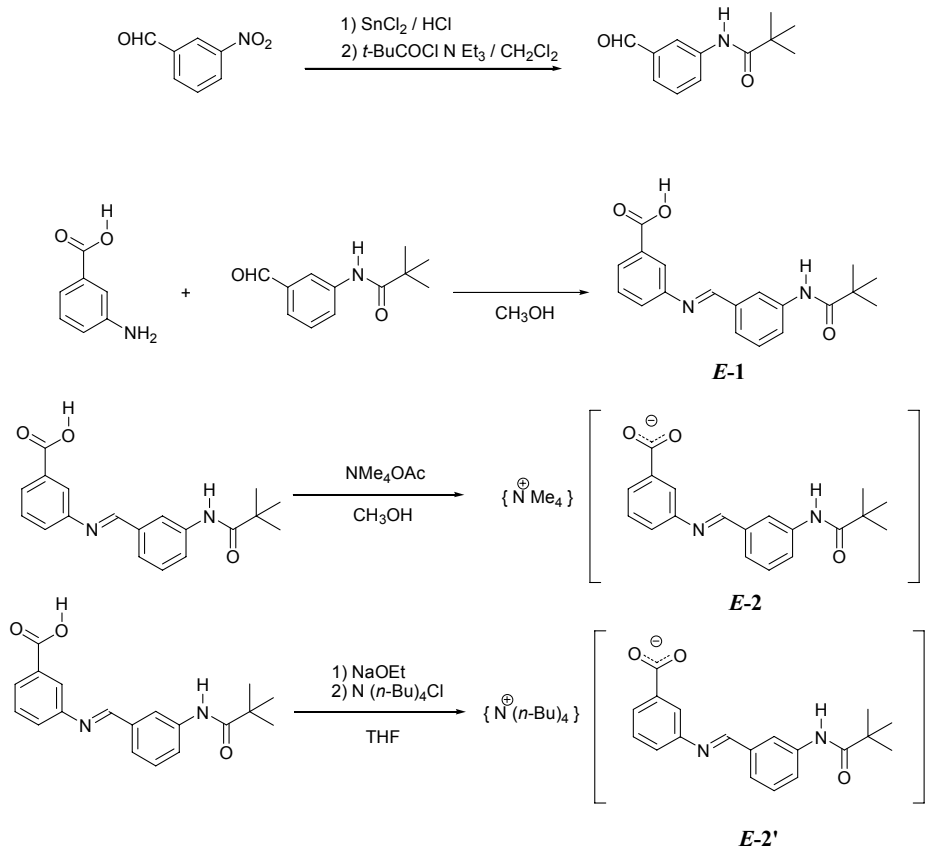

Scheme 3. Synthetic pathway of ***E*-1**, ***E*-2** and ***E*-2'**.

Molecular structure in solid state

The crystal structure of *E*-2 is shown in Figure 1. The intermolecular N'1···O11 distance (2.89 Å) permitted sufficient hydrogen bond formation; this interaction stabilizes the packing structure (N'1 indicates N1 atom at equivalent position (1.5-x, -0.5+y, 1.5-z)). Both of the C···O distances in the carboxylate group, O11···C01 (1.21[8] Å) and O12···C01 (1.26[6] Å), are virtually identical. Solid Fourier transform infrared (FT-IR) spectra of *E*-1 and *E*-2 were measured to determine the existence of an intermolecular hydrogen bond. *E*-1 exhibits an NH band at 3307 cm^{-1}, whereas the ν (NH) band appears at 3218 cm^{-1} in *E*-2, indicating the presence of a stronger NH···O hydrogen bond. These experimental results obtained by X-ray analysis indicate that *E*-2 forms an intermolecular hydrogen bond in the solid state.

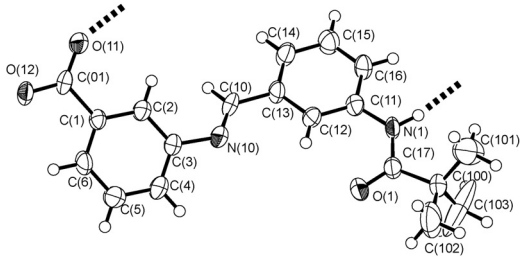

Figure 1. Molecular structure of ***E*-2** (50 % probability).

Molecular structure in solution

The solubility of tetramethylammonium carboxylate (*E*-2) toward tetrahydrofuran (THF) was too low for spectroscopic analysis. Tetra-*n*-butylammonium carboxylate (*E*-2'), which had enhanced solubility by lipophilic cation, was adhibited to measure UV-vis and ^{1}H NMR spectra. The structures in THF-d_8 solution were determined by ^{1}H NMR spectra. ^{1}H NMR spectra of *E*-1 and *E*-2' in THF-d_8 are shown in Figure 2. A positive nuclear overhauser effect (NOE) between He and Ha' or He and Hc' coincided, indicating that the configurations of *E*-1 and *E*-2' are in the *trans* form. The chemical shifts of the amide NH signal are 8.52 ppm in *E*-1 and 10.80 ppm in *E*-2'. The significant downfield shift (Δ = 2.28 ppm) of the NH proton suggests that *E*-2' forms a

strong NH···O hydrogen bond in THF-d_8 solution. However, the temperature dependency of the amide NH chemical shift for *E*-2' was –10.9 ppb K^{-1}, whereas that of *E*-1 was –5.0 ppb K^{-1} in the range of 173 to 303 K. In addition, the upfield shift (Δ = 0.34 ppm) of the NH proton was observed when the solution was diluted from 5 mM to 1 mM. The results show that *E*-2' forms an intermolecular NH···O hydrogen bond in THF-d_8 solution.

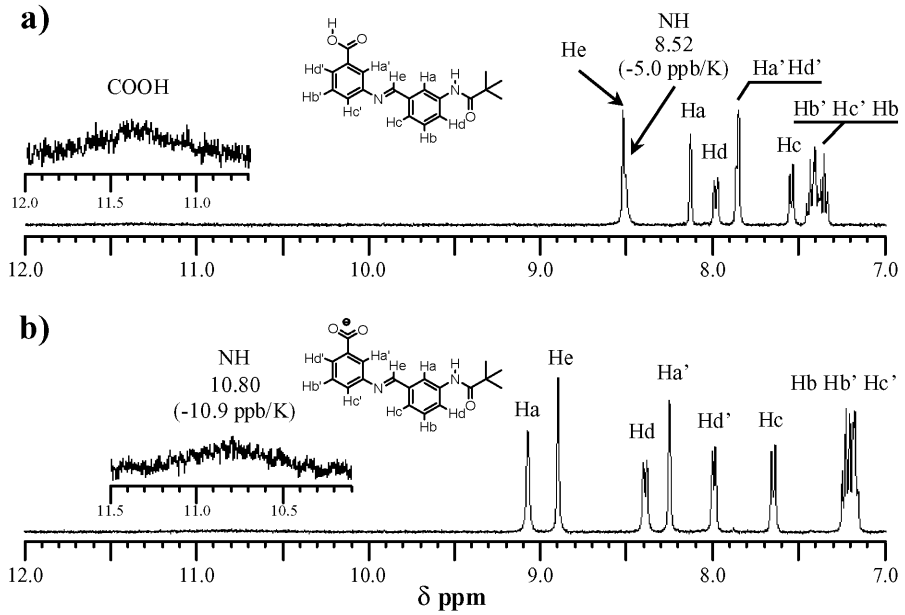

Figure 2. ^{1}H NMR spectra of a) *E*-1 and b) *E*-2', 5 mM in THF-d_8 solution at 303 K.

Direct photoisomerization of *E*-1 and *E*-2'

Although UV irradiation of *trans* diarylazomethines results in extensive conversion into the corresponding *cis* isomers, the *cis* isomers are thermally unstable and cause thermal reversion to *trans* isomers at high temperatures.[5] The *cis* isomers were stable only at temperatures less than *ca.* 203 K.[6] Using UV-vis and ^{1}H NMR measurements at low temperature, the photoisomerization reactions of *E*-1 and *E*-2' were traced. UV-vis

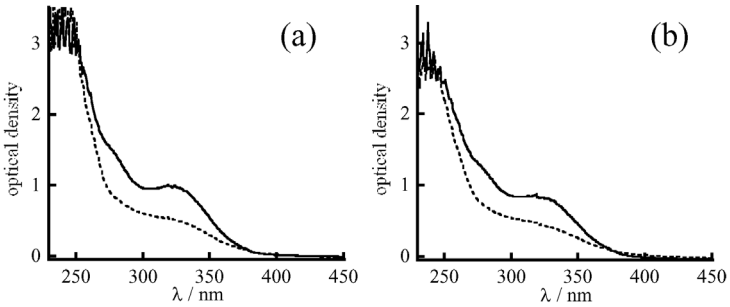

Figure 3. UV-vis spectrum change of a) *E*-1 and b) *E*-2', by UV irradiation of 313 and 365 nm toward 0.08 mM in THF solution at 173K. Before irradiation (solid lines) and after irradiation (dotted lines).

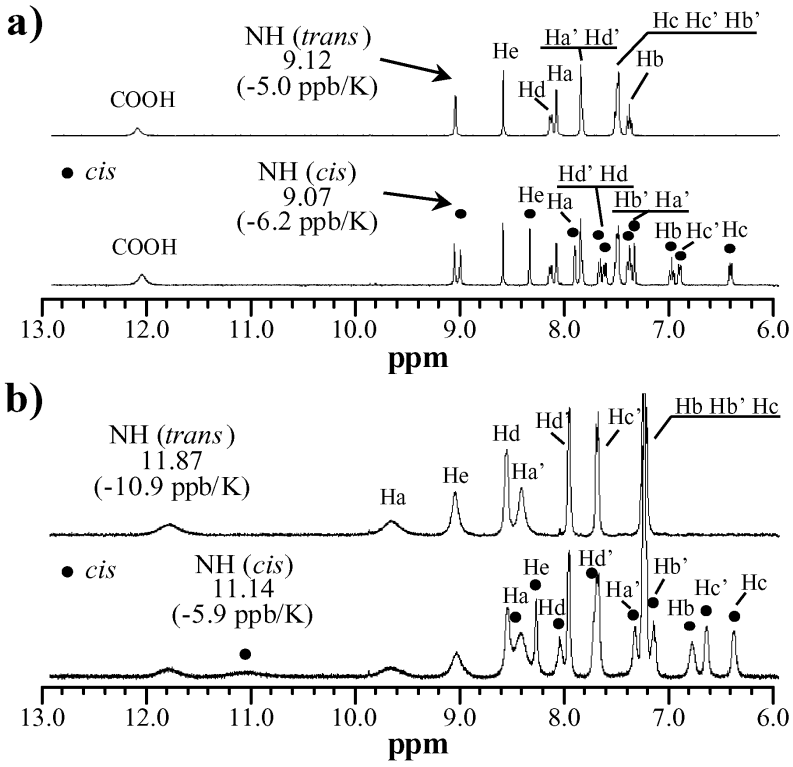

Figure 4. [1]H NMR spectrum change of a) *E*-1 and b) *E*-2', by UV irradiation of 313 nm and 365 nm 5 mM in THF-d_8 solution at 183 K. Before irradiation (upside) and after irradiation (downside).

spectra of *E*-1 and *E*-2' were measured by static method below 203 K. According to photoirradiation in THF solution at 173 K, changes took in the UV-vis spectra of *E*-1 and *E*-2', as shown in Figure 3. *E*-1 and *E*-2' were isomerized and reached a photostationary state (PSS) at 313 and 365 nm UV-light irradiation in the UV-vis spectrometer. Solid lines were those taken before irradiation, corresponding to *trans* isomers, and dotted lines were those observed in PSS. The blue shift of λ_{max} in *cis* compounds indicates that two phenyl rings are not in plane and that the conjugation is interrupted. These changes in the spectra were reversible toward thermal reversion at higher temperatures.

cis Isomers were also observed in ^{1}H NMR spectra. Using a photoirradiation probe (designed for chemically induced dynamic nuclear polarization[CIDNP]), UV light was directly introduced into the NMR equipment. The spectra were taken before and after UV irradiation in THF-d_8 solution at 183 K, using a 200-W xenon–mercury arc passed through a liquid light guide. Irradiation was continued until the establishment of a PSS (about 30 minutes of irradiation). ^{1}H NMR spectra of *trans* compounds (*E*-1 and *E*-2') and their PSS in THF-d_8 solution at 183 K are shown in Figure 4. The signals that newly appeared after irradiation were assigned by correlation of NMR measurements. Exchange spectroscopy (EXSY) spectra under photoirradiation in THF-d_8 solution at 203 K are shown in Figure 5. Because of the fast rate of photoisomerization, equilibrium between *E*-1 and *Z*-1 was achieved and positive cross-peaks based on the photochemical exchange process between the two compounds were observed in Hb, Hc, Hc', Hd, and He (Figure 5a). The homodecoupling measurement coincided with their expected coupling pattern, and the negative NOE between NH and Ha coincided with Ha and Ha' signals. As a consequence, all of the signals derived from *Z*-1 were assigned. In *cis* form, the two rings of diarylazomethine are in close proximity to each other. Significant upfield shift of Hc, Hc' were observed in *Z*-1 because the protons of one ring are in the shielding cone of another ring. The structure in solution of *Z*-1 was estimated based on NOE correlations. NOE correlations of He-Hc' or He-Ha', which were observed characteristically in *E*-1, disappeared in *Z*-1. Instead, the NOE correlation was observed between Ha' and Hc in *Z*-1. These results confirm that the configuration of the photoproduct *Z*-1 is exactly in *cis* form. In *Z*-1, NOE correlations of He-Ha and He-Hc are observed at the same time, which indicates that the amide-side aromatic ring of *Z*-1 rotates easily.

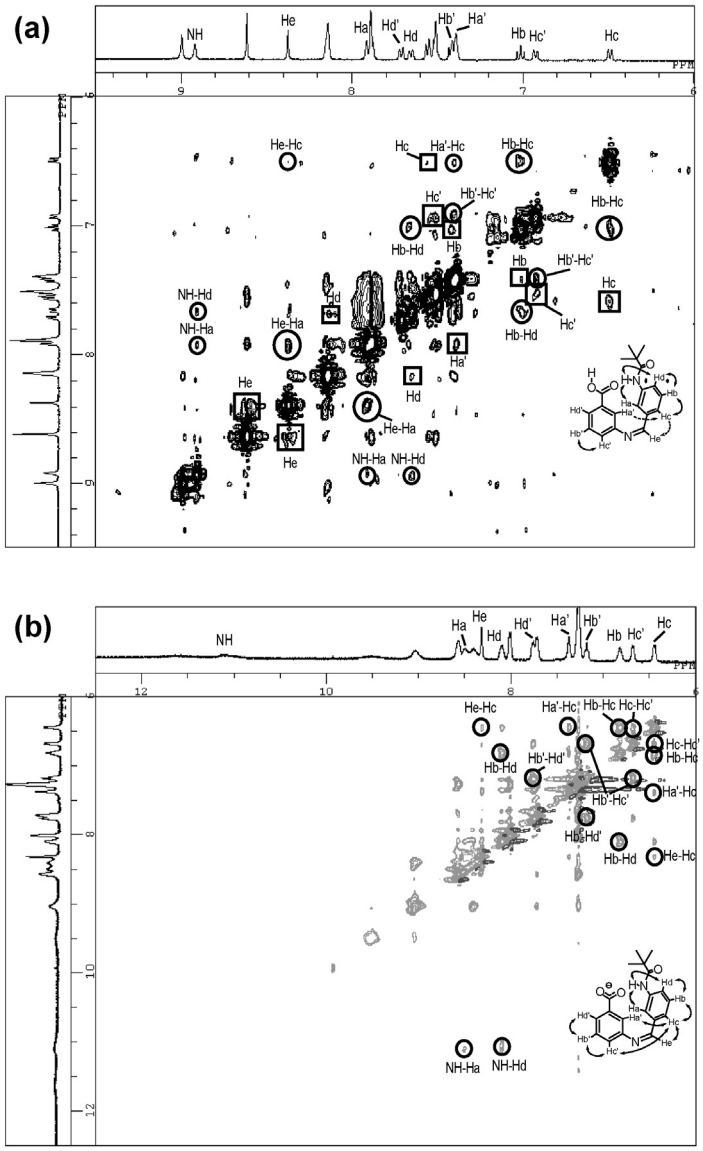

Figure 5. Photoirradiating NOESY NMR spectra of a) carboxylic acid *E*-1/*Z*-1, and b) carboxylate *E*-2'/*Z*-2', 5 mM in THF-d_8 solution at 203 K. The cross peaks in circle indicate the intramolecular NOE signals in *Z* isomers and these in square indicate the EXSY signals between *E* and *Z* isomers.

In contrast to carboxylic acid, the correlation between the two compounds is not clearly observed in carboxylate (Figure 5b). It was also difficult to assign the signals using the homodecoupling method because of broadening of signals at low temperatures. To assign the signals of *Z*-2', correlation spectroscopy (COSY) NMR spectrum in PSS was measured. Two singlets, NH and He, do not have a COSY. One broad signal at 11.10 ppm, which has a large temperature coefficient, is assigned to the NH signal. Another sharp signal at 8.31 ppm is assigned to the He signal. In the nuclear overhauser effect spectroscopy (NOESY) spectrum (Figure 5b), positive NOE of NH-Ha and NH-Hd confirmed the Ha and Hd signals. The COSY NMR spectrum coincided with the Ha', Hb, Hb', and Hc signals. Of two residual signals, an upfield-shifted signal is assigned to Hc' because Hc' is closer to the amide-side aromatic ring than Hd', and Hc' is more affected by the shielding effect of the aromatic ring. A positive NOE was observed in Ha'-Hc and in Hc-Hc' of *Z*-2', which confirms that the configuration of the *Z*-2' is in *cis* form.

When the temperature was raised, the new signals disappeared and only the signals of the *trans* isomer were observed. This reaction cycle (*i.e.,* photoisomerization and thermal reversion) is completely reversible. The ratios of *cis/trans* isomers were 47/53 (*E*-1/*Z*-1) and 40/60 (*E*-2'/*Z*-2') at PSS (173 K), respectively. The chemical shifts of amide NH signals of *cis* isomers at 183 K were 9.07 ppm in *Z*-1 and 11.14 ppm in *Z*-2'. The downfield shift of 2.07 ppm suggests that *Z*-2' forms an NH···O hydrogen bond in the THF-d_8 solution. The decrease in the temperature coefficient during the *trans*-to-*cis* isomerization of *E*-2' (–10.9 ppb K^{-1}) and *Z*-2' (–5.9 ppb K^{-1}), whereas that *E*-1 (–5.0 ppb K^{-1}) and *Z*-1 (–6.2 ppb K^{-1}) has almost same value, indicates that the intramolecular hydrogen bond is predominant in *Z*-2', whereas the intermolecular interaction is formed in *E*-2'.

In contrast to the sharp signals observed in carboxylic acids (*E*-1, *Z*-1), the signals of carboxylates (*E*-2', *Z*-2') were broadened at low temperature. Because of the intermolecular hydrogen bond formed in THF-d_8 solution, *E*-2' assumes an origomeric structure easily because exchange reactions take more slowly at low temperature. It is thought that only signals of carboxylates were broadened at low temperatures because of this equilibrium. Decreasing the temperature also seemed to cause the signals of the aromatic ring protons to shift to a low magnetic field; these signals were observed as a result of the intermolecular deshielding effect produced by the aromatic ring of the other molecule, which became adjacent through the presence of the intermolecular NH···O

hydrogen bond. The intermolecular interaction of *Z*-2' is estimated to be small because the signals those in *E*-2' are broader than those in *Z*-2'.

Z to *E* thermal isomerization

The intramolecular hydrogen bond can influence the ground-state equilibrium between configurational and conformational isomers as well as photophysical and photochemical behavior.[3,4] If the intramolecular hydrogen bond is formed in a *cis* compound, it may decrease the *cis*-to-*trans* thermal reversion rate. Kinetic studies of thermal reversion of diarylazomethine derivatives from *cis*-to-*trans* isomers were reported in a wide temperature range and found to follow first-order kinetics.[5,6] *Z*-1 and *Z*-2' also produce *cis*-to-*trans* thermal reversion in accordance with first-order kinetics. Using the time-course experiments of UV–visible spectra in THF solution, the thermal reversion rates of *Z*-1 and *Z*-2' in the temperature range of 213 to 243 K were measured.

The thermal reversion of *Z*-1 is faster than that of *Z*-2' in the temperature range of 213 to 243 K. This result also suggests that the NH···O intramolecular hydrogen bond forming at *Z*-2' is stronger than the one formed at *Z*-1. Activation energies of *cis*-to-*trans* thermal isomerization were determined using the Arrhenius equation. Arrhenius plots of *Z*-1/*E*-1 and *Z*-2'/*E*-2' are shown in Figure 6. The activation energies of thermal reversion of *Z*-1 and *Z*-2' are 15.1 and 16.9 kcal mol^{-1}, respectively. *Z*-2' has an activation energy that is 1.8 kcal mol^{-1} higher for this reaction. This difference in the revel of activation energy is thought to arise from the formation of an intramolecular NH···O hydrogen bond in *Z*-2'.

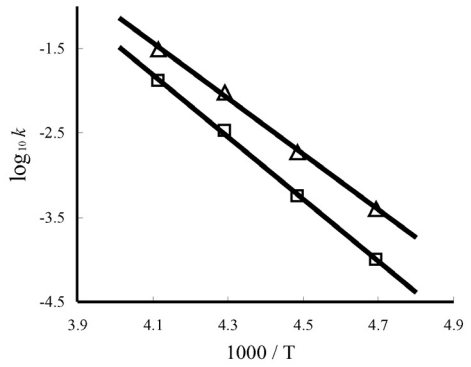

Figure 6. Arrhenius's plots of *Z* to *E* thermal isomerization for *Z*-1 (triangle) and *Z*-2' (square).

Conclusion

In conclusion, carboxylic acid *E*-1 and carboxylate *E*-2', which both have an amide group linked to an azomethine moiety that switches the intramolecular NH···O hydrogen bond through photoirradiation, were synthesized and characterized. *E*-2' was determined to form intermolecular, rather than intramolecular, NH···O hydrogen bonds in the solid state and in the THF solution. Using UV light irradiation, the generation of a *cis* isomer was observed by UV–visible and ^{1}H NMR spectra. The temperature coefficient for the chemical shift of amide NH signals and *cis*-to-*trans* thermal reversion rates of their compounds show that the intramolecular NH···O hydrogen bond of *Z*-2' is stronger than that of *Z*-1.

Experimental

General procedures

All manipulations involving air- and moisture-sensitive compounds were carried out by the use of standard Schlenk technique under argon atmosphere. 3-nitrobenzaldehyde, 2,2-dimethyl-propyonyl chloride were purchased from Tokyo-Kasei Co. 3-aminobenzaldehyde, stannous chloride were purchased from Nacalai tesque Co. Inc. Dichloro-methane was distilled over CaH_2. Tetrahydrofuran was distilled over CaH_2 and dried over Na. Methanol, Ethanol, and Acetonitrile were distilled over CaH_2 and dried over molecular sieves (3A).

Physical measurements

^{1}H (400 and 270 MHz), ^{13}C (100 MHz) NMR spectra were measured on a JEOL JNM-GSX400 or a JEOL JNM-GSX270 spectrometer. ^{1}H (500 MHz), ^{13}C (125 MHz) NMR spectra were measured on a JEOL LA500 spectrometer. When THF-d_8, CD_3CN, and $CDCl_3$ were used as solvent, the ^{1}H NMR and ^{13}C NMR spectra were referenced to the tetramethylsilane protons at δ 0.00, and to the tetramethylsilane carbons at δ 0.00, respectively. When DMSO-d_6 was used as solvent, the ^{1}H NMR and ^{13}C NMR spectra were referenced to the residual solvent protons at δ 2.49, and to the solvent carbons at δ 39.5. Elemental Analysis was performed at Elemental Analysis Center, Faculty of Science, Osaka University. All melting points of the compounds were measured on a micro melting point apparatus of YANAGIMOTO Co. ESI-MS measurements were performed on a Finnigan MAT LCQ ion trap mass spectrometer.zx. FT-IR spectra were measured on a JASCO FT/IR-8300 spectrometer.

Preparation of 3-(2,2-dimethyl-propionylamino)-benzaldehyde

To a conc. HCl (60 mL) suspension of 3-nitrobenzaldehyde (10.0 g, 66 mmol) was added stannous chloride (45.1 g, 240 mmol). The temperature rose rapidly, 3-nitrobenzaldehyde dissolves, and clear, orange solution was obtained. Solution was refluxed for 2 hours, and the solution color turned to red. Solution was cooled in an ice bath, and a pasty orange-red suspension results. Precipitate was collected and washed with the diethylether. Dried over one night in NaOH desiccator under reduced pressure, orange powder obtained (17.3 g). All of the orange powder was suspended in CH_2Cl_2 (70 mL) and cooled in an ice bath (A). 2,2-dimethyl-propyonyl chloride and triethylamine was added to CH_2Cl_2 (40 mL) and cooled in an ice bath (B). (A) was slowly dropped to (B). After the mixture was stirred for 90 min, reactant was washed with 2 % HCl aq., 4 % $NaHCO_3$ aq., water, and with saturated NaCl aq. in a dropping funnel. The organic layer was dried over anhydrous Na_2SO_4. Removal of solvents under reduced pressure followed by recrystallization from ethyl acetate/diethylether gave colorless crystal (4.9 g, 36 %). mp 104-105 ^oC; (Found: C, 70.07; H, 7.34; N, 6.73. Calc. for $C_{12}H_{15}NO_2$: C, 70.22; H, 7.37; N, 6.82 %); δ_H(270 MHz; DMSO-d_6) 1.23 (9H, s, *tert*-butyl), 7.52 (1H, t, *J* 7.6 Hz, Aryl), 7.59 (1H, dt, *J* 7.6 and 1.4, Aryl), 7.95 (1H, dt, *J* 7.6 and 1.4, Aryl), 8.22 (1H, t, *J* 1.4, Aryl), 9.45 (1H, br s, NH) and 9.96 (1H, s, CHO); δ_C(125 MHz; DMSO-d_6) 27.06, 39.18, 120.14, 124.80, 125.96, 129.25, 136.52, 140.15, 176.81 and 192.97; *m/z* (ESI) 204.4 ($[M-H]^+$ requires 204.1).

Preparation of (*E*)-3-{[3-(2,2-dimethyl-propionylamino)-benzylidene]-amino}-benzoic acid (*E*-1)

3-(2,2-Dimethyl-propionylamino)-benzaldehyde (1.0266 g, 5.00 mmol) and 3-aminobenzoic acid (1.3720 g, 10.0 mmol) was dissolved in methanol (70 mL) and stirred over one night at room temperature. Removal of solvents under reduced pressure followed by recrystallization from ethyl acetate/hexane gave white powder (0.5471 g, 33.7 %). mp 185 ^oC; (Found: C, 70.35; H, 6.10; N, 8.62. Calc. for $C_{19}H_{20}N_2O_3$: C, 70.35; H, 6.21; N, 8.64 %); ν_{max}(KBr pellet)/cm^{-1} 3307 (NH), 1700 (C=O), 1655 (C=O) and 1565 (C=N); δ_H(400 MHz; DMSO-d_6) 1.24 (9H, s, *tert*-butyl), 7.44 (1H, t, *J* 7.8 Hz, Aryl), 7.49 (1H, dt, *J* 7.8 and 1.8, Aryl), 7.53 (1H, t, *J* 7.8, Aryl), 7.59 (1H, dt, *J* 7.8 and 1.8, Aryl), 7.76 (1H, t, *J* 1.8, Aryl), 7.81 (1H, dt, *J* 7.8 and 1.8, Aryl), 7.84 (1H, dt, *J* 7.8 and 1.8, Aryl), 8.29 (1H, t, *J* 1.8, Aryl), 8.63 (1H, s, -CH=N-), 9.39 (1H, s, NH) and 13.02 (1H, br s, COOH);); δ_C(150 MHz; THF-d_8) 27.74, 40.23, 120.08, 122.67, 123.88, 125.15, 126.02, 127.74, 129.53, 129.75, 133.04, 137.80, 141.31, 153.27, 161.72, 167.38 and 176.79; *m/z* (ESI) 324.3 ($[M+H]^+$ requires 325.2), 346.3 ($[M+Na]^+$ requires 347.1).

Preparation of (tetramethyl-ammonium) (*E*)-3-{[3-(2,2-dimethyl-propionylamino)-benzylidene-amino]-benzoate (*E*-2)

To a solution of (*E*)-3-{[3-(2,2-Dimethyl-propionyl-amino)-benzylidene]-amino}- benzoic

acid in CH_3CN was added a solution of equivalent amount of tetramethyl-ammonium acetate in CH_3CN. The solution was stirred and concentrated to give orange oil. The oil was washed with ether to give pale orange powder. The powder was recrystalized from hot CH_3CN to give colorless crystal (yield was not certain). mp 245 ^oC; (Found: C, 68.47; H, 7.89; N, 10.40. Calc. for $C_{23}H_{31}N_3O_3$: C, 69.49; H, 7.86; N, 10.57 %); ν_{max}(KBr)/cm^{-1} 3218 (br, NH) and 1668 (CO); δ_H(400 MHz; DMSO-d_6) 1.24 (9H, s, *tert*-butyl), 3.09 (12H, s, NMe_4), 7.12 (1H, dt, *J* 7.8 and 1.6 Hz, Aryl), 7.23 (1H, t, *J* 7.8, Aryl), 7.42 (1H, t, *J* 7.8, Aryl), 7.56 (1H, dt, *J* 7.8 and 1.6, Aryl), 7.65 (1H, t, *J* 1.6, Aryl), 7.66 (1H, dt, *J* 7.8 and 1.6, Aryl), 7.86 (1H, dt, *J* 7.8 and 1.6, Aryl), 8.22 (1H, t, *J* 1.6, Aryl), 8.55 (1H, s, -CH=N-) and 9.39 (1H, s, NH).

Preparation of (tetra-*n*-butyl-ammonium) 3-{[3-(2,2-dimethyl-propionylamino)-benzylidene-amino]-benzoate (*E*-2')

To a solution of (*E*)-3-{[3-(2,2-Dimethyl-propionylamino)-benzylidene]-amino}- benzoic acid (0.0909 g, 2.8×10^{-4} mol) in ethanol (4.0 mL) was added 2.8 M ethanol solution of sodium ethoxide (0.10 mL, 2.8×10^{-4} mol). The solution was stirred over one night and concentrated to give white-yellow powder. The powder was washed with diethyl ether, and then dissolved in ethanol again. A solution of tetra-*n*-butyl-ammonium chloride (0.0778 g, 2.8×10^{-4} mol) in EtOH was added. After stirred for few minutes, solvent was removed under reduced pressure to give pale white-orange powder. The powder was washed by diethyl ether. Recrystallization from THF/hexane gave pale white-orange powder (yield was not certain). (Found: C, 67.23; H, 9.72; N, 6.54. Calc. for $C_{35}H_{55}N_3O_3$ + $(H2O)_{0.3}$: C, 67.23; H, 9.93; N, 6.72 %); δ_H(400 MHz; DMSO-d_6) 0.91 (12H, t, *J*, $-CH_2CH_3\times4$), 1.23 (9H, s, *tert*-butyl), 1.30 (8H, multiplet, $-CH_2CH_3\times4$), 1.56 (8H, multiplet, $-CH_2CH_2CH_3\times4$), 3.15 (8H, multiplet, $N-CH_2-\times4$), 7.12 (1H, dt, *J* 7.8 and 1.6, Aryl), 7.23 (1H, t, *J* 7.8, Aryl), 7.42 (1H, t, *J* 7.8, Aryl), 7.56 (1H, dt, *J* 7.8 and 1.6, Aryl), 7.67 (1H, t, *J* 1.6, Aryl), 7.68 (1H, dt, *J* 7.8 and 1.6, Aryl), 7.87 (1H, dt, *J* 7.8 and 1.6, Aryl), 8.22 (1H, t, *J* 1.6, Aryl), 8.55 (1H, s, -CH=N-) and 9.38 (1H, s, NH) ; δ_C(150 MHz; THF-d_8) 14.01, 20.54, 24.75, 59.19, 120.43, 120.65, 122.46, 125.14, 125.46, 127.81, 128.34, 128.71, 138.23, 142.94, 144.41, 151.64, 160.98, 170.09 and 177.67; *m/z* (ESI) 313.2 ($[M-N(n\text{-butyl})_4]^-$ requires 323.1) and 564.4($[M-H]^-$ requires 564.4).

UV-light irradiation technique for UV-vis spectrum measurement at 173 K

The temperature was controlled in the UV-cell using the DN1704 liquid nitrogen cryostat. A Xe/Hg lamp (MUV-202U, Moritex Co.) was used for UV-light irradiation. The UV-light was directed using a liquid light guide. The sample was prepared under Ar atmosphere and dissolved in the degassed solvent. The sample in the UV-cell was irradiated after the temperature was lowered. After irradiation, the spectrum was measured. During irradiation and spectrum measurements, the sample was always kept at the desired temperature.

UV-light irradiation technique for ^{1}H NMR spectrum measurement at low temperatures

A Xe/Hg lamp was used for UV-light irradiation. The UV-light was directed using a liquid light guide. The sample was dissolved in the degassed solvent and sealed in an NMR tube under Ar atmosphere. After the temperature was lowered, UV-light was irradiated in the NMR spectrometer using a CIDNP probe. After irradiation, the spectrum was measured. During irradiation and spectrum measurements, the sample was always kept at the desired temperature. The schematic illustration of low temperature ^{1}H NMR spectrum was drawn in Figure 7.

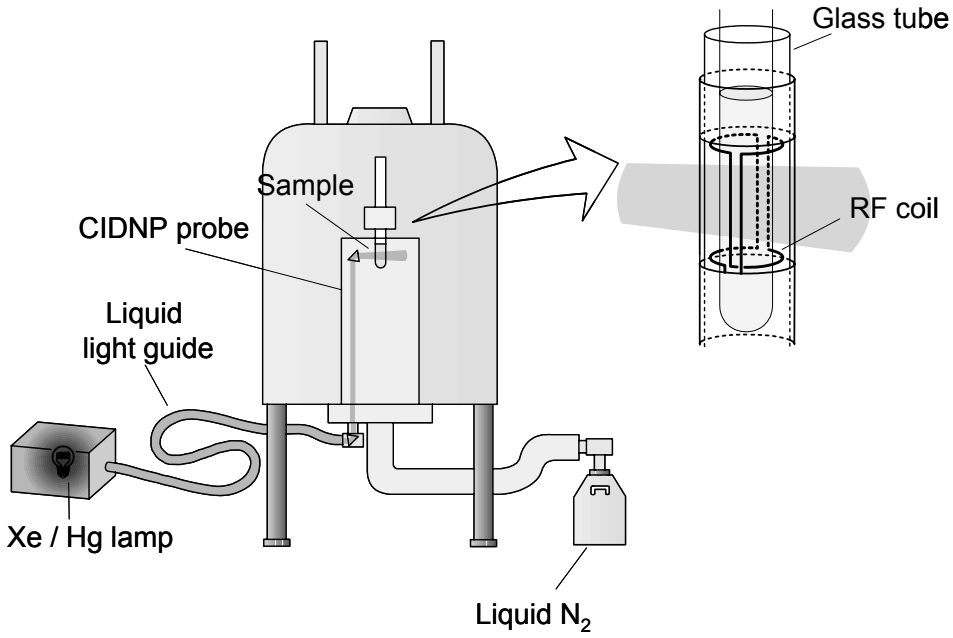

Figure 7. Schematic illustration of low temperature ^{1}H NMR spectrum measurement

First-order kinetics of thermal isomerization of *Z*-1 and *Z*-2'

Thermal reversion rate constants of carboxylic acid *Z*-1 and carboxylate *Z*-2' in the temperature range from 213 to 243 K were measured by using the time course experiments of UV-vis spectra at 313 nm. Thermal reversion rate k was obtained from the equation (1). The thermal reversion rate constants were obtained from the slopes of the plots, $ln\ [A_{trans} / (A_{trans} - A(t))]$ versus time(t).

$kt = ln\,[\,A_{trans} / (\,A_{trans} - A\,(t)\,)]$ (1)

A_{trans} : 313 nm optical density of *trans* isomer,

$A\,(t)$: 313 nm optical density at *t* seconds after irradiation was finished

The thermal reversion rate constants of *Z*-1 and *Z*-2' at several temperatures were shown in Table 1. The thermal reversion of carboxylic acid *Z*-1 was faster than that of carboxylate *Z*-2' in the region from 213 to 243 K. This result indicates that the NH···O intramolecular hydrogen bond forming at carboxylate *Z*-2' is stronger than that of carboxylic acid *Z*-1.

Activation energies of thermal reversion of *Z*-1 and *Z*-2' were obtained from the equation (2), so called *Arrhenius's plot*.

$k = A\,EXP(-E / RT)$ (2)

（ *R* : gas constant, *T* : absolute temperature, *E* : activation energy, *A* : frequency factor ）

Table 1 Thermal Reversion Rates from *Z* to *E* Iisomers

Temp. (K)	*Z*-1 / E-1	*Z*-2' / *E*-2'
243	3.1×10^{-2}	1.3×10^{-2}
233	9.5×10^{-3}	3.4×10^{-3}
223	1.9×10^{-3}	5.6×10^{-4}
213	4.0×10^{-4}	1.0×10^{-4}

Crystallographic data of *E*-2

$C_{23}H_{31}N_3O_3$, *Mr* = 397.52, monoclinic, *a* = 16.08(2) Å, *b* = 8.501(8) Å, *c* = 17.00(3) Å, β = 104.5(1) °, *V* = 2249(16) $Å^3$, *T* = 200 ± 1 K, space group $P2_1/n$, *Z* = 4, $\mu(MoK_\alpha)$ = 0.8 cm^{-1}, Total number of reflection measured 21943, unique reflections 5009 (R_{int} = 0.161), Final *R* indices: *R1* = 0.059, *wR2* = 0.103 for all data.

References

[1] T. Asano, H. Furuta, H. J. Hofmann, R. Cimaraglia, Y. Tsuno, M. Fujino, *J. Org. Chem.* **1993**, *58*, 4418-4423.

[2] K. Maeda, K. A. Muszkat, S. S. Ozeri, *J. Chem. Soc., Perkin Trans 2* **1980**, *9*, 1282-1287.

[3] K. Maeda, E. Fischer, *Israel J. Chem.* **1977**, *16*, 294-298.

[4] R. Behrendt, C. Renner, M. Schenk, F. Wang, J. Wachtveitl, D. Oesterhelt, L. Moroder, *Angew. Chem. Int. Ed.* **1999**, *38*, 2771-2774.

[5] A. Momotake, T. Arai, *Tetrahedron Letter* **2003**, 7277-7280.

[6] R. Behrendt, M. Schenk, H. J. Musiol, L. Moroder, *J. Peptide Sci.* **1999**, *5*, 519-529.

[7] Christophe Dugave, L. D. *Chem. Rev.* **2003**, *103*, 2475-2532.

[8] Krzsztof Palczewski, T. K., Tetsuya Hori, Craig A. Behnke, Hiroyuki Motoshima, Barian A. Fox, Isolde Le Trong, David C. Teller, Tetsuji Okada, Ronald E. Stenkamp, Masaki Yamamoto, Masashi Miyano *Science* **2000**, *289*, 739-745.

[9] Tetsuji Okada, Y. F., Maria Silow, Javier Navarro, Ehud M. Landau, Yoshinori Shichida *Proc. Natl. Acad. Sci. USA* **2002**, *99*, 5982-5987.

[10] Babak Borhan, M. L. S., Hiroo Imai, Yoshinori Shichida, Koji Nakanishi *Science* **2000**, *288*, 2209-2212.

[11] Santosh T. Menon, M. H., Thomas P. Sakmar *Phys. Rev.* **2001**, *81*, 1659-1688.

[12] James B. Hurley, T. G. E., Barry Honig, Michael Ottolenghi *Nature* **1977**, *270*, 540-542.

[13] Tchiya Rosenfeld, A. A., Michael Ottolenghi *J. Phys. Chem.* **1974**, *78*, 336-341.

[14] Istvan Szundi, J. W. L., David S. Kliger. *Biochem.* **2003**, *42*, 5091-5098.

[15] Gregory Choi, J. L., Jhenny Flor Galan, Robert R. Birge, Arlene D. Albert, and Philip L. Yeagle *Biochemistry* **2002**, *41*, 7318-7324.

[16] T. Asano, H. Furuta, and H. Sumi, *J. Am. Chem. Soc.*, **1994**, *116*, 5545-5550.

[17] T. Asano, K. Cosstick, H. Furuta, K. Matsuo, and H. Sumi, *Bull. Chem. Soc. Jpn.*, **1996**, *69*, 551-560.

[18] M. Yoshida, and M. Kobayashi, *Bull. Chem. Soc. Jpn.*, **1981**, *54*, 2395-2398.

[19] T. Hugel, N. B. Holland, A. Cattani, L. Moroder, M. Seitz, and H. E. Gaub, *Science*, **2002**, *296*, 1103-1106.

[20] H. Asamura, T. Ito, T. Yoshida, X. Liang, and M. Komiyama, *Angew. Chem. Int. Ed.*, **1999**, *38*, 2393-2395.

[21] N. Kosaka, T. Oda, T. Hiyama, and K. Nozaki, *Macromolecules*, **2004**, *37*, 3159-3164.

[22] K. Nakayama, M. Endo, and T. Majima, *Chem. Commun.*, **2004**, 2386-2387.

[23] T. Schultz, J. Quenneville, B. Levine, A. Toniolo, T. J. Martinez, S. Lochbrunner, M. Schmitt, J. P. Shaffer, M. Z. Zgierski, and A. Stolow, *J. Am. Chem. Soc.*, **2003**, *125*, 8098-8099.

[24] S. Yagai, T. Karatsu, and A. Kitamura, *Chem. Commun.*, **2003**, 1844-1845.

[25] H. horie, T. Sakano, K. Osakada, and H. Nakao, *Organomettalics*, **2004**, *23*, 18-20.

[26] S. Kume, M. Kurihara, and H. Nishihara, *Inorg. Chem.*, **2003**, *42*, 2194-2196.

[27] M. J. Cook, A. M. Nygard, Z. Wang, and D. A. Russell, *Chem. Commun.*, **2002**, *10*, 1056-1057.

[28] M. Kurihara, A. Hirooka, S. Kume, M. Sugimoto, and H. Nishihara, *I. Am. Chem. Soc.*, **2002**, *124*, 8800-8801.

[29] R. Behrendt, M. Schenk, H., J. Musiol, and L. Moroder, *J. Peptide Sci.*, **1999**, *5*, 519-529.

[30] H. Luecke, B. Schobert, H. T. Richter, J. P. Cartailler, and J. K. Lanyi, *Science*, **1999**, *286,* 255-260.

[31] H. Luecke, B. Schobert, H. T. Richter, J. P. Cartailler, and J. K. Lanyi, *J. Mol. Biol.*, **1999**, *291*, 899-911.

[32] *Organic Synthesis*, **1933**, *13*, 28-30.

[33] A. Onoda, Y. Yamada, J. Takeda, Y. Nakayama, T. Okamura, M. Doi, H. Yamamoto, N. Ueyama, *Bull. Chem. Soc. Jpn.* **2004**, *77*, 321-329.

Chapter 3

Manipulation of an intramolecular NH···O hydrogen bond by photoswitching between stable *E*/*Z* isomers of the cinnamate framework

Introduction

Hydrogen bond switching is thought to very important factor for regulation of the enzymatic reaction in native proteins.[1-4] In a previous study, we investigated the effect of the intramolecular NH···O hydrogen bond toward the oxy anion, such as carboxylate and phenolate. We have proposed that the proximity of the amide NH group and the carboxylic oxygen atoms lowers the pK_a value of the corresponding acid by stabilizing the carboxylate with forming the intramolecular NH···O hydrogen bond.[5-21] Therefore, the switching of the intramolecular NH···O hydrogen bond by external stimulation (such as photoirradiation) is expected to realize the control of the pK_a value.

In this chapter, we designed the novel carboxylic acid derivatives, which allow the switching of an intramolecular NH···O distance stimulated by light irradiation (Figure 1). According to this strategy, photoirradiation stimulates the proximity of the amide NH and carboxyl oxygen according to one-way *E*/*Z* photoisomerization of cinnamic acid framework, which allowed forming intramolecular NH···O hydrogen bond in carboxylate, and lowers the pK_a value of carboxylic acid. Photoisomerization, considered one of the most promising strategies for stimulating these compounds, effectively facilitates the control of molecular structures. There are many investigations using photoisomerization for photoswitching devices.[22-47] For example, the effects of intramolecular NH···N or NH···O hydrogen bonds in *Z* form toward *E/Z*

photoisomerization of the C=C double bond,[33-36] as well as the pK_a change of phenol or carboxylic acid derivatives by the switching of conjugation toward photoisomerization,[38-43] have also been investigated. However, to the best of our knowledge, no previous studies have attempted to control the character of carboxylates by switching an NH···O hydrogen bond. In chapter 2, the author examined the *E*/*Z* photoswitchable benzylideneaniline derivatives, which could switch the intramolecular distance between carboxylic oxygen atoms and the amide group, and revealed that the intramolecular NH···O hydrogen bond formed in carboxylate is stronger than that in carboxylic acid. However, because *Z*-benzylideneaniline derivatives are unstable at room temperature,[44-47] it was difficult to determine the acidity after photoisomerization. In this study, novel carboxylic acid derivatives (*E*-1/*Z*-1, *E*-2/*Z*-2), induced the *E*/*Z* photoswitchable cinnamate frame, were synthesized (Scheme 1). High thermal stabilization of *Z* isomers of cinnamate enables us to isolate each conformation and to investigate detailed properties of them.

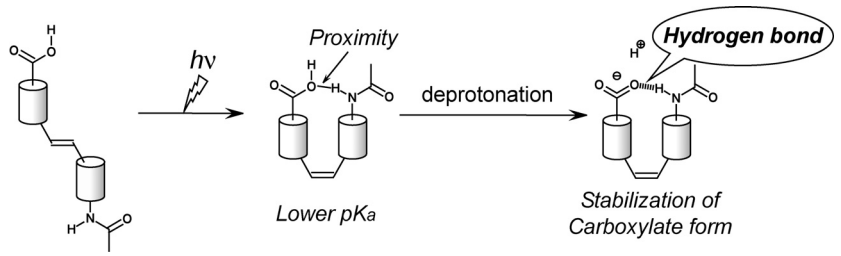

Figure 1. Switching of intramolecular NH···O hydrogen bond by *E*/*Z* photoisomerization of olefin moiety.

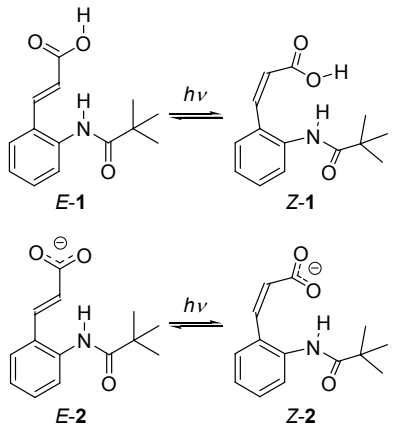

Scheme 1. Photoisomerization equilibriums of cinnamic acid derivatives ***E*-1**/***Z*-1** and ***E*-2**/***Z*-2**

Results and Discussion

Synthesis

Scheme 2 shows the preparation of photoswitching molecules. Cinnamic acid derivative *E*-1 was synthesized using the Heck reaction[48-52] of 2-pivalamidobromobenzene and ethyl propiolate. *E*-2 was prepared through a counter-cation exchange reaction of *E*-1. *Z*-2 was isolated from the photoreaction mixture by recrystallization. *Z*-1 was prepared through an acidification of *Z*-2.

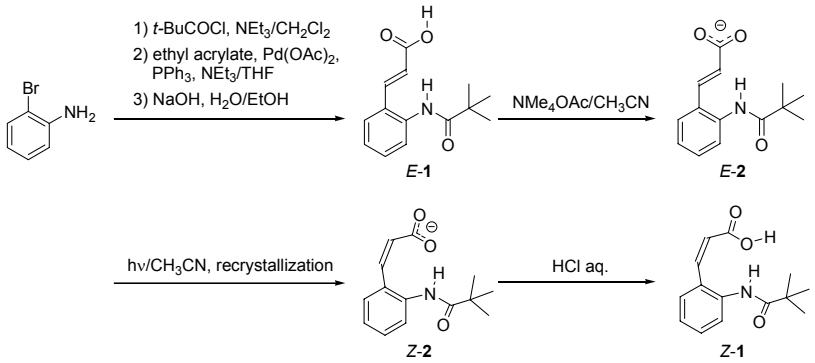

Scheme 2. Synthesis of cinnamic acid derivatives ***E*-1**, ***Z*-1**, ***E*-2** and ***Z*-2**.

Direct photoisomerization of *E*-1 and *E*-2

Photoisomerization of *E*-1 and *E*-2 was traced by UV-visible (UV-vis) spectra. UV-vis spectrum changes of *E*-1 and *E*-2 caused by photoirradiation in dimethyl sulfoxide (DMSO) solution at 293 K are shown in Figure 2. *E*-1 and *E*-2 were isomerized and reached the photostationary state (PSS) at 313 nm UV-light irradiation. Solid lines, corresponding to *E* isomers, are the spectrum measured before irradiation, and broken lines represent the isolated pure *Z* isomers. The absorbance values of *E*-1 and *E*-2 are decreased in accordance with the two-state transition toward irradiation (dotted lines), which indicates that only corresponding *Z* isomers are formed without

any side reactions. The contents of *Z* compounds in the PSS were determined from the integration ratio of ^{1}H NMR spectra. The *E*/*Z* ratio of carboxylate is 7/93, whereas that of carboxylic acid is 25/75. It is difficult to cause the effective *Z* to *E* isomerization in DMSO solution. *Z* compounds are stable for heating, even at 363 K, and there is no suitable wavelength for irradiation which *Z* compounds are preferencially excited. *Z*-1 in chloroform solution allows about 10% of *E*/*Z* photocycle using 254 and 313 nm alternative irradiatoin with decaying by photo-decarbonation (Figure 3).

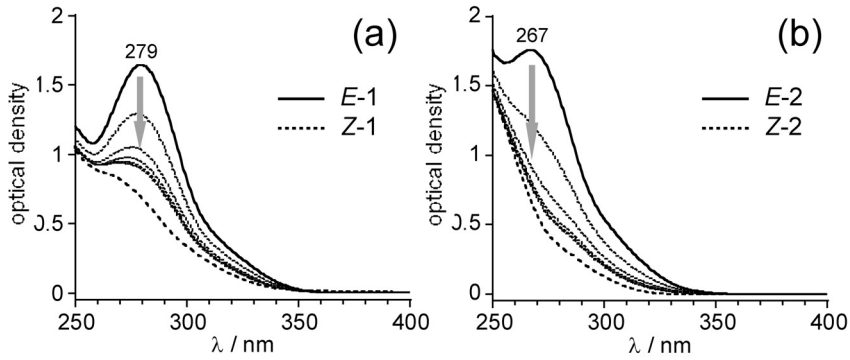

Figure 2. Time course UV-vis spectra changes of ***E*-1** and ***E*-2** toward photoirradiation at 313 nm, 1 mM in DMSO at 293 K.

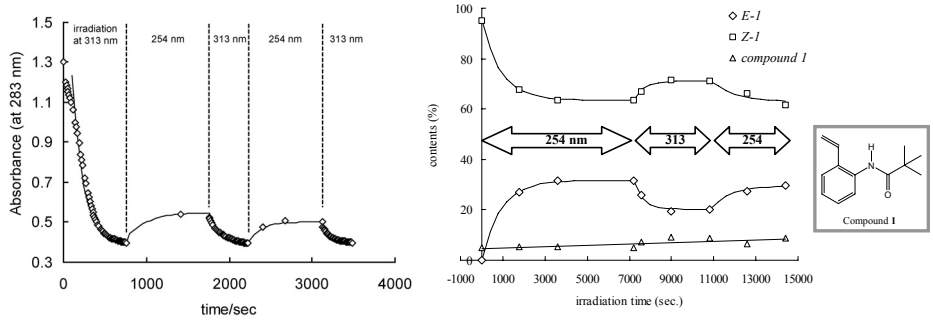

Figure 3. Left) Absorbance change at 283 nm of ***E*-1** imM in chloroform solution traced by UV-vis spectrum at 293 K, Right) Contents change (started from 95% ***Z*-1**) 10 mM in chloroform-*d* solution at 303 K, on alternationg irradiation at λ = 313 and 254 nm.

Molecular structures in solution

The structures in DMSO-d_6 solution of isolated *Z*-1 and *Z*-2 were determined by ^{1}H NMR spectra. The ^{1}H NMR spectra of *E*-1, *E*-2, *Z*-1, and *Z*-2 in DMSO-d_6 at 303 K are shown in Figure 4. All signals were assigned using the nuclear Overhauser effect (NOE) method and the decoupling method. *E*/*Z* configurations of these compounds were confirmed by the $^3J_{HH}$ value of the olefin protons. Generally speaking, the $^3J_{HH}$ coupling constant of olefin protons is about 15 to 16 Hz in the *trans* position and about 12 to 13 Hz in the *cis* position. Observed $^3J_{HH}$ values of the olefin protons of *E*-1 and *E*-2 were 16.0 Hz, whereas those of *Z*-1 and *Z*-2 were 12.5 and 12.7 Hz, respectively. These observed $^3J_{HH}$ values coincide with the typical values of the *trans* and *cis* olefin protons. The configurations of the compounds before irradiation were confirmed to the *E* form, and the photoproducts were confirmed to the *Z* form.

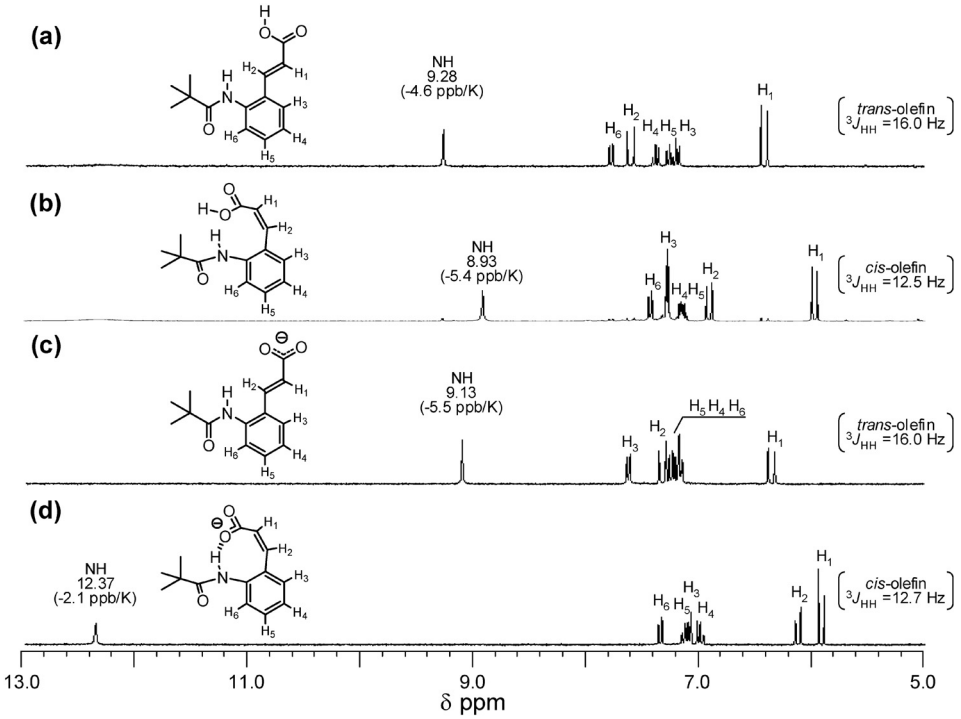

Figure 4. ^{1}H NMR spectra of a) ***E*-1**, b) ***Z*-1**, c) ***E*-2** and d) ***Z*-2**, 5 mM in DMSO-d_6 at 303 K

The structures in solution of carboxylates are estimated based on the nuclear Overhauser enhancement spectroscopy (NOESY) spectra of *E*-2 and *Z*-2 (Figure 5). An NOE correlation between NH and H2 was observed in *E*-2, but no NOE signal was observed between NH and H1 (Figure 5a). This result indicates that the olefin moiety is likely to take the opposite direction toward the amide moiety in *E*-2 (s-*trans* form). In *Z*-2, an NOE correlation between H1 and H2, which was not observed in *E*-2, was characteristically observed (Figure 5b). This correlation confirms that the configuration of photoproduct *Z*-2 was definitely in *Z* form. The correlations of NH-H1 and NH-H2 in *Z*-2 were weaker than that of NH-H6 or H2-H3. This result indicates that the olefin moiety in *Z*-2 is likely to take the same direction toward the amide side (s-*cis* form) and that the carboxylate is in close proximity to the amide moiety.

The chemical shifts of the amide NH signals of *Z* isomers at 303 K were 8.93 ppm in *Z*-1 and 12.37 ppm in *Z*-2 (Figure 4). The significant downfield shift ($\Delta\delta$ = 3.44 ppm) suggests that *Z*-2 forms an NH···O hydrogen bond in DMSO-d_6 solution. The temperature dependency (range, 303-333 K) of the amide NH chemical shift of *Z*-2 is –2.1 ppb·K^{-1}, whereas that of *Z*-1 is –5.4 ppb·K^{-1}. The downfield shift and the decrease in the temperature coefficient of the NH proton suggest that *Z*-2 forms an intramolecular NH···O hydrogen bond in DMSO-d_6 solution.

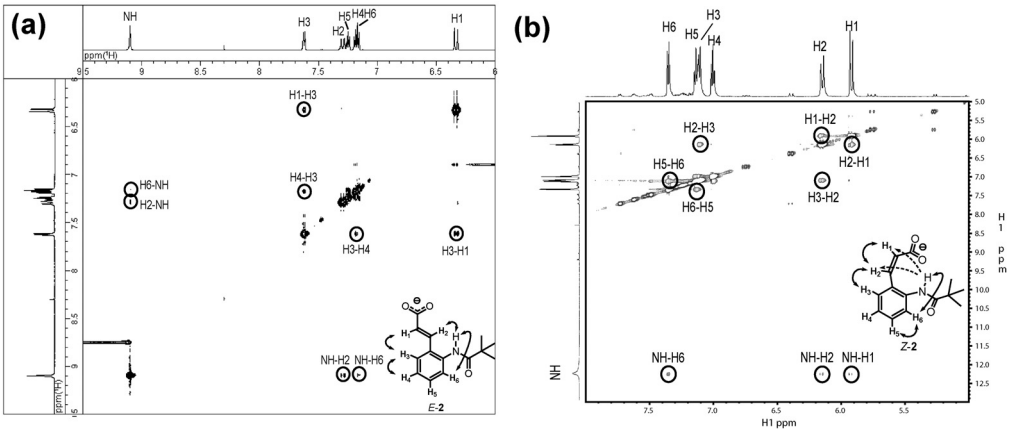

Figure 5. NOESY spectra of a) ***E*-2** and b) ***Z*-2**, 5 mM in DMSO-d_6 at 303 K

Molecular structures in solid state

To confirm the molecular structures in solid state, X-ray crystallography was performed. The crystal structures of *E*-1 and *Z*-2 are shown in Figure 6. Crystal data of *E*-1 and *Z*-2 were shown in the experimental section. All non-hydrogen atoms were refined anisotropically. The coordinates of OH and NH protons were refined using fixed thermal factors, and the other protons were placed in calculated positions. The intramolecular O01···N1 distance (4.854 Å) and the intermolecular O'03···N1 distance (3.235[2] Å) of *E*-1 are too long to form hydrogen bonds; the amide NH of *E*-1 is free from any electrostatic interaction in solid state (O'03 indicates O03 atom at equivalent position [x−1, y, z]). The intermolecular O02···O'01 distance (2.632 Å) of *E*-1 permitted sufficient hydrogen bond formation; the dimerization of carboxylic acid stabilizes the packing structure (O'01 indicates O01 atom at equivalent position [−x, −y+1, −z+1]). The torsion angles of O02-C1-C2-C3 (−3.4[4]°) and C2-C3-C4-C5 (2.6[4]°) indicate that the cinnamic acid frame of *E*-1 is almost in plane. However, the amide moiety is leaning away from this cinnamic acid plane (the torsion angle of C8-C9-N1-C10 is 36.0[3]°). These results inferred that the π-conjugation extends from the aromatic ring toward carboxylic oxygen through the C=C double bond. In contrast, the distances of N1···O1 (2.701[1] Å) and H1···O1 (1.88[1] Å) of *Z*-2 permitted sufficient hydrogen bond formation. The N1-H1-O1 angle of *Z*-2 (154[1]°) is appropriate for hydrogen bonding. These results indicate that *Z*-2 has an intramolecular NH···O hydrogen bond that forms an eight-membered ring structure in the solid state.

On the other hand, no intermolecular interactions (e.g., hydrogen bonding) were detected in *Z*-2. Both of the C···O distances of carboxylate *Z*-2, C1···O1 (1.255[2] Å) and C1···O2 (1.246[2] Å), are virtually identical, whereas C···O distances of carboxylic acid *Z*-1 are C1···O01 (1.281[2] Å) and C1···O02 (1.262[2] Å). The torsion angles of O1-C1-C2-C3 (37.7[2]°), C2-C3-C4-C9 (−65.7[2]°), and C8-C9-N1-C10 (49.5[3]°) are so large that the π-conjugation of cinnamic acid extended in *E*-1 is interrupted in *Z*-2. Solid Fourier transform infrared (FT-IR) spectra of the crystals of *E*-1 and *Z*-2 were measured to determine the existence of an intramolecular NH···O hydrogen bond in *Z*-2. *Z*-2 exhibits the ν (NH) band at 3281 cm^{-1}, whereas the ν (NH) band appears at 3386 cm^{-1} in *E*-1. The low wavenumber shift of the ν (NH) band indicates the presence of a hydrogen bond in *Z*-2. These combined experimental results obtained by X-ray crystallography and FT-IR spectroscopy indicate that *Z*-2 forms an intramolecular NH···O hydrogen bond in crystal.

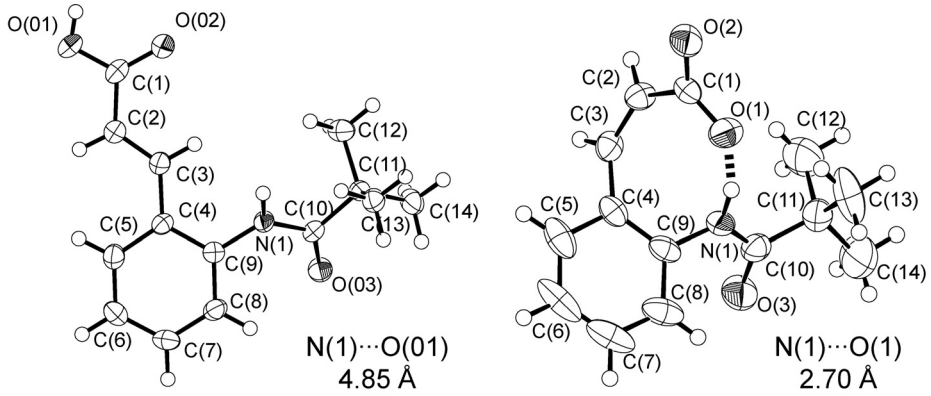

Figure 6. Molecular structures of ***E*-1** (left) and ***Z*-2** (right), 50 % probability

Table 1 Distances and torsion angles of X-ray crystal structure of ***E*-1** and ***Z*-2**

	E-1		*Z*-2
distances (Å)		distances (Å)	
C1-O01, C1-O02	1.281[2], 1.262[2]	C1-O01, C1-O02	1.255[2], 1.246[2]
N1-O3	4.854	N1-O3	2.701[1]
torsion angles (°)		torsion angles (°)	
O02-C1-C2-C3	-3.4[4]	O1-C1-C2-C3	37.7[2]
C2-C3-C4-C9	2.6[4]	C2-C3-C4-C9	-65.7[2]
C8-C9-N1-C10	36.0[3]	C8-C9-N1-C10	49.5[3]

Acidity change through photoisomerization

The pK_a values of *E*-1 and *Z*-1 were measured by potentiometric titration in a 10% Triton X-100 aqueous micellar solution at 298 K. The pK_a value of *Z*-1 was 4.3, which was 0.5 units lower than that of *E*-1 (pK_a = 4.8) (supporting information). When the pK_a value was changed by photoisomerization, the pH value would also be changed. The pH change of *E*-1 by 313 nm photoirradiation in Triton® X-100 aqueous micellar solution at

298 K is shown in Figure 7. In conjugation with the *E* to *Z* photoisomerization, the pK_a value of carboxylic acid was decreased, and the pH value was also decreased from 3.51 to 3.29 (Δ pH = 0.22). This decrease of pH value corresponds to the increase of proton concentration (1.66 times higher).

To discuss the change of acidity in organic solvents, the counter-cation exchange reaction was examined. The difference of pK_a values in organic solvents is determined using the following method. If two acids, AH and BH, are in equilibrium (including the deprotonation process), the equilibrium equation is drawn in equation 1, assuming that all anions have dissociated. The acid dissociation constants of AH and BH are defined as $K_a(1)$ and $K_a(2)$, respectively. The equilibrium constant, $K_{eq,}$ is indicated in equation 2, where K_{eq} is equal to the ratio of acid dissociation constants of AH and BH. The Δ pK_a (= log K_{eq}) value is calculated from $[A^-]/[AH]$ and $[BH]/[B^-]$.

$$AH + B^- \overset{K_{eq}}{\rightleftharpoons} A^- + BH \quad \cdots\cdots \quad ①$$

$$K_{eq} = \frac{[A^-][BH]}{[AH][B^-]} = \frac{[A^-][H^+]}{[AH]} \times \frac{[BH]}{[H^+][B^-]} = \frac{K_a(1)}{K_a(2)} \quad \cdots\cdots \quad ②$$

Carboxylic acid [AH] and carboxylate $[B^-]$ are mixed in DMSO-d_6 solution, and the equilibrium constant is confirmed from the chemical shifts of ^{1}H NMR spectra. Figure 8 shows the ^{1}H NMR spectrum of the mixture of *E*-1 and *Z*-2 in DMSO-d_6 solution. Signals are shifted by mixing, which means that ion exchange reactions have occurred. The deprotonation ratio was estimated by comparing the authentic signals of carboxylic acids and carboxylates. Using the chemical shift of the olefin protons (H2), it was possible to calculate the deprotonation ratio precisely because the signals were sharp and isolated. The chemical shift of the olefin proton of *E* compound was closer to the chemical shift of carboxylic acid *E*-1 than of carboxylate *E*-2, and that of *Z* compound was closer to the *Z*-2 than the *Z*-1. By comparing with the chemical shifts of isolated carboxylic acids and carboxylates, it is estimated that 83% of *E* compound is protonated and that 90% of *Z* compound is deprotonated. According to the results and equation 2, the pK_a value of the *E* compound is 1.63 units lower than the pK_a value of the *Z* compound in DMSO solution.

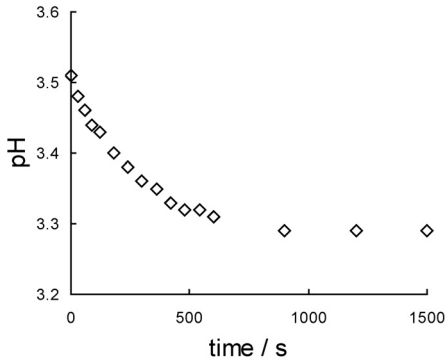

Figure 7. pH change of 10 mM ***E*-1** by 313 nm photoirradiation in 10 % Triton® X-100 aqueous micellar solution at 278 K

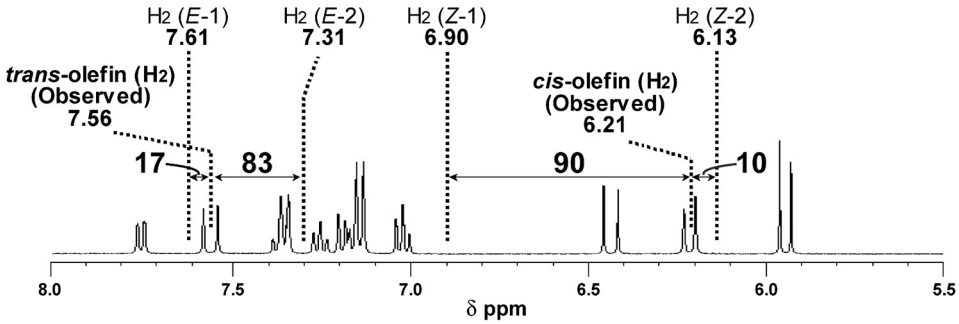

Figure 8. ^{1}H NMR spectrum of the mixture of ***E*-1** and ***Z*-2** in DMSO-d_6 solution at 303 K

Conclusion

In this chapter, one-way photoswitching of the intramolecular NH···O hydrogen bond by using *E* to *Z* photoisomerization of cinnamic acid framework was achieved. We synthesize the carboxylic acid *E*-1/*Z*-1 and carboxylate *E*-2/*Z*-2 derivatives, which have a photoinduced cinnamate frame so as to switch the intramolecular distance between amide NH and carboxylic oxygen atoms by using photoisomerizaization. According to the 313 nm UV light irradiation, *E* to *Z* photoisomerization was progressed. Since *Z* cinnamate compound is thermally stable, *Z*-1 and *Z*-2 are isolated from the mixture of photoisomers. *Z*-2 forms an intramolecular NH···O hydrogen bond both in DMSO-d_6 solution and in solid state. The pK_a value of *Z*-1 was lower than that of *E*-1, not only in an aqueous micellar solution but also in DMSO solution. We propose that the

intramolecular NH···O hydrogen bond formed in carboxylate *Z*-2 encourages the deprotonation process and lowers the pK_a value of the corresponding carboxylic acid *Z*-1.

Experimental

General procedures

All manipulations involving air- and moisture-sensitive compounds were carried out by the use of standard Schlenk technique under argon atmosphere. 2-bromoaniline, 2,2-dimethyl-propyonyl chloride, triphenylphosphine, acrylic acid ethyl ester were purchased from Tokyo-Kasei Co. Palladium acetate, tetramethylammonium acetate were purchased from Aldrich Chemical Company, Inc. Dichloromethane was distilled over CaH_2. Tetrahydrofuran was distilled over CaH_2 and dried over Na. Ethanol, and Acetonitrile were distilled over CaH_2 and dried over molecular sieves (3A).

Physical measurements

^{1}H (270 MHz) NMR spectra were measured on a JEOL JNM-GSX270 spectrometer. NOESY spectra were measured on a Varian UNITYplus 600 MHz spectrometer. The ^{1}H NMR spectra were referenced to the tetramethylsilane protons at δ 0.00. UV-vis spectra was measured on a Shimazu UV-3100PC spectrometer. Elemental Analysis was performed at Elemental Analysis Center, Faculty of Science, Osaka University. All melting points of the compounds were measured on a micro melting point apparatus of YANAGIMOTO Co. ESI-MS measurements were performed on a Finnigan MAT LCQ ion trap mass spectrometer. FT-IR spectra were measured on a JASCO FT/IR-8300 spectrometer, and the solid FT-IR measurement was performed in KBr glass cell with nujol. pK_a measurement was performed using a potentiometric titration in 10 mM micellar solution at 298 K with a Metrohm 716 DMS titrino whtich is combined with Metrohm 728 stirrer and a saturated calomel LL micro pH glass electrode. The saturated calomel micro glass electrode was calibrated with the 0.05 M $KHC_8H_4O_4$ buffer (pH = 4.01) and the 0.0025 M KH_2PO_4 buffer (pH = 6.86) at 298 K. The potentiometric titration was performed three times. pK_a values are estimated by an average value of each measurements.

Preparation of 2-pivaloylamino-bromobenzene

To a solution of 2-bromoaniline (23.5 g, 0.138 mol) and triethylamine (25 mL, 0.18 mol) in

distilled dichloromethane (150 mL) was added a solution of 2,2-dimethyl-propyonyl chloride (16 mL, 0.13 mol) in distilled dichloromethane (50 mL) solution in ice bath. White solid precipitated in orange solution. The mixture was stirred for 21h at room temperature. White solid was filtered off and solution was evaporated to obtain brown oil with a white powder. The mixture was dissolved in diethylether and washed with 2% aqueous hydrochloride, 4% aqueous sodium bicarbonate, water, and brine. Organic layer was dried over anhydrous magnesium sulfate and solvent was removed under reduced pressure to obtain white crystals. (31.2 g, 94 %) m.p. 60-63 ^{o}C; (Found: C, 51.59; H, 5.36; N, 5.57. Calc. for $C_{11}H_{14}BrNO$: C, 51.58; H, 5.51; N, 5.47 %); δ_H(270 MHz; DMSO-d_6) 1.22 (s, 9H; *tert*-Butyl), 7.13 (dt, ^3J(H,H)=7.6 Hz, ^4J(H,H)=1.8 Hz, 1H; Aryl), 7.37 (dt, ^3J(H,H)=7.6 Hz, ^4J(H,H)=1.5 Hz, 1H; Aryl), 7.49 (dd, ^3J(H,H)=7.6 Hz, ^4J(H,H)=1.8 Hz, 1H; Aryl), 7.64 (dd, ^3J(H,H)=7.6 Hz, ^4J(H,H)=1.5 Hz, 1H; Aryl), 8.92 ppm (s, 1H; NH); *m/z* (ESI) 277.9, 279.9 ($[M+Na]^+$ requires 278.0, 280.0).

Preparation of (*E*)-3-(2-pivaloylaminophenyl) acrylic acid ethyl ester

To a two-necked round bottom flask was added acrylic acid ethyl ester (4.35 mL, 4.00 g, 40.0 mmol), 2-pivaloylamino-bromobenzene (5.12 g, 20.0 mmol), palladium acetate (0.133 g, 0.592 mmol), and triphenylphosphine (0.126 g, 0.48 mmol), then suspended in triethylamine/tetrahydrofuran (13.2/10.0 mL, distilled). The mixture was refluxed for 63 h at 110 ^{o}C. The reaction was traced by TLC (ethyl acetate/hexane=1/3; v/v) and by ^{1}H NMR spectrum. The mixture was concentrated to obtain black and white precipitates in orange oil. The mixture were suspended in tetrahydrofuran, and the catalyst was filtered off. The solvent was removed under reduced pressure to obtain orange oil. By TLC and by ^{1}H NMR spectrum, it was confirmed that the orange oil obtained was a mixture of the objective ((*E*)-3-(2-pivaloylaminophenyl) acrylic acid ethyl ester) and reactant (2-pivaloylamino-bromobenzene). The crude products were used for next reaction without further purification.

Preparation of (*E*)-3- (2-pivaloylaminophenyl) acrylic acid (*E*-1)

To a round bottom flask was added the all products that is obtained above reaction (the mixture of 2-pivaloylamino bromobenzene and (*E*)-3- (2-pivaloylaminophenyl) acrylic acid ethyl ester). The oil was dissolved in ethanol (40 mL). 1 M aqueous sodium hydroxide (40 mL, 0.040 mol) was added, and the solution turned to a white suspension. Ethanol (20 mL) was added to dissolve precipitate. The solution was stirred for 24h at room temperature. The reaction was traced by TLC (ethyl acetate/hexane=1/3; v/v). The solution was concentrated to white suspension. Saturated aqueous sodium bicarbonate was added and the suspension was extracted with diethylether. Organic layer was extracted with 4% aqueous sodium bicarbonate for 3 times. Combined aqueous layer was acidified by ice-cooled aqueous sulfuric acid (pH 2~3). Oil-like

white powder floated on white suspension. The suspension was extracted with ethyl acetate, and organic layer was washed with water and with brine. The solution was dried over anhydrous magnesium sulfate. The solvent was removed under reduced pressure to obtain white powder. (1.81 g, 36.6 %) m.p. 178-179 °C; (Found: C, 67.81; H, 6.88; N, 5.72. Calc. for $C_{14}H_{17}NO_3$: C, 68.00; H, 6.93; N, 5.66 %); δ_H(270 MHz; DMSO-d_6) 1.24 (s, 9H; *tert*-Butyl), 6.43 (d, ^3J(H,H)=16.0 Hz, 1H; olefin), 7.19 (dd, ^3J(H,H)=7.8 Hz, ^4J(H,H)=1.2 Hz, 1H; Aryl), 7.26 (dt, ^3J(H,H)=7.8 Hz, ^4J(H,H)=1.2 Hz, 1H; Aryl), 7.39 (dd, ^3J(H,H)=7.8 Hz, ^4J(H,H)=1.6 Hz, 1H; Aryl), 7.62 (d, ^3J(H,H)=16.0 Hz, 1H; olefin), 7.79 (dd, ^3J(H,H)=7.8 Hz, ^4J(H,H)=1.6 Hz, 1H; Aryl), 9.28 (s, 1H; NH), 12.25 ppm (br s, 1H, COOH); *m/z* (ESI) 246.1 ($[M-H]^-$ requires 246.1), 270.3 ($[M + Na]^+$ requires 270.1).

Preparation of [tetramethyl-ammonium](*E*)-3- (2-pivaloylaminophenyl) acrylate (*E*-2)

Tetramethylammonium acetate (53.8 mg, 0.404 mmol) was dissolved in distilled acetonitrile (2 mL). To the solution was added dropwise a solution of (*E*)-3- (2-pivaloylaminophenyl) acrylic acid (100 mg, 0.404 mmol) in distilled acetonitrile (4 mL) using syringe technique. The solution was stirred for several hours, and the solvent was removed under reduced pressure to obtain orange oil. Adding diethylether turns the oil to the gray powder. Supernatant solution was removed and the residue was dried under reduced pressure to obtain gray powder. Yield was not confirmed. δ_H(270 MHz; DMSO-d_6) 1.24 (s, 9H; *tert*-Butyl), 3.09 (s, 12H; NMe_4), 6.33 (d, ^3J(H,H)=16.0 Hz, 1H; olefin), 7.17 (dt, ^3J(H,H)=7.5 Hz, ^4J(H,H)=1.8 Hz, 1H; Aryl), 7.18 (dt, ^3J(H,H)=7.5 Hz, ^4J(H,H)=1.8 Hz, 1H; Aryl), 7.24 (dd, ^3J(H,H)=7.5 Hz, ^4J(H,H)=1.8 Hz, 1H; Aryl), 7.30 (d, ^3J(H,H)=16.0 Hz, 1H; olefin), 7.62 (dd, ^3J(H,H)=7.5 Hz, ^4J(H,H)=1.8 Hz, 1H; Aryl), 9.10 ppm (s, 1H; NH).

Preparation of [tetramethyl-ammonium](*Z*)-3- (2-pivaloylaminophenyl) acrylate (*Z*-2)

To a acetonitrile solution of [tetramethylammonium](*E*)-3-(2-(pivaloylamino)phenyl) acrylate (100 mg) was irradiated by Xe/Hg arc lamp with 313 nm band pass filter for several hours. The content of *Z* isomers were confirmed by ^{1}H NMR spectrum to ensure the photoreaction reached to photostationary state (>80% was *Z* isomer). The solvent was removed under reduced pressure. The obtained powder was recrystallized from hot acetonitrile. The colorless needle crystal was obtained. The crystal was washed with little amount of acetonitrile and with diethylether. Yield was not certain. δ_H(270 MHz; DMSO-d_6) 1.17 (s, 9H; *tert*-Butyl), 3.08 (s, 12H; NMe_4), 5.92 (d, ^3J(H,H)=12.7 Hz, 1H; olefin), 6.13 (d, ^3J(H,H)=12.7 Hz, 1H; olefin), 7.00 (dt, ^3J(H,H)=7.6 Hz, ^4J(H,H)=1.4 Hz, 1H; Aryl), 7.09 (dd, ^3J(H,H)=7.6 Hz, ^4J(H,H)=1.4 Hz, 1H; Aryl), 7.13 (dt, ^3J(H,H)=7.6 Hz, ^4J(H,H)=1.4 Hz, 1H; Aryl), 7.36 (dd, ^3J(H,H)=7.6 Hz, ^4J(H,H)=1.4 Hz, 1H; Aryl), 12.37 ppm (s, 1H; NH).

Preparation of (*E*)-3- (2-pivaloylaminophenyl) acrylic acid (*Z*-1)

The crystal of [tetramethylammonium] (*Z*)-3-(2-pivalamidophenyl) acrylate (186.7 mg, 0.476 mmol) was suspended in ethyl acetate. To the suspension was acidified by adding 2% aqueous hydrochloride, then organic layer turned to a clear solution. The aqueous layer was extracted with ethyl acetate twice, and the combined organic layer was dried over anhydrous magnesium sulfate. The solvent was removed under reduced pressure to obtain colorless oil. The oil was reprecipitated from diethylether/*n*-hexane to obtain white powder. Yield 117.8 mg (81.8 %). m.p. 125 ^{o}C; (Found: C, 66.93; H, 6.99; N, 5.58. Calc. for $C_{14}H_{17}NO_3 \cdot (H_2O)_{0.2}$: C, 67.02; H, 6.99; N, 5.55 %); δ_H(270 MHz; DMSO-d_6) 1.20 (s, 9H; *tert*-Butyl), 5.98 (d, ^3J(H,H)=12.5 Hz, 1H; olefin), 6.91 (d, ^3J(H,H)=12.5 Hz, 1H; olefin), 7.14 (dt, ^3J(H,H)=7.5 Hz, ^4J(H,H)=1.3 Hz, 1H; Aryl), 7.17 (dt, ^3J(H,H)=7.5 Hz, ^4J(H,H)=1.3 Hz, 1H; Aryl), 7.29 (dd, ^3J(H,H)=7.5 Hz, ^4J(H,H)=1.3 Hz, 1H; Aryl), 7.44 (dd, ^3J(H,H)=7.5 Hz, ^4J(H,H)=1.3 Hz, 1H; Aryl), 8.94 (s, 1H; NH), 12.29 ppm (br s, 1H, COOH); *m/z* (ESI) 246.1 ($[M-H]^-$ requires 246.1), 270.1 ($[M + Na]^+$ requires 270.1).

Crystallographic Data Collections and Structure Determinations of *E*-1 and *Z*-2

A suitable single crystals of *E*-1 and *Z*-2 were mounted on a fine nylon loop with nujol and immediately freezed at 200±1 K. All measurements were performed on a Rigaku RAXIS-RAPID Imaging Plate differactometer with graphite monochromated MoKα radiation (λ = 0.71075 Å). The structures were solved by direct method (SIR 92) [53] and the following refinements were performed using SHELXL-97 [54] and teXsan crystallographic software package. All non-hydrogen atoms were refined anisotropically. The coordinates of OH and NH protons were refined by using fixed thermal factors, and the other protons were placed in calculated position. Crystal data for $C_{14}H_{17}NO_3$ (*E*-1): 0.30x0.20x0.10 mm^3, triclinic, $P\bar{1}$ (#2), a = 5.334(4) Å, b = 9.149(7) Å, c = 13.95(1) Å, α = 74.60(3) ^{o}, β = 80.12(3) ^{o}, γ = 82.77(2) ^{o}, V = 644(3) Å^3, Z = 2, ρ_{calcd} = 1.275 g cm^{-3}, μ(MoK$_\alpha$) = 0.89 cm^{-1}, M_w = 247.29. Total number of reflection measured 6238, unique reflections 2885 (R_{int} = 0.031), Final R indices: R_1 = 0.043, wR_2 = 0.120 for all data. GOF (F^2) = 0.86. Crystal data for $C_{18}H_{28}N_2O_3$ (*Z*-2): 0.30x0.20x0.20 mm^3, hexagonal, $P6_3$ (#173), a = 21.127(5) Å, c = 7.522(2) Å, V = 2907(4) Å^3, Z = 6, ρ_{calcd} = 1.098 g cm^{-3}, μ(MoK$_\alpha$) = 0.74 cm^{-1}, M_w = 320.43. Total number of reflection measured 27898, unique reflections 27887 (R_{int} = 0.039), Final R indices: R_1 = 0.041, wR_2 = 0.098 for all data. GOF (F^2) = 1.03. CCDC 603981 and CCDC 603982 contain the supplementary crystallographic data for this paper. These data can be obtained free of charge from Cambridge Crystallographic Data Centre via www.ccdc.cam.ac.uk/data_request/cif.

UV-light irradiation technique for UV-vis and ^{1}H NMR spectrum measurement

Xe/Hg lamp (MUV-202U, Moritex Co.) was used for 313 nm UV-light irradiation. UV-light

was filtered through 6784-t01.uv1 (Asahi tech.) to pick out the 313 nm emission line of Hg gas. TLC lamp was used for 254 nm UV-light irradiation, and UV-light was filtered through a solution filter (aqueous solution of $NiSO_4$, $CoSO_4$ and KI/I_2). Sample was dissolved in the degassed solvent under argon atmosphere and sealed in quarts NMR tube or UV cell. The spectrum was measured before and after irradiation. During irradiation and spectrum measurements, the sample was always kept desired temperature.

Potentiometric titration

pK_a measurements were performed in 10% Triton X-100 aqueous micellar solution at 278 K. The preparation of micellar solutions is as follows. A carboxylic acid derivative (50 μmol) in 5.0 mL of distilled THF solution. To the THF solution was added 0.50 mL of Triton X-100 and stirred for several minutes. The solution was concentrated to remove THF and the residue was added to 4.5 mL of 10 mM sodium perchlorate. The potentiometric titration was performed three times, and pK_a values are estimated by an average value of each measurements.

pH change trace method through photoisomerization

The preparation of micellar solution of carboxylic acid and the measurement of pH value was performed by the same method of potentiometric titration. The pH value through irradiation was measured in temperature controlled bath with persevered stirring.

References

[1] G. O. Borgstahl, D. R. Williams, E. D. Getzoff, *Biochemistry* **1995**, *34*, 6278-6287.

[2] A. Warshel, *Biochemistry* **1981**, *20*, 3167-3177.

[3] Y. Imamoto, M. Kataoka, F. Tokunaga, T. Asahi, H. Masuhara, *Biochemistry* **2001**, *40*, 6047-6052.

[4] Y. Imamoto, Y. Shirahige, F. Tokunaga, T. Kinoshita, K. Yoshihara, M. Kataoka, *Biochemistry* **2001**, *40*, 8997-9004.

[5] A. Onoda, Y. Yamada, J. Takeda, Y. Nakayama, T. Okamura, M. Doi, H. Yamamoto, N. Ueyama, *Bull. Chem. Soc. Jpn.* **2004**, *77*, 321-329.

[6] A. Onoda, Y. Yamada, Y. Nakayama, K. Takahashi, H. Adachi, T. Okamura, A. Nakamura, H. Yamamoto, N. Ueyama, D, Vyprachticky, Y. Okamoto, *Inorg. Chem.* **2004**, *43*, 4447-4455.

[7] N. Ueyama, K. Takahashi, A. Onoda, T. Okamura, H. Yamamoto, *Macromol. Symp.* **2003**, *204*, 287-294.

[8] D. Kanamori, T. Okamura, H. Yamamoto, N. Ueyama, *Angew. Chem. Int. Ed.* **2005**, *44*, 969-972.

[9] D. Kanamori, A. Furukawa, T. Okamura, H. Yamamoto, N. Ueyama, *Otg. Biomol. Chem.* **2005**, *3*, 1453-1459.

[10] D. Kanamori, Y. Yamada, A. Onoda, T. Okamura, S. Adachi, H. Yamamoto, N. Ueyama, *Inorg. Chim. Acta.* **2005**, *358*, 331-338.

[11] K. Takahashi, M. Doi, A. Kobayashi, T. Taguchi, A. Onoda, T. Okamura, H. Yamamoto, N. Ueyama, *J. Cryst. Growth* **2004**, *263*, 552-563.

[12] N. Ueyama, K. Takahashi, A. Onoda, T. Okamura, H. Yamamoto, *Macromol. Symp.* **2002**, *186*, 129-134.

[13] N. Ueyama, H. Kozuki, M. Doi, Y. Yamada, K. Takahashi, A. Onoda, T. Okamura, H. Yamamoto, *Macromolecules* **2001**, *34*, 2607-2614.

[14] A. Onoda, Y. Yamada, M. Doi, T. Okamura, N. Ueyama, *Inorg. Chem.* **2001**, *40*, 516-521.

[15] T. Okamura, S. Takamizawa, N. Ueyama, and A. Nakamura, *Inorg. Chem.*, **1998**, *37*, 18-28.

[16] T. Okamura, N. Ueyama, A. Nakamura, E. Ainscough, A. M. Brodiem and J. M. Waters, *J. Chem. Soc. Chem. Comun.*, **1993**, *21*, 1658-1660.

[17] W. Y. Sun, N. Ueyama, A. Nakamura, *Inorg. Chem.*, **1991**, *30*, 4026-4031

[18] N. Ueyama, T. Okamura, and A. Nakamura, *J. Chem. Soc. Chem. Comun.*, **1992**, *14*, 1019-1020.

[19] N. Ueyama, T. Okamura, and A. Nakamura, *J. Am. Chem. Soc.*, **1992**, *114*, 8129-8137.

[20] N. Ueyama, Y. yamada, T. Okamura, S. Kimura, and A. Nakamura, *Inorg. Chem.*, **1996**, *35*, 6473-6484.

[21] N. Ueyama, T. Terakawa, M. Nakata, and A. Nakamura, *J. Am. Chem. Soc.*, **1983**, *105*, 7098-7102.

[22] M. Irie, T. Fukaminato, T. Sasaki, N. Tamai, T. Kawai, *Nature* **2002**, *420*, 759-760.

[23] M. Irie, O. Miyatake, K. Uchida, T. Eriguchi, *J. Am. Chem. Soc.* **1994**, *116*, 9894-9900.

[24] J. Hayakawa, A. Momotake, T. Arai, *Chem. Commun.* **2003**, 94-95.

[25] J. Hayakawa, A. Momotake, R. Nagahata, T. Arai, *Chem. Lett.* **2003**, *32*, 1008-1009.

[26] H. Tatewaki, T. Mizutani, J. Hayakawa, T. Arai, M. Tarazima, *J. Phys. Chem. A* **2003**, *107*, 6515-6521.

[27] J. H. Yoo, I. Cho, S. Y. Kim, *J. Polym. Sci. part A: Polym. Chem.* **2004**, *42*, 5401-5406.

[28] O. Ohtani, R. Sasai, T. Adachi, I. Hatta, K. Takagi, *Langmuir* **2002**, *18*, 1165-1170.

[29] R. Behrendt, C. Renner, M. Schenk, F. Wang, J. Wachtveitl, D. Oesterhelt, L. Moroder, *Angew. Chem. Int. Ed.* **1999**, *38*, 2771-2774.

[30] R. Behrendt, M. Schenk, H. J. Musiol, L. Moroder, *J. Peptide Sci.* **1999**, *5*, 519-529.

[31] S. Kobatake, S. Takami, H. Muto, T. Ishikawa, M. Irie, *Nature* **2007**, *446*, 778-781.

[32] F. D. Lewis, B. A. Yoon, T. Arai, T. Iwasaki, K. Tokumaru, *J. Am. Chem. Soc.* **1995**, *117*,

3029-3036.

[33] T. Arai, M. Moriyama, K. Tokumaru, *J. Am. Chem. Soc.* **1994**, *116*, 3171-3172.

[34] A. Masumoto, K. Maeda, T. Arai, *J. Phys. Chem. A* **2003**, *107*, 10039-10045.

[35] M. Ikegami, T. Arai, *Bull. Chem. Soc. Jpn.* **2003**, *76*, 1783-1792.

[36] M. Ikegami, T. Arai, *Chem. Lett.* **2005**, *34*, 492-493.

[37] T. Asano, H. Furuta, H. J. Hofmann, R. Cimaraglia, Y. Tsuno, M. Fujino, *J. Org. Chem.* **1993**, *58*, 4418-4423.

[38] Y. Odo, K. Matsuda, M. Irie, *Chem. Eur. J.* **2006**, *12*, 4283-4288.

[39] S. H. Kawai, S. L. Gilat, J. M. Lehn, *Eur. J. Org. Chem.* **1999**, 2359-2366.

[40] M Irie, Y Hirano, S Hashimoto, K Hayashi, *Macromolecules* **1981**, *14*, 262-267.

[41] K Ishihara, T Matsuo, K Tsunemitsu, I Shinohara, *Journal of Polymer Science: Polymer Chemistry Ed.* 1984, *22*, 3687-3695.

[42] Richard Fuchs, Jordan J. Bloomfield *J. Org. Chem.* **1966**, *31*, 3423-3425.

[43] T. Asano, H. Furuta, H. J. Hofmann, R. Cimaraglia, Y. Tsuno, M. Fujino, *J. Org. Chem.* **1993**, *58*, 4418-4423.

[44] K. Maeda, K. A. Muszkat, S. S. Ozeri, *J. Chem. Soc., Perkin Trans 2* **1980**, *9*, 1282-1287.

[45] K. Maeda, E. Fischer, *Israel J. Chem.* **1977**, *16*, 294-298.

[46] R. Behrendt, C. Renner, M. Schenk, F. Wang, J. Wachtveitl, D. Oesterhelt, L. Moroder, *Angew. Chem. Int. Ed.* **1999**, *38*, 2771-2774.

[47] A. Momotake, T. Arai, *Tetrahedron Letter* **2003**, 7277-7280.

[48] P. Ayyappan, O. R. Evans, W. Lin, *Inorg. Chem.* 2002, **41**, 3328-3330.

[49] I. D. Kostas, B. R. Steels, A. Terzis, S. V. Amosova, *Tetrahedron* 2003, **59**, 3467-3473.

[50] M. Buback, T. Perkovic, S. Redlich, A. Meijere, *Eur. J. Org. Chem.* 2003, 2375-2382.

[51] J. H. Kim, H. Lee, *Chem. Mater.* 2002, **14**, 2270-2275; e) H. Li, Y. Li, J. Zhai, G. Cui, H. Liu, S. Xiao, Y. Liu, F. Lu, L. Jiang, D. Zhu, *Chem. Eur. J.* 2003, **9**, 6031-6038.

[52] I. K. Spiliopoulos, J. A. Mikroyannidis, *J. Polym. Sci., Part A: Polym. Chem.* 2002, **40**, 2591-2600; g) M. Pan, Z. Bao, L. Yu, *Macromolecules* 1995, **28**, 5151-5153

[53] A. Altomare, M. C. Burla, M. Camalli, M. Cascarano, C. Giacovazzo, A. Guagliardi, G. Polidori, *J. Appl. Crystallogr.* 1994, **27**, 435.

[54] G. M. Sheldrick, SHELXS-97, Program for the Refinement of Crystal Structures, University of Göttingen, Göttingen (Germany), 1997.

Chapter 4

Acidity control by ON/OFF switching of an intramolecular NH···O hydrogen bond by *E*/*Z* photoisomerization of the cinnamate framework

Introduction

In chapter 3, the author showed the OFF to ON one-way switching of an intramolecular NH···O hydrogen bond accompanying with the *E* to *Z* photoisomerization of cinnamate framework. And NH···O hydrogen bond formed in *Z* form lowered the pK_a value of the *Z* carboxylic acid derivative. The author conceived an idea that the carboxylic acid derivative, which is introduced cinnamate framework, and interrupt an intramolecular NH···O hydrogen bond according to photoisomerization (that means ON to OFF switching of hydrogen bonding), will achieve to increase the pK_a value of the corresponding carboxylic acid. According to this strategy, the author designed the carboxylic acid derivatives. Scheme 1 shows the one-way switching of the intramolecular NH···O hydrogen bond of ON→OFF type compounds (*E*-3/*Z*-3, *E*-4/*Z*-4) and that of OFF→ON type compounds (*E*-1/*Z*-1, *E*-2/*Z*-2). The characters of OFF→ON switching type compounds were already described in previous chapter.[1] The formation of intramolecular NH···O hydrogen bonding in *E* carboxylate form of ON→OFF type compound was promised by the previous investigation of the similar compounds which don't have an aromatic ring.[2-11] Chart 1 shows the mono amidated maleic acid investigated by *Takahashi et al.* that forms OH···O=C hydrogen bond in carboxylic acid and forms NH···O hydrogen bond in carboxylate by seven membered ring.[10, 11] In this chapter, the author expanded the π-conjugation of the compound shown in chart 1 by introducing the cinnamate framework, to accelerate the photoisomerization reaction.

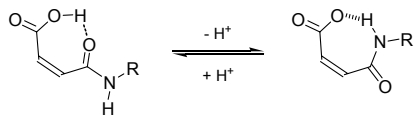

Chart 1.

OFF→ON switching type

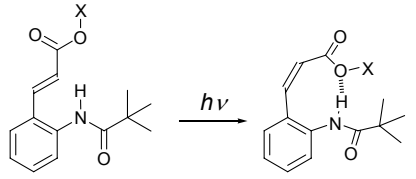

X=H (*E*-1) **X=H (*Z*-1)**
X=NMe$_4$ (*E*-2) **X=NMe$_4$ (*Z*-2)**

ON→OFF switching type

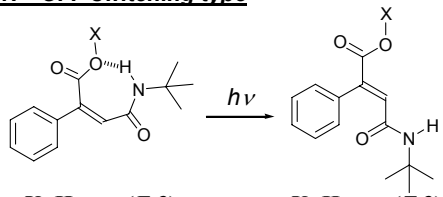

X=H (*E*-3) **X=H (*Z*-3)**
X=NMe$_4$ (*E*-4) **X=NMe$_4$ (*Z*-4)**

Scheme 1. OFF→ON (***E*-1**, ***Z*-1**, ***E*-2**, ***Z*-2**) and ON→OFF (***E*-3**, ***Z*-3**, ***E*-4**, ***Z*-4**) switching of intramolecular NH···O hydrogen bond by *E* to *Z* photoisomerization of cinnamate framework.

Results and Discussion

Synthesis

The synthesis of ON→OFF type compounds (*E*-3, *Z*-3, *E*-4, *Z*-4) were shown in Scheme 2. *E*-3 was synthesized through a coupling of phenylmaleic anhydride and *tert*-butylamine. In this procedure, it is expected that two isomers should be produced (chart 2). Only one product was obtained after purification. The configuration of the product was confirmed to *E*-1 by long range coupling correlation of olefin proton and amidecarbonyl carbon using HSQC method. *Z*-3 was isolated from photoreaction

mixture through an addition of hydrochloric acid. *E*-3 was hydrolyzed by acid addition, and removed through washing by the water, to obtain isolated *Z*-3. *E*-4 and *Z*-4 were synthesized through a counter-cation exchange reaction of corresponding acids.

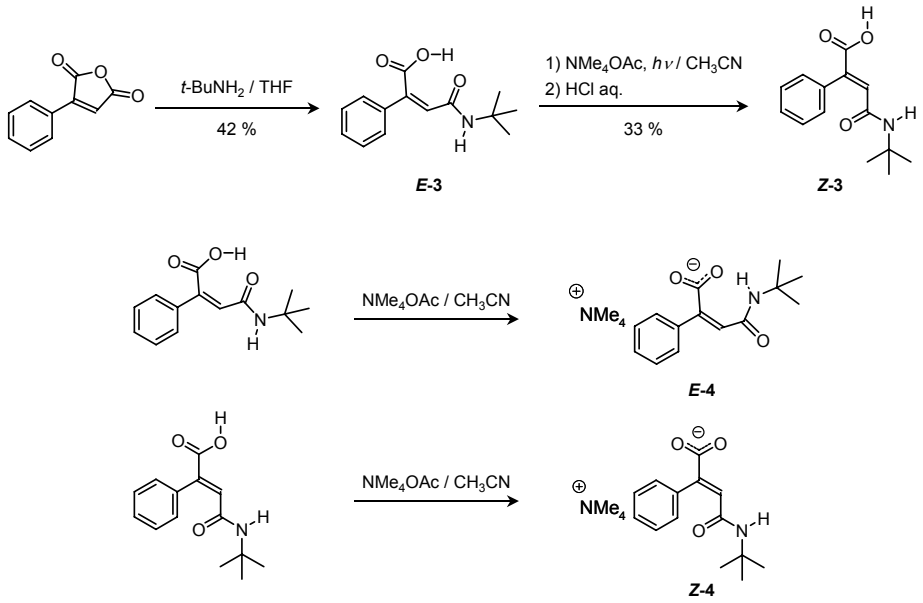

Scheme 2. Synthesis of ON→OFF switching type compounds (***E*-3**, ***Z*-3**, ***E*-4**, ***Z*-4**).

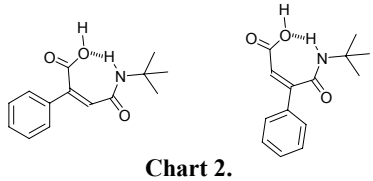

Chart 2.

Direct photoisomerization of *E*-1, *E*-2, *E*-3 and *E*-4

E/Z Photoisomerization were traced by UV-visible (UV-vis) spectra. UV-vis spectrum changes of *E*-1, *E*-2, *E*-3 and *E*-4 according to photoirradiation in dimethylsulfoxide (DMSO) solution at 293 K are shown in Figure 1. Each *E* compounds are isomerized and reached to photostationary state (PSS) at 313 nm UV-light irradiation. Solid lines are those taken before irradiation, corresponding to *E* isomers, and broken lines are the isolated pure *Z* isomers. The absorbances of E isomers are decreased in accordance with

two-stete transition toward irradiation (dotted lines), which indicating that only corresponding *Z* isomers are formed without any side reaction. The contents of *Z* compounds in PSS were determined from the integration ratio of ^{1}H NMR spectra. The *E*/*Z* ratios in PSS are 25/75 (*E*-1/*Z*-1), 7/93 (*E*-2/*Z*-2), 15/85 (*E*-3/*Z*-3) and 16/84 (*E*-4/*Z*-4) respectively.

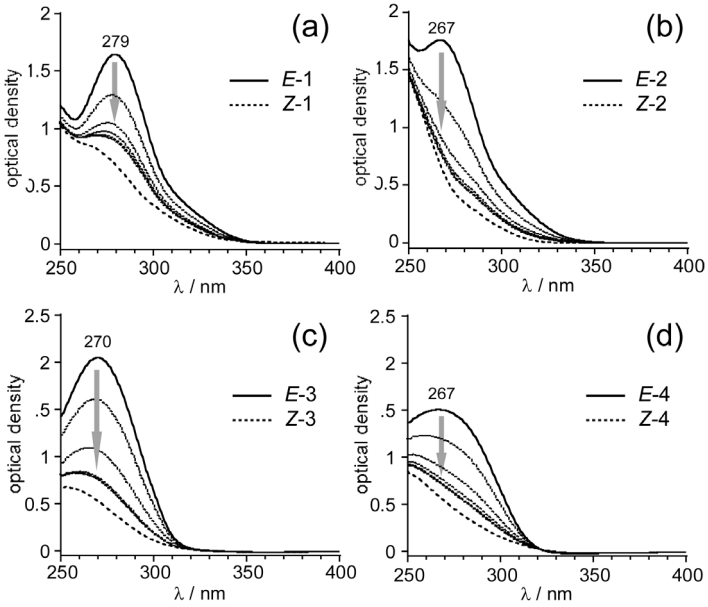

Figure 1. Time course UV-vis spectra changes of ON→OFF type compounds (***E*-3, *E*-4**) comparing with OFF→ON type compounds (***E*-1, *E*-2**), toward photoirradiation at 313 nm, 1 mM in DMSO at 293 K.

Molecular structures in solution

The structures in solution of isolated Z compounds were determined by ^{1}H NMR spectra. ^{1}H NMR spectra of carboxylates *E*-2, *Z*-2, *E*-4, and *Z*-4 in DMSO-d_6 at 303 K are shown in Figure 2. All signals are assigned by nuclear overhauser effect (NOE) and decoupling method. *E*/*Z* configurations of OFF-ON type compounds, *E*-1/*Z*-1 and *E*-2/*Z*-2, were confirmed by $^3J_{HH}$ value of the olefin protons. Generally speaking, typical $^3J_{HH}$ coupling constant of the olefin protons is about 15-16 Hz in *trans* position, and is about 12-13 Hz in *cis* position. Observed $^3J_{HH}$ values of the olefin protons of *E*-1 and

E-2 were 16.0 Hz, and those of *Z*-1 and *Z*-2 were 12.5 and 12.8 Hz respectively. It coincides the typical values of the *trans* and *cis* olefin protons, and the configurations of the compounds before irradiation were confirmed to *E* form, and the photoproducts were confirmed to *Z* form. However, ON-OFF type compounds, *E*-3/*Z*-3 and *E*-4/*Z*-4, don't have the olefin coupling. The structures in solution of the ON-OFF type compounds are estimated based on the NOESY spectra (Figure 3). NOE correlations between olefin and phenyl proton were observed in *E*-3 and *E*-4 (Figure 3a, 3c), whereas correlations between *tert*-butyl and phenyl proton were observed in *Z*-3 and *Z*-4 (Figure 3b, 3d); the results confirm their configurations. NOE correlation between amide NH and olefin proton was observed in *E*-3. That means, amide carbonyl (C=O) is close to the carboxylic acid (COOH) moiety. This NOE correlation of amide NH and olefin proton observed in *E*-3 was disappeared in *E*-4; indicates that the amide plane was reversed according to the deprotonation, and the amide NH was strongly strained toward the direction of carboxylate oxygen in *E*-4.

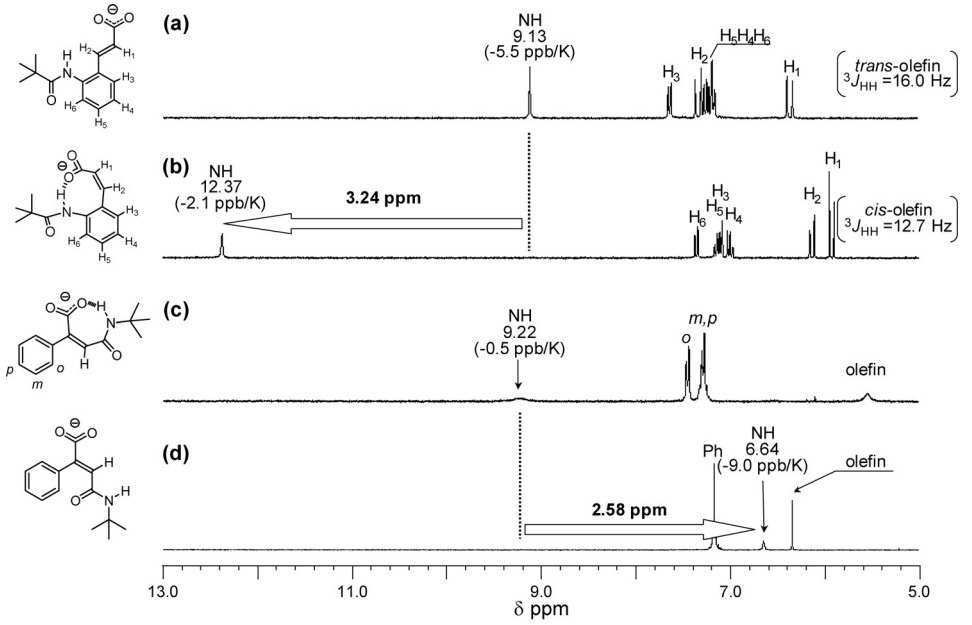

Figure 2. ^{1}H NMR spectra changes of isolated ON→OFF type carboxylate derivatives c) ***E*-4**, d) ***Z*-4**, comparing with OFF→ON type a) ***E*-1**, b) ***E*-2**, 5 mM in DMSO-d_6 at 303 K.

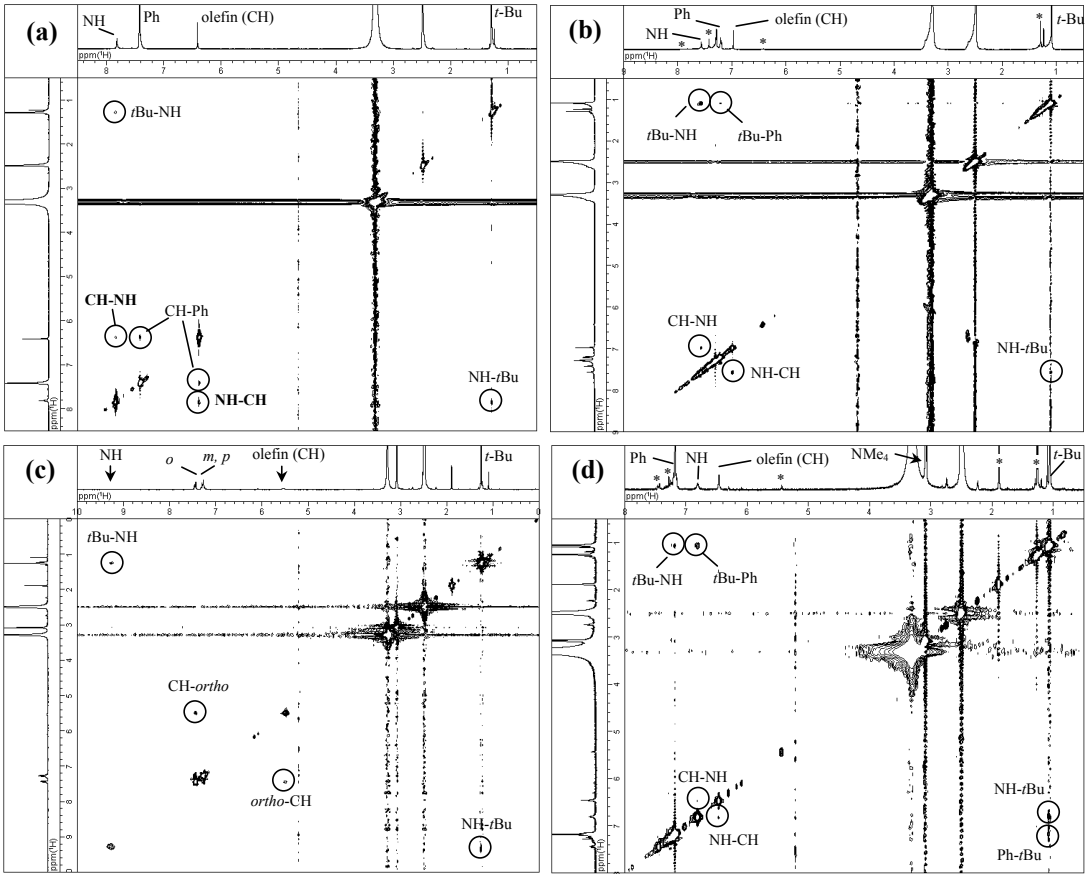

Figure 3. NOESY NMR spectra of a) ***E*-3**, b) ***Z*-3**, c) ***E*-4**, d) ***Z*-4**, in DMSO-d_6 at 303 K.

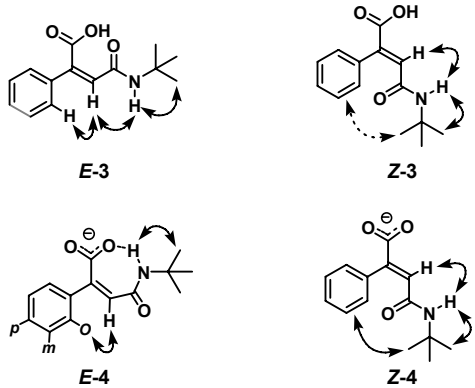

Chart.

The chemical shifts of the amide NH signals of OFF-ON type compounds were 9.13 ppm in *E*-2 and 12.37 ppm in *Z*-2 at 303 K (Figure 2). The significant downfield shift ($\Delta\delta$ = 3.24 ppm) suggests that *Z*-2 forms an NH···O hydrogen bond in DMSO-d_6 solution. The temperature dependency of the amide NH chemical shift of *Z*-2 was –2.1 ppb K^{-1}, whereas that of *E*-2 was –5.5 ppb K^{-1} in the range of 303 to 333 K. The downfield shift and the decrease of temperature coefficient of the NH proton suggest that *Z*-2 forms an intramolecular NH···O hydrogen bond in DMSO-d_6 solution. In contrast to the OFF-ON type compounds, amide NH chemical shift of ON-OFF type compounds was 9.22 ppm in *E*-4 and 6.64 ppm in *Z*-4 at 303 K (Figure 2). The temperature dependency of the amide NH chemical shift of *Z*-4 was –9.0 ppb K^{-1}, whereas that of *E*-4 was –0.5 ppb K^{-1} in the range of 303 to 333 K. The upfield shift ($\Delta\delta$ = 2.58 ppm) and the increase of temperature coefficient suggest that an intramolecular NH···O hydrogen bond formed in *E*-4 was interrupted in *Z*-4.

Acidity change through photoisomerization

pK_a values of *E*-1 and *Z*-1 were measured by potentiometric titration in a 10 % Triton X-100 aqueous micellar solution at 298 K. pK_a value of *Z*-1 is 4.3, which shifts 0.6 unit lower than that of *E*-1 (4.8). In ON-OFF type compounds, the pK_a value of *Z*-3 was obtained to 4.3, but that of the *E*-3 was not obtained accurately because of the hydrolysis of the amide bond. This hydrolysis reaction doesn't proceed in some organic solvents like DMSO. Thus, we approached to determine relative acidity in such organic solvent.

To discuss about the acidity change in organic solvent, counter cation exchange reaction was examined. The difference of pK_a values in organic solvent is obtained by following method. If two acids, AH and BH, are in equilibrium including deprotonation process, the equilibrium equation is drawn in equation 1. (It is assumed that all anions have dissociated. The acid dissociation constant of AH and BH are defined as $K_a(1)$ and $K_a(2)$, respectively.) The equilibrium constant K_{eq} is indicated in equation 2, and K_{eq} is equal to the ratio of acid dissociation constants of AH and BH. Δ pK_a (= log K_{eq}) is

calculated from [A^-]/[AH] and [BH]/[B^-]. (Generally speaking, it is preferable to make [A^-]/[AH] and [BH]/[B^-] for 0.8 from 0.2, to reduce the error margin.)

$$AH + B^- \underset{}{\overset{K_{eq}}{\rightleftharpoons}} A^- + BH \quad \cdots\cdots \quad ①$$

$$K_{eq} = \frac{[A^-][BH]}{[AH][B^-]} = \frac{[A^-][H^+]}{[AH]} \times \frac{[BH]}{[H^+][B^-]} = \frac{K_a(1)}{K_a(2)} \quad \cdots\cdots \quad ②$$

Carboxylic acid [AH] and carboxylate [B^-] are mixed in DMSO-d_6 solution and equilibrium constant is confirmed from the chemical shift of ^{1}H NMR spectra. Panels a, b, and c in Figure 4 shows the ^{1}H NMR spectra of the mixtures of *E*-1 and *Z*-2, *E*-4 and *Z*-3, *Z*-2 and *Z*-3, respectively in DMSO-d_6 solution. Signals are shifted by mixing, which means ion exchange reaction have occurred. Comparing with authentic signals of carboxylic acids and carboxylates, the deprotonation ratios are estimated. By using the chemical shift of the olefin protons, of which signals are sharp and isolated, deprotonation ratio was calculated precisely. In the case of the OFF-ON type isomers (*E*-1, *Z*-2), the chemical shift of the olefin proton of *E* compound was close to the chemical shift of carboxylic acid *E*-1 than carboxylate *E*-2, and that of *Z* compound was close to the *Z*-2 than *Z*-1 (Figure 4a). Comparing with the chemical shifts of isolated carboxylic acids and carboxylates, it is estimated that the 83 % of *E* compound is protonated, and 90 % of *Z* compound is deprotonated. The result and the equation 2 indicate that *E* compound has 1.63 unit lower pK_a value than *Z* compound in DMSO solution. Estimating in a uniform manner, *E*-3 has 0.92 unit lower pK_a value than *Z*-3 (Figure 4b), and *Z*-1 has 0.39 unit lower pK_a value than *Z*-3 (Figure 4c) in DMSO solution. Figure 5 shows the pK_a differences in DMSO solution described on a straight line. According to photoisomerization, the pK_a value of carboxylic acid was lowered in OFF-ON type compounds, and increased in ON-OFF type compounds; acidity was reversed after photoisomerization. The pK_a value was controlled arbitrarily by photoswitching of intramolecular NH···O distances.

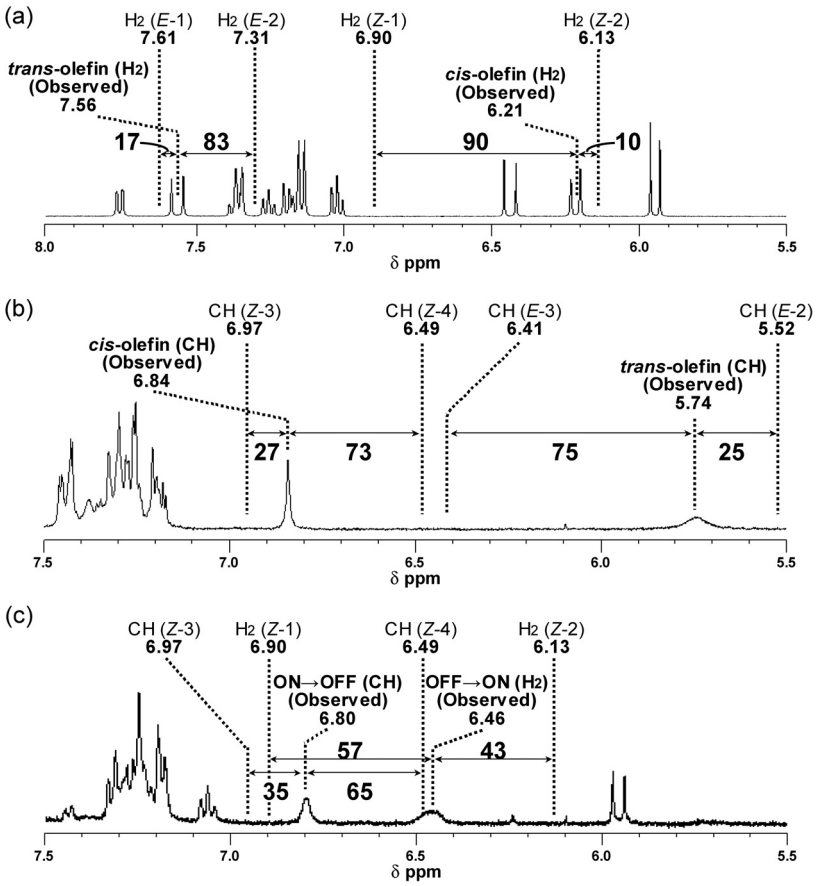

Figure 4. [1]H NMR spectrum of the mixture of a) ***E*-1** and ***Z*-2**, b) ***E*-4** and ***Z*-3**, c) ***Z*-2** and ***Z*-3** in DMSO-d_6 solution at 303 K

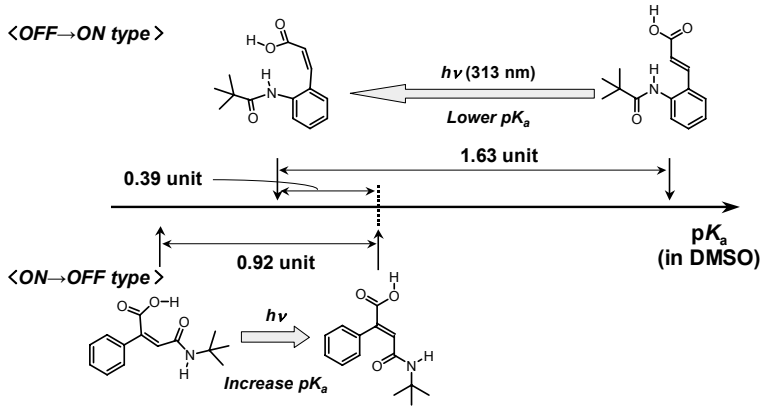

Figure 5. pK_a differences of OFF→ON and ON→OFF type carboxylic acids in DMSO solution obtained from [1]H NMR analysis of ion exchange reaction.

Conclusion

In this chapter, OFF→ON (*E*-1/*Z*-1, *E*-2/*Z*-2) and ON→OFF (*E*-3/*Z*-3, *E*-4/*Z*-4) photoswitching of the intramolecular NH···O hydrogen bond by using *E* to *Z* photoisomerization of cinnamic acid framework was achieved. *E* carboxylate derivative *E*-4 forms an intramolecular NH···O hydrogen bond in DMSO-d_6 solution, and that hydrogen bond was interrupted in *Z* carboxylate *Z*-4 according to photoisomerization of cinnamate framework. The pK_a value of *Z*-3 was higher than that of *E*-3 in DMSO solution. We propose that the intramolecular NH···O hydrogen bond interrupted in *Z* conformation discourages the deprotonation process and increases the pK_a value of the corresponding carboxylic acid *Z*-3. As a result, the pK_a value of carboxylic acid was lowered in OFF→ON type compounds, and increased in ON→OFF type compounds. The auther found that the acidity of ON→OFF and OFF→ON type compound was reversed after photoisomerization in DMSO solution.

Experimental

General procedures

All manipulations involving air- and moisture-sensitive compounds were carried out by the use of standard Schlenk technique under argon atmosphere. phenylmaleic acid anhydride and tetramethylammonium acetate were purchased from Aldrich Chemical Company, Inc. Tetrahydrofuran, diethylether, *n*-hexane, and acetonitrile were distilled over CaH_2 and dried over molecular sieves (3A).

Physical measurements

^{1}H (270 MHz) NMR spectra were measured on a JEOL JNM-GSX270 spectrometer. NOESY spectra were measured on a JEOL JNM-GSX400 spectrometer spectrometer. The ^{1}H NMR spectra were referenced to the tetramethylsilane protons at δ 0.00. UV-vis spectra was measured on a Shimazu UV-3100PC spectrometer. Elemental Analysis was performed at Elemental Analysis Center, Faculty of Science, Osaka University. All melting points of the compounds

were measured on a micro melting point apparatus of YANAGIMOTO Co. ESI-MS measurements were performed on a Finnigan MAT LCQ ion trap mass spectrometer. pK_a measurement was performed using a potentiometric titration in 10 mM micellar solution at 298 K with a Metrohm 716 DMS titrino whtich is combined with Metrohm 728 stirrer and a saturated calomel LL micro pH glass electrode. The saturated calomel micro glass electrode was calibrated with the 0.05 M $KHC_8H_4O_4$ buffer (pH = 4.01) and the 0.0025 M KH_2PO_4 buffer (pH = 6.86) at 298 K. The potentiometric titration was performed three times. pK_a values are estimated by an average value of each measurements.

UV-light irradiation technique for UV-vis and ^{1}H NMR spectrum measurement

Xe/Hg lamp (MUV-202U, Moritex Co.) was used for 313 nm UV-light irradiation. UV-light was filtered through 6784-t01.uv1 (Asahi tech.) to pick out the 313 nm emission line of Hg gas. Sample was dissolved in the distilled solvent under argon atmosphere and sealed in NMR tube or UV cell. The spectrum was measured before and after irradiation. During irradiation and spectrum measurements, the sample was always kept desired temperature.

Preparation of (*Z*)-3-(*tert*-butylcarbamoyl)-2-phenylacrylic acid (*E*-3)

To a phenylmaleic acid anhydride (400 mg, 2.296 mmol) solution in distilled THF (10 mL) was added dropwise a *tert*-butyl amine (2.4 mL, 22.96 mmol) solution in distilled THF (10 mL) in an ice-water bath, and stirred at room temperature for16 hours. 3.5 % HCl aqueous solution (20 mL) was added to the solution to obtain yellow solid in white suspension. The suspension was filtered, and washed with water to obtain white powder (213.5 mg, 37.6 %). mp 113 ^oC; (Found: C, 66.85; H, 7.02; N, 5.68. Calc. for $C_{14}H_{17}NO_3$: C, 68.00; H, 6.93; N, 5.66 %); δ_H(270 MHz; Me_2SO-d_6) 1.29 (9H, s, *tert*-butyl), 6.42 (1H, s, olefin), 7.38-7.44 (5H, Aryl), 7.81 (1H, s, NH) and 12.93 (1H, br s, COOH); δ_C(67.5 MHz; Me_2SO-d_6) 28.43, 50.25, 121.04, 125.92, 128.72, 129.13, 134.59, 143.60, 162.86 and 169.10 ; *m/z* (ESI) 246.1 (M^- requires 246.1).

Preparation of [Tetramethylammonium] (*Z*)-3-(*tert*-butylcarbamoyl)-2-phenylacrylate (*E*-4)

To an acetonitrile solution of (*Z*)-3-(*tert*-butylcarbamoyl)-2-phenylacrylic acid (50.0 mg, 0.202 mmol) was added an acetonitrile solution of tetramethyl-ammonium acetate (26.93 mg, 0.202 mmol). The solution was stirred for 2 hours and concentrated to give colorless oil. The oil was reprecipitated from ether/*n*-hexane to give white powder (yield was not certainly obtained). δ_H(270 MHz; Me_2SO-d_6) 1.26 (9H, s, *tert*-butyl), 3.08 (12H, s, NMe_4), 5.54 (1H, br s, olefin), 7.22-7.32 (3H, Aryl), 7.45 (2H, dd, Aryl) and 9.23 (1H, br s, NH).

Preparation of (*E*)-3-(*tert*-butylcarbamoyl)-2-phenylacrylic acid (*Z*-3)

To a (*Z*)-3-(*tert*-butylcarbamoyl)-2-phenylacrylic acid (*maleic*-CPA, 100 mg, 0.4044 mmol)

solution in acetonitrile (40 mL) was added tetramethylammonium acetate (107.7 mg, 0.8088 mmol). The reaction mixture was irradiated at 313 nm for 15 hours. The solution was acidified by aqueous hydrochloride (pH 2) and stirred over one night. The solution was concentrated to obtain white suspension. The precipitate was filtered and washed with water. The white powder was dried over phosphorous pentoxide under reduced pressure (38.1 mg, 38 %). mp 178 ^{o}C; (Found: C, 66.91; H, 6.79; N, 5.47. Calc. for $C_{14}H_{17}NO_3 \cdot (H_2O)_{0.2}$: C, 67.02; H, 6.99; N, 5.58 %); δ_H(270 MHz; DMSO-d_6) 1.09 (9H, s, *tert*-butyl), 7.20 (2H, Aryl), 7.26-7.32 (3H, Aryl), 7.56 (1H, s, NH) and 12.89 (1H, br s, COOH); δ_C(125 MHz; DMSO-d_6) 28.09, 50.28, 122.74, 127.16, 127.38, 129.12, 134.18, 139.52, 164.05 and 167.93 ; *m/z* (ESI) 248.1 ($[M+H]^+$ requires 248.1), 270.0 ($[M+Na]^+$ requires 270.1); pK_a 4.3 (in 10% Triton® X-100 micellar solution).

Preparation of [Tetramethylammonium] (*E*)-3-(*tert*-butylcarbamoyl)-2-phenylacrylate (Z-4)

To an acetonitrile solution of (*E*)-3-(*tert*-butylcarbamoyl)-2-phenylacrylic acid (10.0 mg, 0.0404 mmol) was added an acetonitrile solution of tetramethylammonium acetate (5.4 mg, 0.0404 mmol). The solution was stirred for 2 hours and concentrated to give colorless oil. The oil was washed with diethylether to obtain white powder. δ_H(270 MHz; DMSO-d_6) 1.05 (9H, s, *tert*-butyl), 3.11 (12H, s, NMe_4), 6.34 (1H, olefin), 6.64 (1H, s, NH), and 7.10-7.21 (5H, Aryl).

References

[1] T. Matsuhira, H. Yamamoto, T. Okamura, N. Ueyama, *Org. & Biomol. Chem.*, in press.

[2] Jose' V. Herma'ndaz, Euan R. Kay, David A. Leigh, *Science*, **2004**, *306*, 1532-1537.

[3] A. Altieri, G. Bottari, F. Dehez, David A. Leigh, Jenny K. Y. Wong, F. Zerbetto, *Angew. Chem. Int. Ed.* **2003**, *42*, 2296-2300.

[4] Francesco G. Gatti, S. Leo'n, Jenny K. Y. Wong, G. Bottari, A. Altieri, M. Angeles Farran Morales, Simon J. Teat, C. Frochot, David A. Leigh, Albert M. Brouwer, F. Zerbetto, *Proc. Natl. Acad. Sci. U. S. A.*, **2003**, *100*, 10-14.

[5] G. Campari, M. Fagnoni, M Mella, A. Albini, *Tetrahedron: Asymmetry*, **2000**, *11*, 1891-1906.

[6] F. G. Gatti, D. A. Leigh, S. A. Nepogodiev, A. M. Z. Slawin, S. J. Teat, J. K. Y. Wong, *J. Am. Chem. Soc.* **2001**, *123*, 5983-5989.

[7] G. Brancato, F. Coutrot, D. A. Leigh, A. Murphy, J. K. Y. Wong, F. Zerbetto, *Proc. Natl. Acad. Sci. U. S. A.* **2002**, *99*, 4967-4971.

[8] V. Bermudaz, N. Capron, T. Gase, F. G. Gatti, F. Kajzar, D. A. Leigh, F. Zerbetto, S. W. Zhang, *Nature* **2000**, *406*, 608-611.

[9] L. Frkanec, M. Jokic', J. Makarevic', K. Wolsperger, M. Zyinic, *J. Am. Chem. Soc.* **2002**, *124*, 9716-9717.

[10] K. Takahashi, T. Okamura, H. Yamamoto, N. Ueyama, *Acta Crystallogr.*, *Sect. E: Struct. Rep. Online* **2004**, *E60*, o448-449.

[11] K. Takahashi, M. Doi, A. Kobayashi, T. Taguchi, A. Onoda, T. Okamura, H. Yamamoto, N. Ueyama, *Chem. Lett.* **2002**, *33*, 192-193.

Chapter 5

The artificial photocycle containing protonation and deprotonation process of phenol derivative

Introduction

Photoactive Yellow Protein (PYP) is one of the photo-acceptable proteins that concerned with the negative cursoriality of purple photosynthetic bacteria.[1-13] The photocycle of PYP around the chromophore indicate that hydrogen bond between phenolate oxygen and hydroxyl moiety of Glu 46 or Tyr 42 formed in ground state were interrupted by *E*/*Z* photoisomerization of *para*-coumaric acid framework, accompanying the protonation and deprotonation process of phenol moiety (Figure 1). Not only in PYP, but also in other native proteins like hydrolytic enzymes, rearrangement of the hydrogen bond network around the active site is believed to play a substantial role in regulating reactivity of enzymatic reactions.[14-30] They induce dynamic switching of the overall protein structure triggered by external stimulation such as substance binding, pH change, temperature change or photoillumination, to switch the hydrogen bond network. We propose that the small molecule that switch their conformation by external stimulation will achieve to switch the intramolecular hydrogen bonding artificially, by controlling the distance between hydrogen bond donor and acceptor (Figure 2).

To drive these compounds, a photoisomerization is one of the most promising strategies and enables to control of molecular structures in an elegant way. Recently, much attention has been focused on the isomerization reaction of photochromic compounds as a photo-induced switching devices.[31-40] For example, also the effect of intramolecular NH···N or NH···O hydrogen bonds in *Z* form toward *E/Z* photoisomerization of the C=C double bond,[41-44] and the pK_a change of phenol or carboxylic acid derivatives by the switching of conjugation toward photoisomerization[45-48] have investigated.

Previously, we have proposed that the hydrogen bond between the amide NH and the oxy-anion, such as carboxylate and phenolate, stabilizes and decreases the nucleophilicity of the anions and lower the pK_a values of the corresponding acids.[49-61] In this chapter, we designed *ortho*-coumaric acid derivatives (*E*-1/*Z*-1, *E*-2/*Z*-2), both of which have an amide group linked with a photoinduced olefin moiety (Scheme 1). These compounds are expected to have an intramolecular OH· · · O=C hydrogen bond in *Z*-1 and an intramolecular NH···O hydrogen bond in *Z*-2 forming eight-membered ring structures. And they are expected to construct an artificial cycle containing protonation and deprotonation process, like that of PYP photocycle.

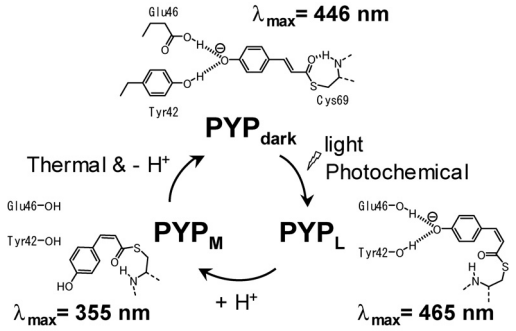

Figure 1. Photocycle of Photoactive Yellow Protein (PYP)

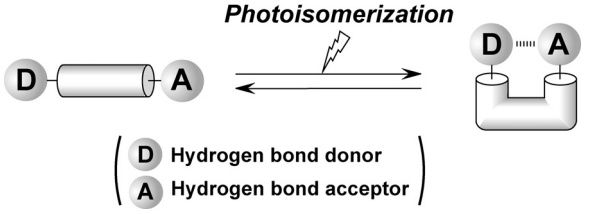

Figure 2. Switching of intramolecular distance of hydrogen bond donor and acceptor, by external stimulation.

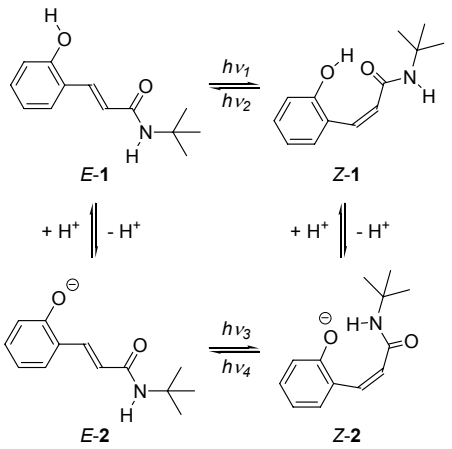

Scheme 1. Photoisomerization equilibriums of cinnamic acid derivatives *E*-1/*Z*-1 and *E*-2/*Z*-2.

Results and Discussion

Synthesis

The synthetic method was shown in Scheme 2. *E*-1 was synthesized through DCC (dicyclohexyl carbodiimide) coupling of *ortho*-coumaric acid and *tert*-butyl amine. *Z*-1 was isolated from photoreaction mixture by recristallization. *E*-2 and *Z*-2 were prepared through counter-cation exchange reaction of corresponding phenol derivatives (*E*-1 and *Z*-1) with tetraethylammonium hydroxides.

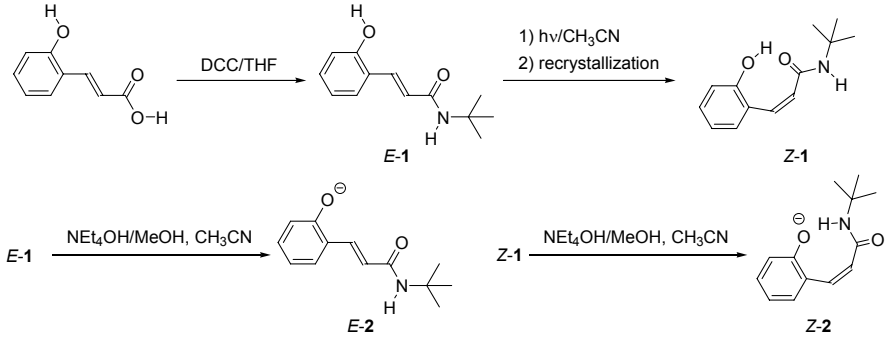

Scheme 2 Synthesis of cinnamic acid derivatives *E*-1, *Z*-1, *E*-2 and *Z*-2.

Molecular structures in solid state

To confirm the molecular structures in solid state, X-ray crystallography was appropriated. The crystal structures of *E*-1 and *Z*-1 are shown in Figure 3. Crystal data of *E*-1 and *Z*-2 were shown in experimental section. All non-hydrogen atoms were refined anisotropically. The coordinates of OH and NH protons were refined by using fixed thermal factors, and the other protons were placed in calculated position. The intrermolecular O01···O'02 (2.645[2] Å) and O01···N"1 (3.099[3] Å) distances of *E*-1 permitted the hydrogen bond formation; these intermolecular NH···O and OH···O=C hydrogen bonds are thought to stabilize the packing structure of *E*-1 [O'02 indicates O02 atom at equivalent position (-x+1, y+1/2, -z+1/2), and N"1 indicates N1 atom at equivalent position (x+1/2, y, -z+1/2)]. The torsion angles of C5-C6-C7-C8 (16.5 [4] °) and C7-C8-C9-O02 (20.3[4] °) indicate that *ortho*-coumaric frame of *E*-1 is almost in plane; inferred that the π-conjugation is extended from phenol oxygen toward amidecarbonyl oxygen through C=C double bond.

By contrast, the distances of O01···O02 (2.516[2] Å) and H01···O01 (1.63[2] Å) of *Z*-1 permitted sufficient hydrogen bond formation (whereas O01···O02 distance of *E*-1 was 4.933 Å). The O01-H01-O03 angle of *Z*-1 (164[2] °) is appropriate to form hydrogen bonding. These results indicate that *Z*-1 has an intramolecular OH· · · O=C hydrogen bond forms eight-membered ring structure in the solid state. The intrermolecular O1···N'1 distance (2.971 Å) of *Z*-1 permitted the intermolecular hydrogen bond formation; and thought to stabilize the packing structure of *Z*-1 (N'1 indicates N1 atom at equivalent position). The torsion angles of C5-C6-C7-C8 (–137.4[3] °) and C7-C8-C9-O02 (–27.0 [4] °) are so large that π-conjugation extended in *E*-1 is interrupted in *Z*-2.

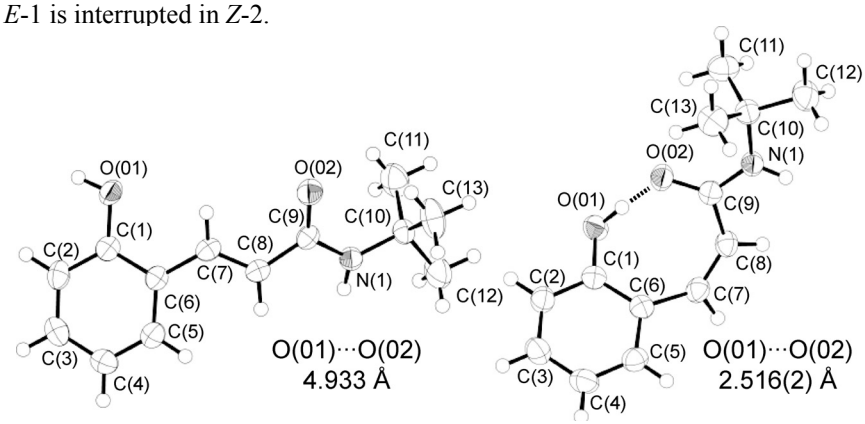

Figure 3. Molecular structures of *E*-**1** (left) and *Z*-**1** (right), 50 % probability.

Molecular structures in solution

The structures in solution of isolated isomers were determined by ^{1}H NMR spectra. The ^{1}H NMR spectra of *E*-1, *E*-2, *Z*-1 and *Z*-2 in acetonitrile-d_3 at 303 K are shown in Figure 4. All signals are assigned by nuclear Overhauser effect (NOE) and decoupling method. *E*/*Z* configurations of these compounds were confirmed by $^3J_{HH}$ value of the olefin protons. Generally speaking, $^3J_{HH}$ coupling constant of the olefin protons is about 15-16 Hz in *trans* position, and is about 12-13 Hz in *cis* position. Observed $^3J_{HH}$ values of the olefin protons of *E*-1 and *E*-2 were 15.8 and 15.5 Hz, and those of *Z*-1 and *Z*-2 were 13.0 Hz respectively. It coincides the typical values of the *trans* and *cis* olefin protons, and the configurations of the compounds before irradiation were confirmed to *E* form, and the photoproducts were confirmed to *Z* form. The chemical shifts of the OH signals of phenol compounds at 303 K were 7.33 ppm in *E*-1 and 9.87 ppm in *Z*-1 (Figure 4). The significant downfield shift ($\Delta\delta$ = 2.54 ppm) suggests that *Z*-1 forms an OH· · · O=C hydrogen bond in acetonitrile-d_3 solution. The temperature dependency of the OH signal chemical shift of *E*-1 and *Z*-1 are –7.2 and –7.5 ppb K^{-1} in the range of 233 to 303 K. These results indicate a hydrogen bond formation of that phenol OH

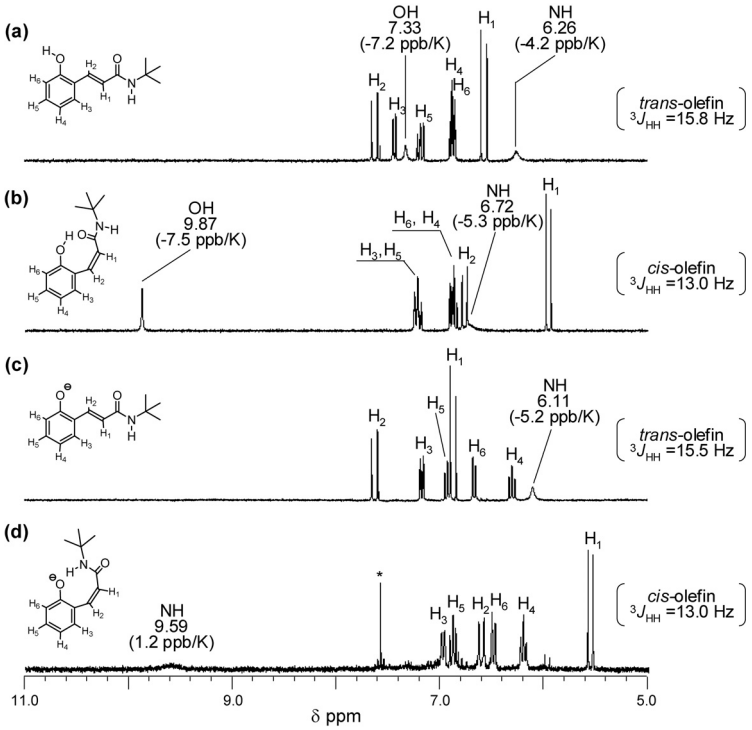

Figure 4. ^{1}H NMR spectra of a) *E*-1, b) *Z*-1, c) *E*-2 and d) *Z*-2, 5 mM in acetonitrile-d_3 at 303 K.

moiety in *Z*-1; including not only intramolecular but also intermolecular interaction. The chemical shifts of the amide NH signals of phenolates at 303 K were 6.11 ppm in *E*-2 and 9.59 ppm in *Z*-2 (Figure 4). The temperature dependency of the amide NH chemical shift of *Z*-2 is 1.2 ppb K^{-1} (in the range of 233 to 303 K), whereas that of *E*-2 is –5.4 ppb K^{-1} (263 to 333 K). The significant downfield shift ($\Delta\delta$ = 3.48 ppm) and the decrease of temperature coefficient of the NH proton signal suggest that *Z*-2 forms an intramolecular NH···O hydrogen bond in acetonitrile-d_3 solution.

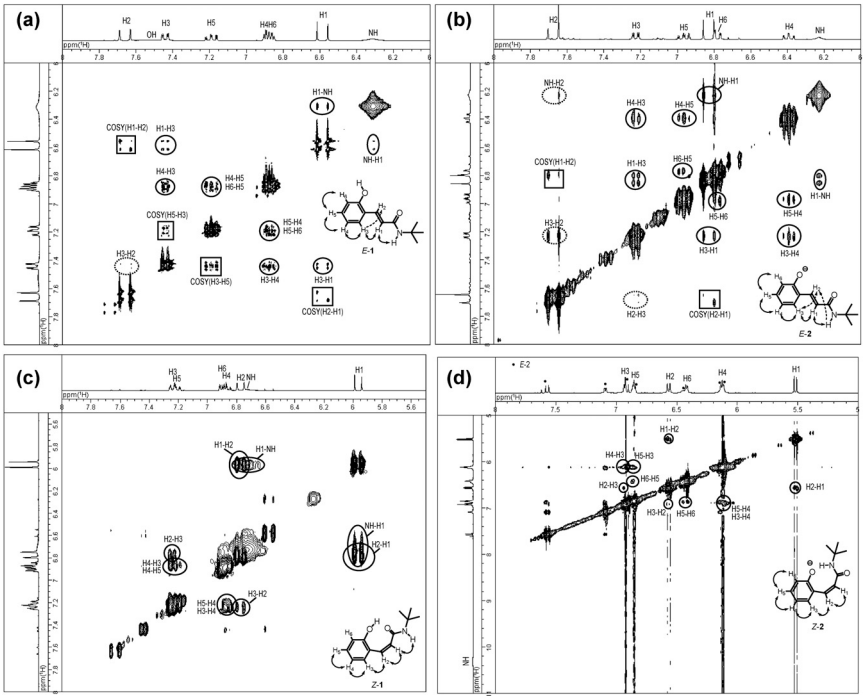

Figure 5. NOESY spectra of a) *E*-2 and b) *Z*-2, 5 mM in acetonitrile-d_3 at 303 K

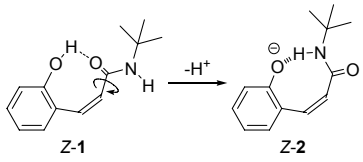

Scheme 3 The flipping of amide plane according to deprtonation of *Z*-1

The nuclear Overhauser enhancement spectroscopy (NOESY) spectra were measured to discuss about the structure in solution (Figure 5). A negative NOE correlation between NH and H1 was observed in *E*-1, whereas no NOE signal was observed between NH and H2 (Figure 5a). And the correlation of H1-H3 was stronger than that of H2-H3. These results indicate that *E*-1 seems to take the conformation as shown in Figure 5a, which amide carbonyl takes the same direction toward olefin moiety (s-*cis* form) and the hydroxyl moiety takes the opposite direction toward olefin moiety (s-*trans* form), in acetonitrile-d_3 solution. This structure of *E*-1 consists with the solid structure obtained X-ray crystallography (Figure 3). The characteristic positive-negative correlation pattern of H1-H2 and H5-H3 are predicated to the correlated spectroscopy (COSY) signal caused by spin coupling. The correlation of hydroxyl OH proton was not observed but exchange spectroscopy (EXSY) signal with water protons. NOE pattern of *E*-2 was almost same as *E*-1, and *E*-2 seems to take the structure as shown in Figure 5b in solution. The correlation of H1-H2 in *E*-2 was the COSY signal as well as that in *E*-1.

In *Z*-1, the negative NOE correlation between H1 and H2 was observed (Figure 5c). This correlation is characteristically observed in *cis* configuration of the olefin protons, therefore the configuration of *Z*-1 is determined to definitely in *Z* form. Correlations of NH-H1 and H2-H3 were observed, and no NOE signal was observed around OH protons. These results indicate that *Z*-1 seems to take the structure in solution as shown in Figure 5c, whose hydroxyl proton is in close proximity toward the amide carbonyl oxygen and allows to form intramolecular OH···O=C hydrogen bond. In *Z*-2, an NOE correlation of NH-H1, which was characteristically observed in *Z*-1, was disappeared (Figure 5d). Additionally, correlation of H2-H3 was observed. These results ascribed to the flipping of the amide plane by switching of the intramolecular hydrogen bond from OH· · · O=C to NH···O^-, accompanying with the deprotonation of phenol moiety (Scheme 3).

Direct photoisomerization

Figure 6 shows the UV-visible (UV-vis) spectra of isolated compounds (*E*-1, *E*-2, *Z*-1, *Z*-2), in acetonitrile at 303 K. The wavenumber of absorbance maximum (λ_{max}) in phenolate derivatives (*E*-2, *Z*-2) were longer than that in corresponding phenol

derivatives (*E*-1, *Z*-1). The red shift of λ_{max} according to the deprotonation ascribed to the electron delocalization in phenolate derivatives. The UV-vis spectra in Figure 6 indicate that the available wavelength of emission of mercury lamp for photoexcitation are 313 and 365 nm in phenol derivatives, and 313, 365, 405, and 436 nm in phenolate derivatives, without using any photosensitizer. According to photoirradiation, *E*/*Z* isomerization was progressed without any effective side reaction. *E*/*Z* ratio in photostationary state (PSS) depends on the irradiation wavelength. The contents in PSS at relative wavelength were shown in Table 1. At 313 nm irradiation, the contents in PSS were *Z* configuration rich in phenol derivatives (*E*-1/*Z*-1 = 11/89), and was *E* configuration rich in phenolate derivatives (*E*-2/*Z*-2 = 51/49). At 365 nm irradiation, phenol and phenolate derivatives generate *Z* isomer rather than *E* isomer (*E*-1/*Z*-1 = 11/89, *E*-2/*Z*-2 = 13/87). The phenolate derivatives generate the most *Z* compound in PSS by irradiation at 405 nm (*E*-2/*Z*-2 = 16/84), whereas phenol derivative takes no photoreaction by 405 nm irradiation because *E*-1 and *Z*-1 have no absorption at this wavelength. The phenolate derivative progresses the reversible photoisomerization that takes *E* to *Z* isomerization by 405 nm irradiation, and *Z* to *E* reversion by 313 nm irradiation.

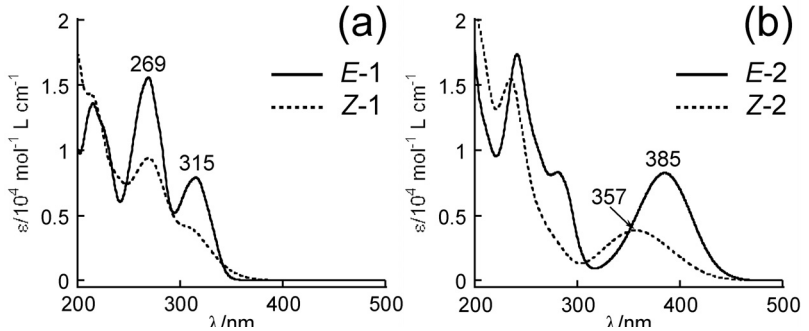

Figure 6. UV-vis spectra of *E*-1/*Z*-1 and *E*-2/*Z*-2, 1 mM in acetonitrile at 293 K.

Table 1 *E*/*Z* contents at photostationary state (PSS) by irradiation of various wavelengths

	irradiation wavelength			
	313 nm	365 nm	405 nm	436 nm
E-1/*Z*-1	11/89	18/82	no reaction	no reaction
E-2/*Z*-2	51/49	13/87	16/84	30/70

Acidity change through photoisomerization

pK_a values of *E*-1 and *Z*-1 were measured by potentiometric titration traced with UV-vis spectra in a 10 % lauryl ether aqueous micellar solution at 303 K. UV-vis spectra change by adding aqueous sodium hydroxide solution (0.100 mol L^{-1}) were shown in Figure 7. According to raising pH value, the absorbances of phenol derivatives (323 nm in *E*-1 and 311 nm in *Z*-1) were decreased, and that of phenolate derivatives (380 nm in *E*-2 and 357 nm in *Z*-2) were increased. The titration curves were shown in Figure 8. *Henderson-Hasselbalch* equation of acid dissociation in buffering region shows that the pK_a value is equal to the pH value when the concentration of phenolate has an accordant with that of phenol.

$$[HA] \rightleftharpoons [H^+] + [A^-]$$

〈*Henderson-Hasselbalch* equasion〉

$$pH = pK_a + \log [A^-] - [AH]$$

Thus the pH value at the cross point of titration curves of phenol and phenolate in Figure 8 stimulates the pK_a value of the corresponding phenol derivatives. The pK_a value of *Z*-1 was 10.24, which shifts 0.13 unit lower than that of *E*-1 (10.37). We propose that the stabilization of *Z* phenolate derivative (*Z*-2) by forming an intramolecular NH···O hydrogen bond decreases the pK_a value of *Z* phenol derivative (*Z*-1). Figure 9 shows the comparison of titration curves of phenol derivatives. In the pH region arround pK_a values of *E*-1 and *Z*-1, which is a buffering region, *E* compound was protonated and Z compound was deprotonated, preferentially. We propose that photoisomerization of synthesized compound in this pH region will achieve the protonation and deprotonation control of phenolic hydroxyl moiety.

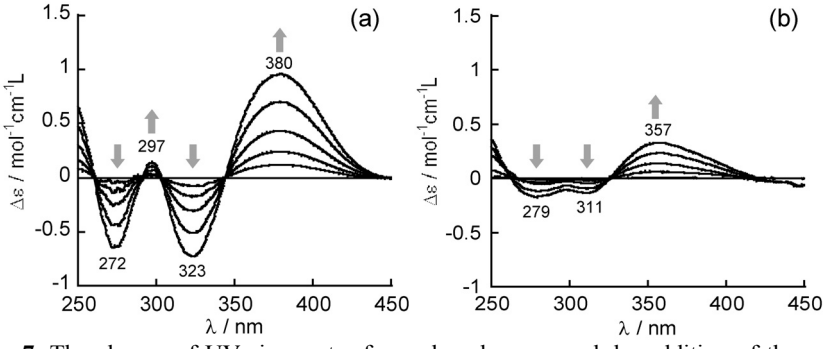

Figure 7. The change of UV-vis spectra from phenol compound, by addition of the sodium hydroxide aqueous solution, a) *E*-1 and b) *Z*-1, 5 mM in 10% raurilether aqueous micellar solution at 303 K.

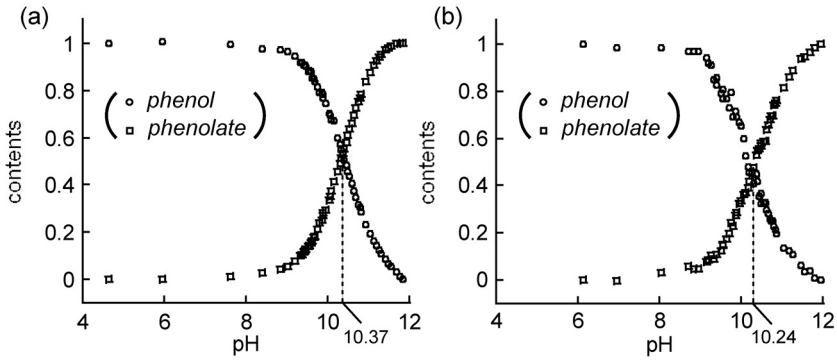

Figure 8. Titration curves of a) *E*-1 and b) *Z*-1.

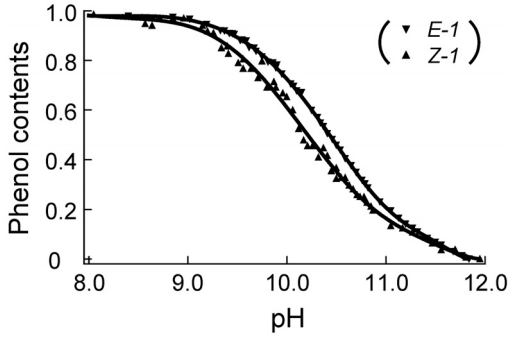

Figure 9. Comparison of titration curves of *E*-1 and *Z*-1; contents changes of phenol components depend on pH.

Proposed artificial photocycle

The decrease of pK_a value in *Z* phenol compound, and the difference of *E*/*Z* ratio at PSS toward 313 nm irradiation between phenol and phenolate derivatives, indicate that the artificial photocycle would be constructed like PYP photocycle containing protonation and deprotonation process (Scheme 4). In this photocycle, *E* phenol derivative photoisomerize toward *Z* phenol by 313 nm UV-light irradiation. Then, deprotonation process progressed because of the decrease of pK_a value in *Z* phenol. *Z* phenolate takes photoisomerization toward *E* isomer by same UV-light irradiation wavelength (313 nm), and *E* phenolate turns back to the initial state by protonation process. Through a series of the processes of this photocycle, phenolate was protonated

far from the amide moiety, and phenol was deprotonated near the amide moiety. That means proton transport from far side toward near side of amide moiety, that owing the light energy as a driving force. It is the achievement of a light-driven proton pumping system using an artificial small molecule.

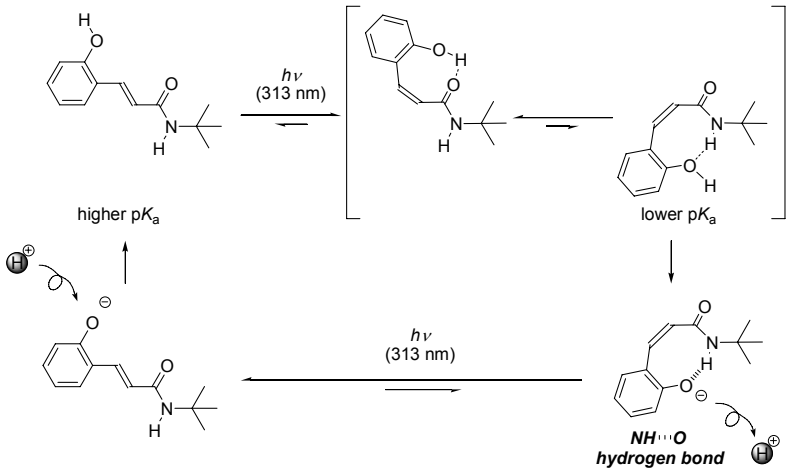

Scheme 4 Proposed photocycle.

Conclusion

The author designed the artificial photocycle consist of phenol *E*-1/*Z*-1 and phenolate *E*-2/*Z*-2 derivatives, which modeling the PYP photocycle. *Z*-1 is found to form an intramolecular OH· · · O=C hydrogen bond both in acetonitrile-d_3 solution and in solid state, and *Z*-2 is determined to form an intramolecular NH···O hydrogen bond in acetonitrile-d_3 solution. *Ortho*-coumaric acid moiety has an extended π-conjugation in phenolate, thus the red shift of the absorption maximum was observed. Because of the difference of the absorption wavelength, phenol and phenolate have different *E*/*Z* ratio whereas same wavelength light irradiation. 313 nm UV light irradiation generate *Z* form in phenol and generate *E* form in phenolate, preferentially. The pK_a value of the phenol compound was lowered in *Z* compound by stabilizing the *Z* phenolate with formation of

an intramolecular NH···O hydrogen bond. The change of *E*/*Z* ratio in phenol and phenolate, and the decrease of pK_a value in *Z* phenol compound, indicate that the artificial photocycle was constructed like PYP photocycle containing protonation and deprotonation process.

Experimental

General Procedure

All manipulations involving air- and moisture-sensitive compounds were carried out by the use of standard Schlenk technique under argon atmosphere. *E*-*ortho*-coumaric acid, 25% tetraethylammonium bydroxide in methanol solution were purchased from Tokyo-Kasei Co. Dicyclohyxylcarbodiimide was purchased from Peptide Institute, Inc. Dichloromethane was distilled over CaH_2. Methanol, tetrahydrofuran, diethylether, *n*-hexane, and acetonitrile were distilled over CaH_2 and dried over molecular sieves (3A).

Physical measurements

^{1}H (270 MHz) NMR spectra were measured on a JEOL JNM-GSX270 spectrometer. NOESY spectra were measured on a JEOL JNM-GSX400 spectrometer and Varian UNITYplus 600 MHz spectrometer. The ^{1}H NMR spectra were referenced to the tetramethylsilane protons at δ 0.00. UV-vis spectra was measured on a Shimazu UV-3100PC and Ocean Optics Inc. TP300-UV/VIS spectrometers. Elemental Analysis was performed at Elemental Analysis Center, Faculty of Science, Osaka University. All melting points of the compounds were measured on a micro melting point apparatus of YANAGIMOTO Co. ESI-MS measurements were performed on a Finnigan MAT LCQ ion trap mass spectrometer. FT-IR spectra were measured on a JASCO FT/IR-8300 spectrometer, and the solid FT-IR measurement was performed in KBr glass cell with nujol. pK_a measurement was performed using a potentiometric titration in 10 mM micellar solution at 298 K with a Metrohm 716 DMS titrino whtich is combined with Metrohm 728 stirrer and a saturated calomel LL micro pH glass electrode. The saturated calomel micro glass electrode was calibrated with the 0.05 M $KHC_8H_4O_4$ buffer (pH = 4.01) and the 0.0025 M KH_2PO_4 buffer (pH = 6.87) at 303 K. The potentiometric titration was performed three times. pK_a values are estimated by an average value of each measurements.

Preparation of (*E*)-*N*-*tert*-butyl-3-(2-hydroxyphenyl) acrylamide (*E*-1)

To a 1L tetrahydrofuran solution of *E*-*ortho*-coumaric acid (2.01 g, 12.2 mmol) and *tert*-butylamine (2.6 mL, 24.4 mmol) were added dicyclohyxylcarbodiimide (DCC, 4.44 g, 24.4 mmol). The white suspension was stirred at room temperature for 2 days. The solvent was

removed under reduced pressure to ontain white solid. The solid was dissolved in 100 mL of 0.8 mol L^{-1} sodium hydroxide aqueous solution. The yellow solution was moved to dropping funnel and washed with 150 mL of ethylacetate/diethylether (1/1, v/v). The organic layer was extracted again by 0.8 M aqueous sodium hydroxide solution for three times. Combined aqueous layer was washed with 100 mL of *n*-hexane. Cooling in ice bath, the aqueous layer was acidified by sulfuric acid aqueous solution (pH 6-7).Orange solution was turned to white suspension. The mixture was extracted with ethylacetate/diethylether (1/1, v/v) for three times. Organic layer was washed by 4% sodium bicarbonate aqueous solution for three times. Organic layer was dried over anhydrous magnesium sulfate, and thesolvent was removed under reduced pressure. The white powder was recrystallized from hot acetonitrile to obtain colorless crystal (1.25 g 46.8%). m.p. 229-230 ^{o}C; (Found: C, 71.14; H, 7.90; N, 6.53. Calc. for $C_{13}H_{17}NO_2$: C, 71.21; H, 7.81; N, 6.39 %); ν_{max}(in nujol mull)/cm^{-1} 3357 (NH), 3130-3047(OH), and 1657 (C=O); δ_H(270 MHz; acetonitrile-d_3) 1.36 (s, 9H; *tert*-Butyl), 6.26 (br s, 1H; NH), 6.58 (d, ^3J(H,H)=15.8 Hz, 1H; olefin), 6.87 (dd, ^3J(H,H)=8.2 Hz, ^4J(H,H)=1.2 Hz, 1H; Aryl), 6.88 (dt, ^3J(H,H)=8.2 Hz, ^4J(H,H)=1.2 Hz, 1H; Aryl), 7.18 (dt, ^3J(H,H)=8.2 Hz, ^4J(H,H)=1.2 Hz, 1H; Aryl), 7.33(br s, 1H; OH), 7.44 (dd, ^3J(H,H)=8.2 Hz, ^4J(H,H)=1.2 Hz, 1H; Aryl), 7.63 ppm (d, ^3J(H,H)=15.8 Hz, 1H; olefin); *m/z* (ESI) 218.3 ($[M-H]^-$ requires 218.1), 220.1 ($[M + Na]^+$ requires 220.1), 242.2 ($[M + Na]^+$ requires 242.1), 461.0 ($[2M + Na]^+$ requires 461.2); pK_a = 9.84 (10 mM in 10% aqueous micellar solution of Triton® X-100).

Preparation of (*Z*)-*N*-*tert*-butyl-3-(2-hydroxyphenyl) acrylamide (*Z*-1)

(*E*)-*N*-*tert*-butyl-3-(2-hydroxyphenyl) acrylamide (*E*-1, 441.2 mg, 2.01 mmol) was dissolved in 50 mL of acetonitrile. UV-light was irradiated to the solution for 400 minutes. The solvent was removed under reduced pressure. The residue was reprecipitated from diethylether/*n*-hexane. White precipitate was collected by filteration and the powder was suspended in ice-cooled chroloform. The suspension was filtered and the filterate was concentrated under reduced pressure. Pale yellow powder was recrystallized from ehtylacetate/*n*-hexane to obtain colorless crystal (154.4 mg, 35%). δ_H(270 MHz; acetonitrile-d_3) 1.32 (s, 9H; *tert*-Butyl), 5.97 (d, ^3J(H,H)=13.0 Hz, 1H; olefin), 6.72 (br s, 1H; NH), 6.77 (d, ^3J(H,H)=13.0 Hz, 1H; olefin), 6.87 (dt, ^3J(H,H)=7.5 Hz, ^4J(H,H)=1.2 Hz, 1H; Aryl), 6.89 (dd, ^3J(H,H)=7.5 Hz, ^4J(H,H)=1.2 Hz, 1H; Aryl), 7.22 (dt, ^3J(H,H)=7.5 Hz, ^4J(H,H)=1.2 Hz, 1H; Aryl), 7.23(dd, ^3J(H,H)=7.5 Hz, ^4J(H,H)=1.2 Hz, 1H; Aryl), and 9.87 ppm (br s, 1H; OH); pK_a = 9.70 (10 mM in 10% aqueous micellar solution of Triton® X-100).

Preparation of [tetraethyl-ammonium] 2-((*E*)-2-(*tert*-butylcarbamoyl)vinyl) phenolate (*E*-2)

(*E*)-*N*-*tert*-butyl-3-(2-hydroxyphenyl) acrylamide (*E*-1, 100.9 mg, 0.46 mmol) was dissolved in 1 mL of methanol. To the solution was added 25% tetraethylammonium bydroxide solution in methanol (0.25 mL, 0.41 mmol). The solution was stirred for 2 hours and the solvent was removed under reduced pressure. The residue was washed with 10 mL of diethylether twice. The powdeer was recrystallized from acetonitrile/diethylether to obtain yellow crystalline. δ_H(270 MHz; acetonitrile-d_3) 1.20 (t, ^3J(H,H)=7.3 Hz, 12H; NEt_4), 1.35 (s, 9H; *tert*-Butyl), 3.15 (q, ^3J(H,H)=7.3 Hz, 8H; NEt_4), 6.11 (s, 1H; NH), 6.31 (dt, ^3J(H,H)=7.3 Hz, ^4J(H,H)=1.2 Hz, 1H; Aryl), 6.67 (dd, ^3J(H,H)=7.3 Hz, ^4J(H,H)=1.2 Hz, 1H; Aryl), 6.88 (d, ^3J(H,H)=15.5 Hz, 1H; olefin), 6.92 (dt, ^3J(H,H)=7.3 Hz, ^4J(H,H)=1.2 Hz, 1H; Aryl), 7.18 (dd, ^3J(H,H)=7.3 Hz, ^4J(H,H)=1.2 Hz, 1H; Aryl), 7.62 ppm (d, ^3J(H,H)=15.5 Hz, 1H; olefin).

Preparation of [tetraethyl-ammonium] 2-((*E*)-2-(*tert*-butylcarbamoyl)vinyl) phenolate (*Z*-2)

(*Z*)-*N*-*tert*-butyl-3-(2-hydroxyphenyl) acrylamide (*E*-1, 100.9 mg, 0.46 mmol) was dissolved in 1 mL of methanol. To the solution was added 25% tetraethylammonium bydroxide solution in methanol (0.25 mL, 0.41 mmol). The solution was stirred for 2 hours and the solvent was removed under reduced pressure. The residue was washed with 10 mL of diethylether twice. The powdeer was recrystallized from acetonitrile/diethylether to obtain yellow crystalline. δ_H(270 MHz; acetonitrile-d_3) 1.21 (t, ^3J(H,H)=7.4 Hz, 12H; NEt_4), 1.23 (s, 9H; *tert*-Butyl), 3.16 (q, ^3J(H,H)=7.4 Hz, 8H; NEt_4), 5.57 (d, ^3J(H,H)=13.0 Hz, 1H; olefin), 6.21 (dt, ^3J(H,H)=7.6 Hz, ^4J(H,H)=1.8 Hz, 1H; Aryl), 6.50 (dd, ^3J(H,H)=7.6 Hz, ^4J(H,H)=1.8 Hz, 1H; Aryl), 6.61 (d, ^3J(H,H)=13.0 Hz, 1H; olefin), 6.89 (dt, ^3J(H,H)=7.6 Hz, ^4J(H,H)=1.8 Hz, 1H; Aryl), 6.98 (dd, ^3J(H,H)=7.6 Hz, ^4J(H,H)=1.8 Hz, 1H; Aryl), 9.58 ppm (br s, 1H; NH).

Crystallographic Data Collections and Structure Determinations of *E*-1 and *Z*-1

A suitable single crystals of *E*-1 and *Z*-1 were mounted on a fine nylon loop with nujol and immediately freezed at 200±1 K. All measurements were performed on a Rigaku RAXIS-RAPID Imaging Plate differactometer with graphite monochromated MoKα radiation (λ = 0.71075 Å). The structures were solved by direct method (SIR 92) [62] and the following refinements were performed using SHELXL-97 [63] and teXsan crystallographic software package. All non-hydrogen atoms were refined anisotropically. The coordinates of OH and NH protons were refined by using fixed thermal factors, and the other protons were placed in calculated position. Crystal data for $C_{13}H_{17}NO_2$ (*E*-1): 0.35x0.30x0.02 mm^3, orthorhombic, Pbca (#61), a = 12.940(5) Å, b = 9.252(5) Å, c = 20.60(1) Å, V = 2466(3) $Å^3$, Z = 8, ρ_{calcd} = 1.181 g cm^{-3}, μ (MoK_α) = 0.79 cm^{-1}, M_w = 219.28. Total number of reflection measured 23376, unique reflections 21726 (R_{int} = 0.174), Final R indices: R_1 = 0.058, wR_2 = 0.128 for all data. GOF (F^2) = 1.03. Crystal data for $C_{13}H_{17}NO_2$ (*Z*-2): 0.40x0.35x0.08 mm^3, monoclinic, $P2_1/c$ (#14), a =

11.000(6) Å, b = 12.346(16) Å, c = 9.398(7) Å, β = 103.58(2) °, V = 1240(1) Å^3, Z = 4, ρ_{calcd} = 1.174 g cm^{-3}, μ (MoK$_\alpha$) = 0.79 cm^{-1}, M_w = 219.28. Total number of reflection measured 11695, unique reflections 11384 (R_{int} = 0.089), Final R indices: R_1 = 0.070, wR_2 = 0.129 for all data. GOF (F^2) = 1.04. CCDC xxxxx and CCDC xxxxx contain the supplementary crystallographic data for this paper. These data can be obtained free of charge from Cambridge Crystallographic Data Centre via www.ccdc.cam.ac.uk/data_request/cif.

UV-light irradiation technique for UV-vis and ^{1}H NMR spectrum measurement

Xe/Hg lamp (MUV-202U, Moritex Co.) was used for 313 nm UV-light irradiation. UV-light was filtered through 6784-t01.uv1 (Asahi tech.) to pick out the 313 nm emission line of Hg gas. For 365, 405, and 436 nm irradiation, the filters of #43-155 FILTER INT 365NM 50.8mm SQ, #43-156 FILTER INT 405NM 50.8mm SQ, and #43-161 FILTER INT 436NM 50.8mm SQ (Edmund Optics Inc.) are used respectively. Sample was dissolved in the distilled solvent under argon atmosphere and sealed in NMR tube or UV cell. The spectrum was measured before and after irradiation. During irradiation and spectrum measurements, the sample was always kept desired temperature.

Potentiometric titration traced by UV-vis spectrum

To the solution of phenol derivative dissolved in distilled THF was added raurilether, and the solution was stirred for several minutes. THF was removed under reduced pressure, and the residue was added to sodium perchlorate aqueous solution. The UV-vis spectrum and the pH value were measured at the same time, by using reaction tracing system of fiber UV-vis spectrometer. During each measurements, the sample was always kept at 303 K in temperature controlled bath.

References

[1] G. O. Borgstahl, D. R. Williams, E. D. Getzoff, *Biochemistry* **1995**, *34*, 6278-6287.

[2] A. Warshel, *Biochemistry* **1981**, *20*, 3167-3177.

[3] Y. Imamoto, M. Kataoka, F. Tokunaga, T. Asahi, H. Masuhara, *Biochemistry* **2001**, *40*, 6047-6052.

[4] Y. Imamoto, Y. Shirahige, F. Tokunaga, T. Kinoshita, K. Yoshihara, M. Kataoka, *Biochemistry* **2001**, *40*, 8997-9004.

[5] U. K. Genick, S. M. Soltis, P. Kuhn, I. L. Canestrelli, E. D. Getzoff, *Nature*, **1998**, *392*, 206-209.

[6] M. Baca, G. E. Borgstahl, M. Boissinot, P. M. Burke, D. R. Williams, K. A. Slater, E. D.

Getzoff, *Biochemistry*, **1994**, *33*, 14369-14377.

[7] M. Kim, R. A. Mathiesm W. D. Hoff, K. J. Hellingwerf, *Biochemistry*, **1995**, *34*, 12669-12672.

[8] B. Perman, V. Srajer, Z. Ren, T. Teng, C. Pradervand, T. Ursby, D. Bourgeois, F. Schotte, M. Wulff, R. Kort, K. Hellingwerf, K. Moffat, *Science*, **1998**, *279*, 1946-1950.

[9] U. K. Genick, G. E. O. Borgstahl, Z. R. Kingham Ng, C. Pradervand, P. M. Burke, V. Srajer, T. Y. Teng, W. Schildkamp, D. E. McRee, K. Moffat, E. D, Getzoff, *Science*, **1997**, *275*, 1471-1475.

[10] A. Xie, W. D. Hoff, A. R. Kroon, K. J. Hellingwerf, *Biochemistry*, **1996**, *35*, 14671-14678.

[11] A. Xie, L. Kelemen, J. Hendriks, B. J. White, K. J. Hellingwerf, W. D. Hoff, *Biochemistry*, **2001**, *40*,1510-1517.

[12] Y. Imamoto, K. Mihara, O. Hisatomi, M. Kataoka, F. Tokunaga, N. Bojkova, K. Yoshihara, *J. Biol. Chem.*, **1997**, *272*, 12905-12908.

[13] G. Rubinstenn, G.. W. Vuister, F. A. Mulder, P. E. Dux, R. Boelens, K. J. Hellingwerf, R. Kaptein, *Struct. Biol.*, **1998**, 568-570.

[14] D. P. H. Cruikahank, K. W., and D. J. Tholen, *Nature*, **1985**, *315*, 122-124.

[15] M. C. Fujinaga, M. M., N. I. Tarosova, S. C. Morimann, and M. N. G. James, *Protein Science*, **1995**, 960-972.

[16] M. J. Millar, R. J. K. Mohano, J. Leis and A. Wlodawer, *Nature*, **1989**, *337*, 576-579.

[17] A. M. C. Silva, E. R., H. L. Cham, and J. W. Erickson, *J. Mol. Biol.*, **1996**, *255*, 324-346.

[18] K. B. suguna, R. R., E. A. Padlan, E. Subramanian, S. Scheriff, G.. H. Cohen, D. R. Davis, *J. Mol. Biol.*, **1987**, *196*, 877-900.

[19] A. M. Wlodawer, M. Jaskolski, and B. K. Sathyanarayama, *Science*, **1989**, *245*, 616-621.

[20] B. V. A. Cheesman, and D. L. Rabenstein, *J. Am. Chem. Soc.*, **1988**, *110*, 6359-6364.

[21] Z. R. W. Gan, and W. W., *J. Biol. Chem.*, **1987**, *262*, 6704-6707.

[22] H. C. F. Hawkins, *Biochem. J.*, **1991**, 335-339.

[23] S. D. R. Katti, *Protein Sci.*, **1995**, *4*, 1998-2005.

[24] S. D. J. Lewis, F. A., and J. A. Shafer, *Biochemistry*, **1976**, *15*, 5009-5017.

[25] S. D. J. Lewis, F. A., and J. A. Shafer, *Biochemistry*, **1981**, *20*, 48-51.

[26] S. Z. P. J. Liu, W. W. Johnson, G. L. Gilliland, and R. N. Armstrong, *J. Biol. Chem.*, **1992**, *267*, 4296-4299.

[27] J. L. B. Martin, J. C. A., J. Kuriyan, *Nature*, **1993**, *365*, 464-468.

[28] J. W. C. Nerson, T. E., *Biochemistry*, **1994**, *33*, 5974-5983.

[29] U. M. Srinivasan, J.J., *Biochemistry*, **1997**, *36*, 3199-3206.

[30] C. Mattos, D. A. Giammona, G. A. Petsko, D. Ringe, *Biochemistry*, **1995**, *34*, 3193-3203.

[31] M. Irie, T. Fukaminato, T. Sasaki, N. Tamai, T. Kawai, *Nature* **2002**, *420*, 759-760.

[32] M. Irie, O. Miyatake, K. Uchida, T. Eriguchi, *J. Am. Chem. Soc.* **1994**, *116*, 9894-9900.

[33] J. Hayakawa, A. Momotake, T. Arai, *Chem. Commun.* **2003**, 94-95.

[34] J. Hayakawa, A. Momotake, R. Nagahata, T. Arai, *Chem. Lett.* **2003**, *32*, 1008-1009.

[35] H. Tatewaki, T. Mizutani, J. Hayakawa, T. Arai, M. Tarazima, *J. Phys. Chem. A* **2003**, *107*, 6515-6521.

[36] J. H. Yoo, I. Cho, S. Y. Kim, *J. Polym. Sci. part A: Polym. Chem.* **2004**, *42*, 5401-5406.

[37] O. Ohtani, R. Sasai, T. Adachi, I. Hatta, K. Takagi, *Langmuir* **2002**, *18*, 1165-1170.

[38] R. Behrendt, C. Renner, M. Schenk, F. Wang, J. Wachtveitl, D. Oesterhelt, L. Moroder, *Angew. Chem. Int. Ed.* **1999**, *38*, 2771-2774.

[39] R. Behrendt, M. Schenk, H. J. Musiol, L. Moroder, *J. Peptide Sci.* **1999**, *5*, 519-529.

[40] S. Kobatake, S. Takami, H. Muto, T. Ishikawa, M. Irie, *Nature* **2007**, *446*, 778-781.

[41] F. D. Lewis, B. A. Yoon, T. Arai, T. Iwasaki, K. Tokumaru, *J. Am. Chem. Soc.* **1995**, *117*, 3029-3036.

[42] T. Arai, M. Moriyama, K. Tokumaru, *J. Am. Chem. Soc.* **1994**, *116*, 3171-3172.

[43] A. Masumoto, K. Maeda, T. Arai, *J. Phys. Chem. A* **2003**, *107*, 10039-10045.

[44] M. Ikegami, T. Arai, *Bull. Chem. Soc. Jpn.* **2003**, *76*, 1783-1792; e) M. Ikegami, T. Arai, *Chem. Lett.* **2005**, *34*, 492-493.

[45] Y. Odo, K. Matsuda, M. Irie, *Chem. Eur. J.* **2006**, *12*, 4283-4288.

[46] S. H. Kawai, S. L. Gilat, J. M. Lehn, *Eur. J. Org. Chem.* **1999**, 2359-2366.

[47] M Irie, Y Hirano, S Hashimoto, K Hayashi, *Macromolecules* **1981**, *14*, 262-267.

[48] K Ishihara, T Matsuo, K Tsunemitsu, I Shinohara, *Journal of Polymer Science: Polymer Chemistry Ed.* 1984, *22*, 3687-3695.

[49] A. Onoda, Y. Yamada, J. Takeda, Y. Nakayama, T. Okamura, M. Doi, H. Yamamoto, N. Ueyama, *Bull. Chem. Soc. Jpn.* **2004**, *77*, 321-329.

[50] A. Onoda, Y. Yamada, Y. Nakayama, K. Takahashi, H. Adachi, T. Okamura, A. Nakamura, H. Yamamoto, N. Ueyama, D, Vyprachticky, Y. Okamoto, *Inorg. Chem.* **2004**, *43*, 4447-4455.

[51] N. Ueyama, K. Takahashi, A. Onoda, T. Okamura, H. Yamamoto, *Macromol. Symp.* **2003**, *204*, 287-294.

[52] D. Kanamori, T. Okamura, H. Yamamoto, N. Ueyama, *Angew. Chem. Int. Ed.* **2005**, *44*, 969-972.

[53] D. Kanamori, A. Furukawa, T. Okamura, H. Yamamoto, N. Ueyama, *Otg. Biomol. Chem.* **2005**, *3*, 1453-1459.

[54] D. Kanamori, Y. Yamada, A. Onoda, T. Okamura, S. Adachi, H. Yamamoto, N. Ueyama, *Inorg. Chim. Acta.* **2005**, *358*, 331-338.

[55] K. Takahashi, M. Doi, A. Kobayashi, T. Taguchi, A. Onoda, T. Okamura, H. Yamamoto, N.

Ueyama, *J. Cryst. Growth* **2004**, *263*, 552-563.

[56] N. Ueyama, K. Takahashi, A. Onoda, T. Okamura, H. Yamamoto, *Macromol. Symp.* **2002**, *186*, 129-134.

[57] N. Ueyama, H. Kozuki, M. Doi, Y. Yamada, K. Takahashi, A. Onoda, T. Okamura, H. Yamamoto, *Macromolecules* **2001**, *34*, 2607-2614.

[58] A. Onoda, Y. Yamada, M. Doi, T. Okamura, N. Ueyama, *Inorg. Chem.* **2001**, *40*, 516-521.

[59] A. Onoda, H. Yamamoto, Y. Yamada, K. Lee, S. Adachi, T. Okamura, K. Yoshizawa-Kumagaye, K. Nakajima, T. Kawakami, S. Aimoto, N. Ueyama, *Biopolymers*, **2005**, *80* (2 and 3), 233-248.

[60] D. Kanamori, Y. Yamada, A. Onoda, T. Okamura, S. Adachi, H. Yamamoto, N. Ueyama, *Inorganic Chim. Acta* **2005**, *358*, 85-92.

[61] N. Ueyama, M. Inohara, A. Onoda, T. Ueno, T. Okamura, A. Nakamura, *Inorganic Chem.* **1999**, *38*, 4028-4031.

[62] A. Altomare, M. C. Burla, M. Camalli, M. Cascarano, C. Giacovazzo, A. Guagliardi, G. Polidori, *J. Appl. Crystallogr.* **1994**, *27*, 435.

[63] G. M. Sheldrick, SHELXS-97, Program for the Refinement of Crystal Structures, University of Göttingen, Göttingen (Germany), **1997**.

Chapter 6

The conformation change of oligopeptide by photoswitching of multiple intramolecular NH···O hydrogen bonds

Introduction

In native proteins, the switching of intramolecular hydrogen bond network plays an important role to construct the characteristic second or third dimension structures. Particularly in α-helix structure, terminal residues plays an important role for construct their structure,[1,2] because the terminal NH···O hydrogen bond stabilizes and supports the forward hydrogen bond (Figure 1). β-turn structure were also have been investigated.[3-7] *Onoda et al.* investigated the conformation change of the tripeptide (Asp-Val-Gly), which have similar residues around the active site of pepsin, and reported that the deprotonation of aspartic acid causes the linear to turn conformation change.[8, 9] The conformation change caused by the switching of intramolecular NH···O hydrogen bond was also investigated in artificial compound. Chair to boat transformation of cyclohexyl skeleton was observed by switching of intramolecular NH···O hydrogen bond according with the deprotonation of Kemp's acid.[10]

The author introduced the concept of OFF→ON switching device of intramolecular NH···O hydrogen bond, which introduced in chapter 3 (*E*-1/*Z*-1 and *E*-2/*Z*-2), toward the C-terminal of oligopeptide (Scheme 1). The designed compounds are expected to switch the conformation from linear to turn, not only triggered by deprotonation process, but

also by *E*/*Z* photoisomerization. The *Z* carboxylate of dipeptide introduced compound, *Z*-6, is expected to form three intramolecular NH···O hydrogen bond, and to form turned structure.

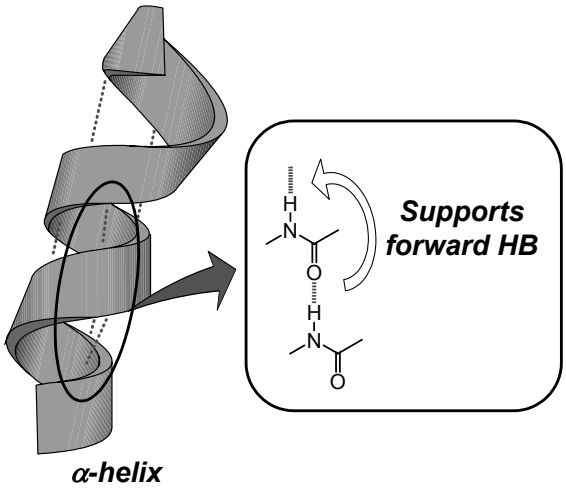

Figure 1. Schematic figure of the effect of terminal NH···O hydrogen bond.

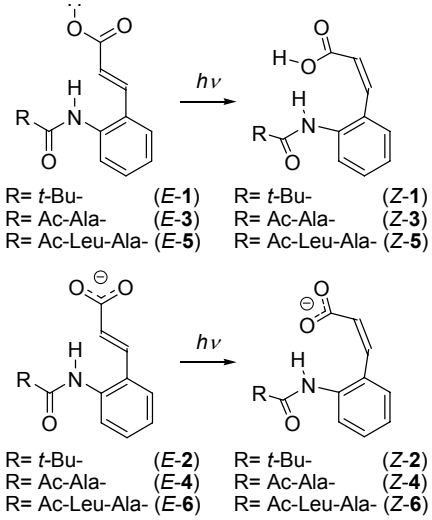

Scheme 1. *E* to *Z* photoisomerization of cinnamic acid derivatives *E*-1 ~ *E*-6, and *Z*-1 ~ *Z*-6.

Results and Discussion

Synthesis

The synthetic method was shown in Scheme 2. Objectives were synthesized from *ortho*-amino cinnamic acid derivatives by stepwise elongation of N-terminal. Carboxylates were prepared through counter-cation exchange reaction of corresponding carboxylic acid derivatives with tetramethylammonium acetate.

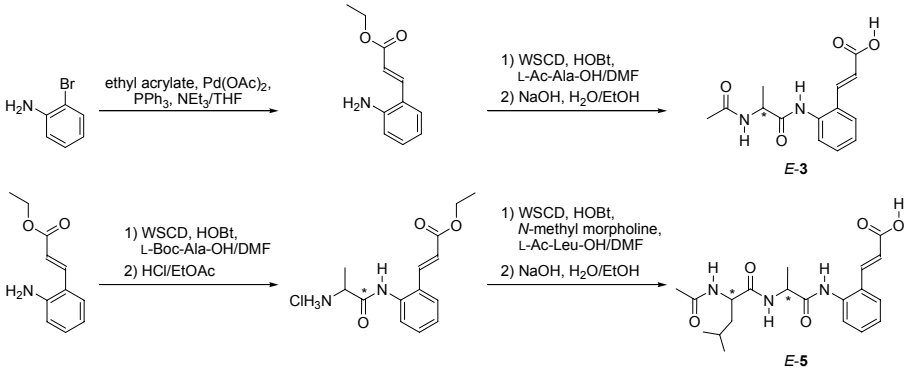

Scheme 2. Synthesis of cinnamic acid derivatives, monopeptide introduction *E*-3 and dipeptide introduction *E*-6.

Direct photoisomerization

Photoisomerization reaction was traced by UV–visible (UV–vis) spectra. UV–vis spectrum changes of *E*-3, *E*-4, *E*-5 and *E*-6 caused by photoirradiation in dimethyl sulfoxide (DMSO) solution at 293 K are shown in Figure 2. *E*-3, *E*-4, *E*-5 and *E*-6 were isomerized from *E* to *Z* configurations, and reached the photostationary state (PSS) at 313 nm UV-light irradiation. Solid lines, corresponding *E* isomers, are the spectra measured before irradiation, and broken lines represent the estimated spectra of *Z* isomers obtained from the *E*/*Z* ratio in photosteady state (PSS) by ^{1}H NMR spectrum. The spectra were almost same whereas the peptide moiety was changed. The elongation of peptide doesn't affect the π-conjugation of cinnamic acid moiety. The absorbance values of *E* compounds were decreased in accordance with the two-state transition following irradiation (broken lines), which indicates that only corresponding *Z* isomers are formed without any side reactions. The fraction of *Z* compounds in the PSS was determined from the integration ratio of ^{1}H NMR spectra. The *E*/*Z* ratio of the carboxylates are 18/82 in *E*-4/*Z*-4 and 20/80 in *E*-6/*Z*-6, whereas that of the carboxylic acids are 31/69 in *E*-3/*Z*-3 and 32/68 in *E*-5/*Z*-5.

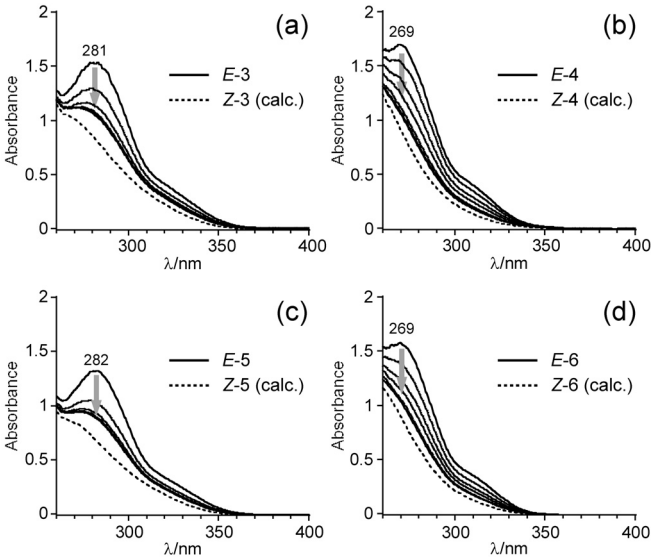

Figure 2. Time course UV-vis spectra changes of a) *E*-3, b) *E*-4, c) *E*-5, and d) *E*-6, 1 mM in acetonitrile at 293 K. Solid lines are those before irradiation, and broken lines are calculated spectrum of *Z* compounds.

Molecular structures in solution

The ^{1}H NMR spectra before and after photoirradiation toward *E*-3 and *E*-4 are shown in Figure 3, and that toward *E*-5 and *E*-6 are shown in Figure 4, in DMSO-d_6 at 303 K. All signals are assigned by using nuclear Overhauser effect (NOE) and decoupling method. The signals were newly appeared after irradiation (dotted signals of panels b and d in Figure3, and panels b and d in Figure 4). The configurations of photoproducts were confirmed by $^{3}J_{HH}$ value of the olefin protons, which appeared after irradiation was observed around 12-13 Hz. It coincides the typical values of the *cis* olefin protons, and the compounds generated after irradiation were confirmed to have *Z* configuration.

The chemical shifts of amide NH signals are focused to discuss about the hydrogen bond formation. In monopeptide, compound 3 and 4, the chemical shifts of the aromatic amide NH (Aryl-NH) signals of *Z* isomers at 303 K were 9.41 ppm in *Z*-3 and 12.58 ppm in *Z*-4 (Figure 3). The temperature dependency (range, 303-333 K) of the Aryl-NH chemical shift of *Z*-4 is –1.1 ppb·K^{-1}, whereas that of *Z*-3 is –5.9 ppb·K^{-1}. The significant downfield shift ($\Delta\delta$ = 3.17 ppm) and the decrease of temperature dependency

suggest that Aryl NH of *Z*-4 forms a strong intramolecular NH···O hydrogen bond in DMSO-d_6 solution like that formed in *Z*-2. However, all of the chemical shifts of the alanyl amide NH (Ala-NH) signals were found around 8 ppm, at 8.16 ppm in *Z*-3 and 8.04 ppm in *Z*-4, and the temperature coefficients (range, 303-333 K) were almost same large value (–5.0 ppb·K^{-1} in Z-3 and in Z-4). These results indicate that Ala-NH doesn't form strong intramolecular hydrogen bond in *Z*-4 (Chart 1).

In dipeptide, compound 5 and 6, the chemical shift of Aryl-NH was downfield shifted and the temperature coefficient was decreased in *Z*-6 (12.72 ppm, –1.2 ppb·K^{-1}) (Figure 4). The result indicate that Aryl-NH of Z-6 forms an strong intramolecular NH···O hydrogen bond like that of *Z*-4 or *Z*-2. The temperature coefficient of Ala-NH was decreased in *Z*-6 comparing with *Z*-5 (–5.8 toward –4.8 ppb·K^{-1}). That means that Ala-NH of *Z*-6 forms the intramolecular interaction, such as hydrogen bonding. The chemical shifts of leucyl NH (Leu-NH) protons were found at 7.98 ppm (–4.5 ppb·K^{-1}) in *Z*-5 and 8.22 ppm (–2.4 ppb·K^{-1}) in *Z*-6. The downfiled shift and significant decrease of temperature dependency indicate that Leu-NH proton in *Z*-6 forms intramolecular NH···O hydrogen bond. The Leu-NH of *E*-6 was found in the most downfield shifted region (8.74 ppm), at the smallest temperature coefficient (–1.0 ppb·K^{-1}). This result indicate that Leu-NH proton of *E*-6 forms the intramolecular NH···O hydrogen bond by forming turn conformation, which is stronger than that formed in *Z*-6 (Scheme 3). The formation of multiple hydrogen bonds must affect to weaken the strength of each hydrogen bond.

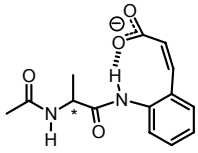

Chart 1.

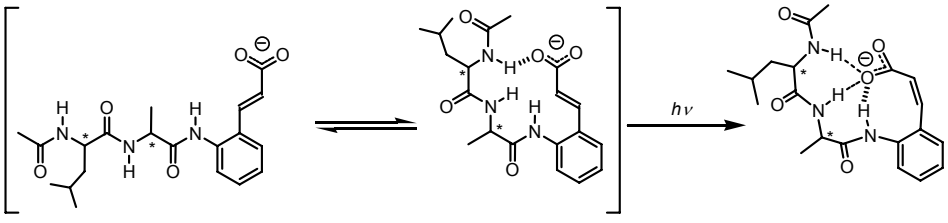

Scheme 3. Intramolecular hydrogen bond formation of *E*-6 and *Z*-6.

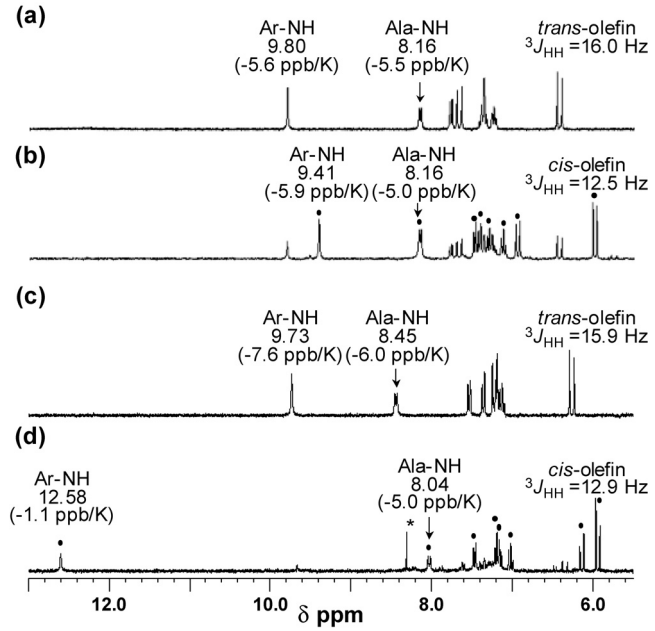

Figure 3. [1]H NMR spectra of *E*-3, a) before, and b) after 313 nm irradiation, and *E*-4 c) before and d) after 313 nm irradiation, 5 mM in DMSO-d_6 at 303 K.

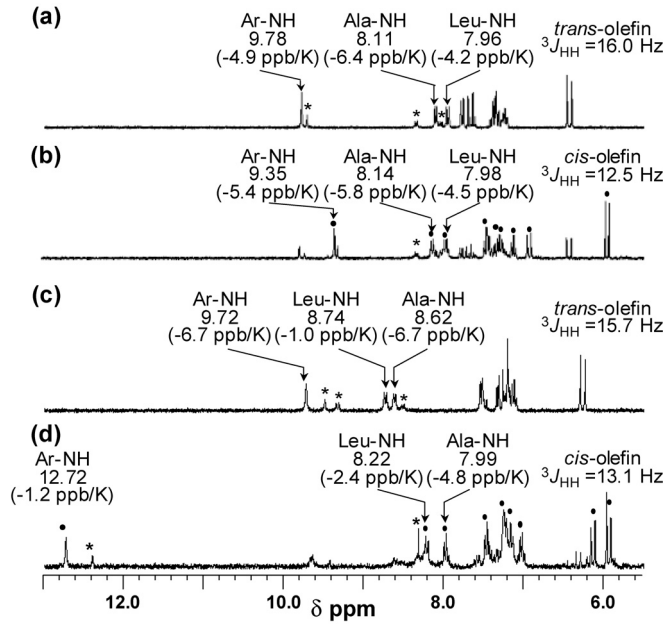

Figure 3. [1]H NMR spectra of *E*-5, a) before, and b) after 313 nm irradiation, and *E*-6 c) before and d) after 313 nm irradiation, 5 mM in DMSO-d_6 at 303 K.

The nuclear Overhauser enhancement spectroscopy (NOESY) spectra were measured for *E*-6 and *Z*-6, to discuss about the peptide conformation in DMSO-d_6 solution (Figure 5). In *E*-6, 21 kinds of NOE signals are found (Figure 6). Especially, NOE correlation between Ala-NH and Leu-γH, and correlation between Ala-βH and Aryl-NH were found. This NOE pattern of *E*-6 renounces the turn conformation (Scheme 3 middle), but persists the linear conformation (Scheme 3 left). However, the NOE signals between olefin protons (H1, H2) and side chain of peptide (Ala-βH, Leu-βH, Leu-γH) were observed at the same time. This NOE pattern of *E*-6 persists the turn conformation (Scheme 3 middle). These results indicate that *E*-6 forms linear conformation and turn conformation in equilibrium, in DMSO solution. Figure 5b shows the NOESY spectrum of *Z*-6. 21 kinds of NOE signals are found. Particularly, the NOE correlations between Aryl-NH and Ala-NH, between olefin proton (H2) and aryl proton (H3), and between Leu-δH and olefin proton (H1) were observed. These correlations, which were not observed in *E*-6, indicate that *Z*-6 is able to form the turn conformation in DMSO-d_6 solution like shown in Figure 6. It is attributed that three intramolecular NH···O hydrogen bonds formed in *Z*-6 contribute to stabilize the turn conformation. These results confirm the hydrogen bond switching as shown in Scheme 4.

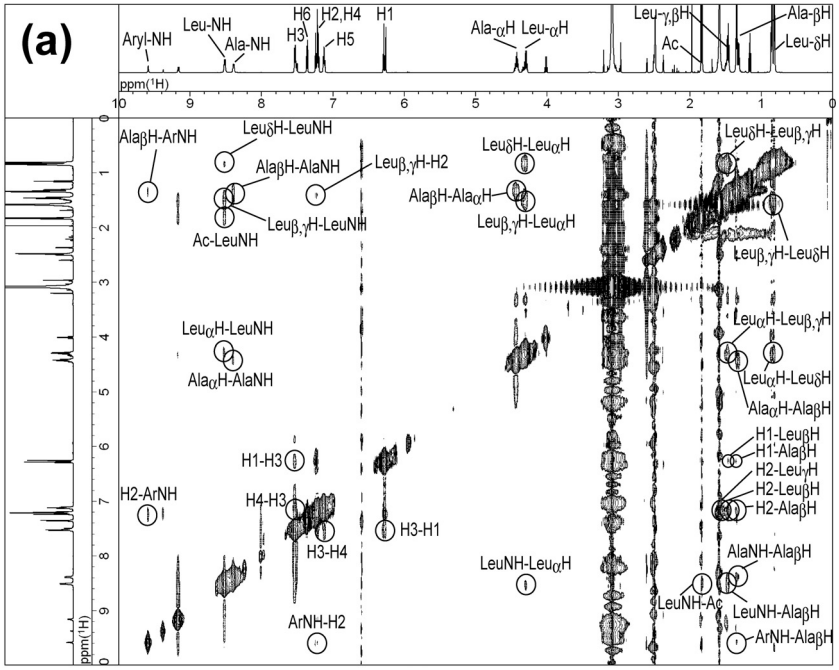

Figure 5a. NOESY spectra of *E*-6 in DMSO-d_6 solution at 303 K

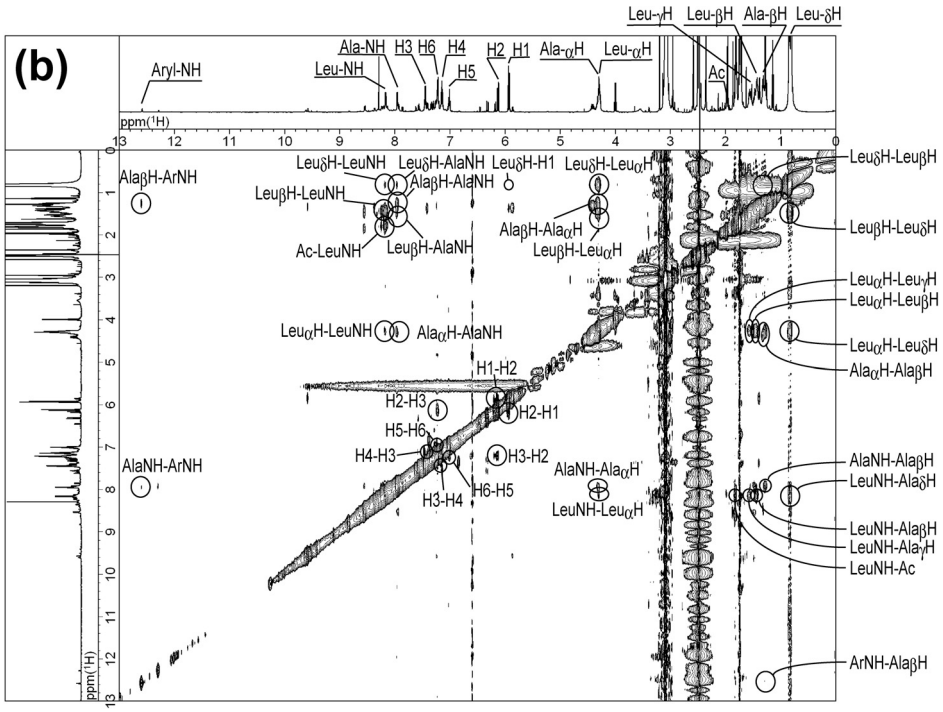

Figure 5b. NOESY spectra of *Z*-6 (photostationary state) in DMSO-d_6 solution at 303 K

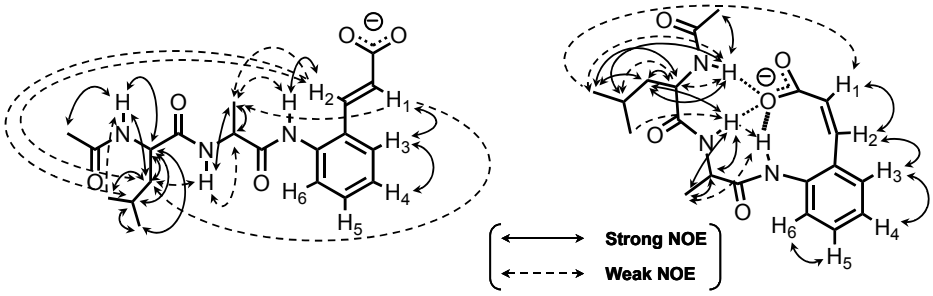

Figure 6. NOESY correlations of *E*-6 and Z-6.

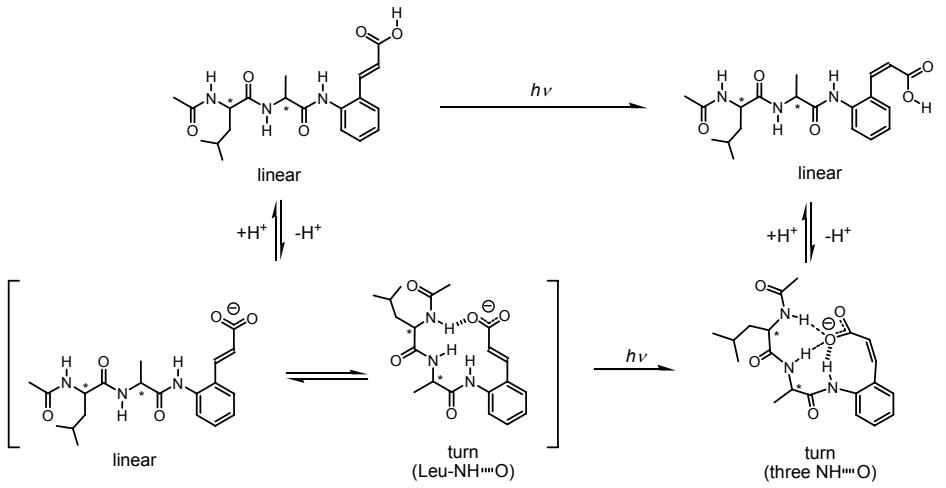

Scheme 4. Proposed conformation changes and photoswitching of intramolecular NH···O hydrogen bond network of *E*-5/*Z*-5 and *E*-6/*Z*-6.

Conclusion

The photoswitching of multiple hydrogen bonds between the amide NH of oligopeptide or arylamide and carboxylate oxygen were photoswitched by *E*/*Z* photoisomerization of cinnamate framework and deprotonation process. Monopeptide derivative (Ac-Ala-NH-C_6H_4-CH=CH- COOH) forms one intramolecular NH···O hydrogen bond in *Z* carboxylate (*Z*-4) between aryl NH and carboxyl oxygen; the amide NH of Ala moiety was free from any interaction. Dipeptide derivative (Ac-Leu-Ala-NH-C_6H_4-CH=CH-COOH) forms one intramolecular NH···O hydrogen bond in *E* carboxylate (*E*-6) between Leu NH and carboxyl oxygen, and forms three intramolecular NH···O hydrogen bonds in *Z* carboxylate (*Z*-6). Elongation of peptide moiety may stabilize the *Z* carboxylate by forming multiple intramolecular NH···O hydrogen bonds. The switching of intramolecular NH···O hydrogen bond of terminal amino acids indicate the possibility of photocontrol of second dimension structure of longer peptide, such as α-helix to random coil conversion.

Experimental

General procedures

All manipulations involving air- and moisture-sensitive compounds were carried out by the use of standard Schlenk technique under argon atmosphere. *N*-acetyl-L-leucine, 2-bromoaniline, triphenylphosphine, acrylic acid ethyl ester were purchased from Tokyo-Kasei Co. Palladium acetate, tetramethylammonium acetate were purchased from Aldrich Chemical Company, Inc. Boc-L-alanine, HOBt were purchased from Peptide Institute, Inc. *N*-acetyl-L-alanine was perchased from Wako Pure Chemical Industries, Ltd.. Dichloromethane was distilled over CaH_2. Methanol, tetrahydrofuran, diethylether, *n*-hexane, and acetonitrile were distilled over CaH_2 and dried over molecular sieves (3A).

Physical measurements

^{1}H (270 MHz) NMR spectra were measured on a JEOL JNM-GSX270 spectrometer. NOESY spectra were measured on a JEOL JNM-GSX400 spectrometer and Varian UNITYplus 600 MHz spectrometer. The ^{1}H NMR spectra were referenced to the tetramethylsilane protons at δ 0.00. UV-vis spectra was measured on a Shimazu UV-3100PC and Ocean Optics Inc. TP300-UV/VIS spectrometers. Elemental Analysis was performed at Elemental Analysis Center, Faculty of Science, Osaka University. All melting points of the compounds were measured on a micro melting point apparatus of YANAGIMOTO Co.

(*E*)-ethyl 3-(2-aminophenyl)acrylate (*E-ortho*-aminocinnamic acid ethyl ester)

To a two-necked round bottom flask was added acrylic acid ethyl ester (32.0 mL, 0.291 mol), 2-bromoaniline (25.0 g, 0.146 mol), palladium acetate (1.63 g, 7.3 mmol), and triphenylphosphine (3.83 g, 14.6 mmol), then suspended in distilled triethylamine (60 mL). The mixture was refluxed over one night in 130 ºC oil bath. The reaction was traced by TLC (ethyl acetate/hexane=1/3; v/v). Triethylamine hydrobromide and Pd catalyst are filtered off, and the solution was concentrated to obtain red oil. The mixture was dissolved in diethylether, washed with aqueous sodium bicarbonate for twice, and extracted by 2 % aqueous hydrochloride for 10 times. Combined aqueous hydrochloride layer was washed with diethylether/*n*-hexane (1/1;v/v), and alkalinized with solid sodium bicarbonate (pH 8~9). Yellow oily paste floated on a yellow suspension. The mixture was extracted with diethylether for 3 times. The combined organic layer was washed with brine, and dried over anhydrous magnesium sulfate. The solvent was removed under reduced pressure to obtain yellow oil. The oil was dissolved in diethylether and reprecipitated by *n*-hexane to obtain yellow powder. (Yield, 13.15 g, 47.3 %). δ_H(270 MHz; DMSO-d_6) 1.24 (3H, t, -CH_2-CH_3), 4.16 (2H, q, -CH_2-CH_3), 5.55 (2H, s, NH_2), 6.33 (1H, d, J = 15.8 Hz, olefin), 6.53 (1H, dt, J = 7.5 and 1.0, Aryl), 6.68 (1H, dd, J = 7.5 and 1.0, Aryl), 7.06

(1H, dt, J = 7.5 and 1.0, Aryl), 7.43 (1H, dd, J = 7.5 and 1.0, Aryl) and 7.85 (1H, d, J = 15.8, olefin).

Preparation of (*E*)-ethyl 3-(2-(*N*-acetyl-L-alanyl) amido phenyl)acrylate

(*E*)-ethyl 3-(2-aminophenyl)acrylate (810.6 mg, 4.24 mmol), *N*-acetyl-L-alanine (617.6 mg, 4..71 mmol), and 1-hydroxybenzotriazole (HOBt; 700.1 mg, 5.18 mmol) were dissolved in *N*,*N*-dimethylformamide (DMF, distilled, 5 mL). To the solution was added water soluble carbodiimide (WSCD, 1-Ethyl-3-(3-dimethylaminopropyl) carbodiimide; 804.2 mg, 5.18 mmol) at –20 ^{o}C. The solution was stirred at this temperature for 2 hours, and stirred at room temperature for 2 days. The solution was concentrated under reduced pressure to obtain white-yellow powder, and ethylacetate was added to obtain suspension. The precipitate was collected by filteration and washed with ethylacetate, 2 % aqueous hydrochloride solution, 4 % aqueous sodium bicarbonate solution, and diethylether. The white powder was dried under reduced pressure. White powder (1st. 694.9 mg). The organic solutions are combined and washed with with 2 % aqueous hydrochloride solution for 5 times, with 4 % aqueous sodium bicarbonate solution for 5 times, with water once, and with brine once. The organic layer was dried over anhydrous magnesium sulfate, and the solvent was removed under reduced pressure. The obtained yellow powder was suspended in a little amount of diethylether and the precipitate was collected by filteration. White powder (2nd. 359.4 mg). Total Yield was 1054.3 mg (81.7%). δ_H(270 MHz; DMSO-d_6) 1.25 (t, ^3J(H,H)= 7.0 Hz, 3H; -CH_2CH_3), 1.33 (d, ^3J(H,H)= 7.1 Hz, 3H; Ala βH), 1.86 (s, 3H; acetyl), 4.17 (m, ^3J(H,H)= 7.0 Hz, 2H; -CH_2CH_3), 4.47 (m, 1H; Ala αH), 6.53 (d, ^3J(H,H)=15.9, 1H; olefin), 7.25 (dt, ^3J(H,H)=7.4 Hz, ^4J(H,H)=2.0 Hz, 1H; Aryl), 7.33 (dd, ^3J(H,H)=7.4 Hz, ^4J(H,H)=2.0 Hz, 1H; Aryl), 7.41 (dt, ^3J(H,H)=7.4 Hz, ^4J(H,H)=2.0 Hz, 1H; Aryl), 7.71 (d, ^3J(H,H)=15.9, 1H; olefin), 7.81 (dd, ^3J(H,H)=7.4 Hz, ^4J(H,H)=2.0 Hz, 1H; Aryl), 8.15 (d, ^3J(H,H)=7.1 Hz, 1H; Ala NH), and 9.83 ppm (s, 1H; Aryl NH).

Preparation of (*E*)-3-(2-(*N*-acetyl-L-alanyl) amido phenyl)acrylic acid (*E*-3)

(*E*)-ethyl 3-(2-(*N*-acetyl-L-alanyl) amido phenyl)acrylate (1.04 g, 3.41 mmol) was dissolved in ethanol. 10.0 mL of 1.0 M sodium hydroxide aqueous solution (10.0 mmol) and 10.0 mL of water were added to the solution to obtain light yellow suspension. Ethanol was added to dissolve precipitate. The solution was stirred for 2 days at room temperature. The reaction was traced by TLC method (ethyl acetate/hexane=2/1; v/v). The solution was concentrated to white paste. The paste was dissolved in saturated sodium bicarbonate aqueous solution and washed with a little amount of ethyl acetate. The organic layer was extracted with satulated sodium bicarbonate aqueous solution again, and the combined aqueous layer was acidified by ice-cooled sulfuric acid aqueous solution toward pH 4, and extracted with ethylacetate for 3 times. Organic layer was dried over brine and over magnesium sulfate. Solvent was removed

under reduced pressure to obtain white powder. The powder was reprecipitated from diethylether/*n*-hexane. (white powder, 439.7 mg, 46.8%) m.p. 232 ^{o}C; (Found: C, 60.83; H, 5.82; N, 10.00. Calc. for $C_{14}H_{16}N_2O_4$: C, 60.86; H, 5.84; N, 10.14 %); δ_H(270 MHz; DMSO-d_6) 1.33 (d, ^3J(H,H)= 7.0 Hz, 3H; Ala βH), 1.87 (s, 3H; Ac), 4.48 (m, 1H; Ala αH), 6.45 (d, ^3J(H,H)=15.9, 1H; olefin), 7.25 (dt, ^3J(H,H)=7.4 Hz, ^4J(H,H)=2.0 Hz, 1H; Aryl), 7.36 (dd, ^3J(H,H)=7.4 Hz, ^4J(H,H)=2.0 Hz, 1H; Aryl), 7.40 (dt, ^3J(H,H)=7.4 Hz, ^4J(H,H)=2.0 Hz, 1H; Aryl), 7.68 (d, ^3J(H,H)=15.9, 1H; olefin), 7.78 (dd, ^3J(H,H)=7.4 Hz, ^4J(H,H)=2.0 Hz, 1H; Aryl), 8.16 (d, ^3J(H,H)=7.1, 1H; Ala N*H*), 9.80 (s, 1H; Aryl N*H*) and 12.28 ppm (s, 1H; COO*H*).

Preparation of (*E*)-ethyl 3-(2-(*N-tert*-butoxycarbonyl-L-alanyl) amido phenyl)acrylate

(*E*)-ethyl 3-(2-aminophenyl)acrylate (2.43 g, 12.7 mmol), *N-tert*-butoxycarbonyl-L-alanine (Boc-Ala-OH; 2.67 g, 14.1 mmol), and HOBt (2.10 g, 15.6 mmol) were dissolved in DMF (10 mL, distilled). To the solution was added WSCD (2.41 mg, 15.6 mmol) at –20 ^{o}C. The solution was stirred at this temperature for 30 minutes, at 0 ^{o}C for 2 hours, and at room temperature for 2 days. The solution was concentrated under reduced pressure to obtain orange oil, and ethylacetate was added to obtain orange-white suspension. The suspension was moved to the dropping funnel and washed with with 10 % aqueous citric acid solution for 4 times, with 4 % aqueous sodium bicarbonate solution for 3 times, and with brine once. The organic layer (orange solution) was dried over anhydrous magnesium sulfate, and the solvent was removed under reduced pressure. The obtained yellow powder was reprecipitated from diethylether/*n*-hexane. White powder (3.810 g, 82.6%) δ_H(270 MHz; DMSO-d_6) 1.25 (t, ^3J(H,H)= 7.0 Hz, 3H; -CH_2CH_3), 1.32 (d, ^3J(H,H)= 7.1 Hz, 3H; Ala βH), 1.38 (s, 9H; *t*-Bu), 4.17 (m, 3H; Ala αH, -CH_2CH_3), 6.53 (d, ^3J(H,H)=15.9, 1H; olefin), 7.00 (d, ^3J(H,H)=6.5 Hz, 1H; Ala N*H*), 7.24 (dt, ^3J(H,H)=7.4 Hz, ^4J(H,H)=2.0 Hz, 1H; Aryl), 7.35 (dd, ^3J(H,H)=7.4 Hz, ^4J(H,H)=2.0 Hz, 1H; Aryl), 7.41 (dt, ^3J(H,H)=7.4 Hz, ^4J(H,H)=2.0 Hz, 1H; Aryl), 7.73 (d, ^3J(H,H)=15.9, 1H; olefin), 7.81 (dd, ^3J(H,H)=7.4 Hz, ^4J(H,H)=2.0 Hz, 1H; Aryl), and 9.77 ppm (s, 1H; Aryl N*H*).

Preparation of (*E*)-ethyl 3-(2-(L-alanyl) amido phenyl)acrylate hydrochloride

(*E*)-ethyl 3-(2-(*N-tert*-butoxycarbonyl-L-alanyl) amido phenyl)acrylate (3.2647 g, 9.01 mmol) was dissolved in 35 mL of hydrochloride satulated ethylacetate. After stirring 5 minutes, the yellow solution turned to the white suspension. The suspension was stirred for a day. The precipitate was collected by filteration and washed with a little amount of ethyl acetate. The white powder was dried under reduced pressure in desiccator using sodium hydroxide as a desiccant. White powder (2.69 g, 99.8%) δ_H(270 MHz; DMSO-d_6) 1.25 (t, ^3J(H,H)= 7.0 Hz, 3H; -CH_2CH_3), 1.54 (d, ^3J(H,H)= 7.1 Hz, 3H; Ala βH), 4.14 (m, 1H; Ala αH), 4.18 (q, ^3J(H,H)= 7.0 Hz, 2H; -CH_2CH_3), 6.59 (d, ^3J(H,H)=15.9, 1H; olefin), 7.30 (dt, ^3J(H,H)=7.4 Hz,

^4J(H,H)=2.0 Hz, 1H; Aryl), 7.37 (dd, ^3J(H,H)=7.4 Hz, ^4J(H,H)=2.0 Hz, 1H; Aryl), 7.45 (dt, ^3J(H,H)=7.4 Hz, ^4J(H,H)=2.0 Hz, 1H; Aryl), 7.73 (d, ^3J(H,H)=15.9, 1H; olefin), 7.87 (dd, ^3J(H,H)=7.4 Hz, ^4J(H,H)=2.0 Hz, 1H; Aryl), 8.35 (br s, 3H; -NH_3Cl) and 10.50 ppm (s, 1H; Aryl N*H*).

Preparation of (*E*)-ethyl 3-(2-(*N*-acetyl-L-leucyl-L-alanyl-) amido phenyl)acrylate

(*E*)-ethyl 3-(2-(L-alanyl) amido phenyl)acrylate hydrochloride (1.00 g, 3.35 mmol), *N*-acetyl-L-leucine (644.1 g, 3.72 mmol), and HOBt (552.7 g, 4.09 mmol) were dissolved in DMF (8 mL, distilled). To the solution was added WSCD (634.9 mg, 4.09 mmol) at –20 ^oC. The solution was stirred at this temperature for 30 minutes, and at room temperature for 2 days. The solution was concentrated under reduced pressure to obtain yellow-white wet solid. 10% Citric acid aqueous solution was added to obtain white suspension. Precipitate was filtered and washed with 2% hydrochloric acid aqueous solution, water, and 4% sodium bicarbonate aqueous solution. The white powder was dried under reduced pressure. (836.2 mg, 59.8%) δ_H(270 MHz; DMSO-d_6) 0.84 (m, 6H; Leu δH), 1.25 (t, ^3J(H,H)= 7.0 Hz, 3H; -CH_2CH_3), 1.36 (d, ^3J(H,H)= 7.1 Hz, 3H; Ala βH), 1.44 (m, 2H; Leu βH), 1.59 (m, 1H; Leu γH), 1.83 (s, 3H; Ac), 4.17 (q, ^3J(H,H)= 7.0 Hz, 2H; -CH_2CH_3), 4.30 (m, 1H; Leu αH), 4.46 (m, 1H; Ala αH), 6.54 (d, ^3J(H,H)=15.9, 1H; olefin), 7.25 (dt, ^3J(H,H)=7.4 Hz, ^4J(H,H)=2.0 Hz, 1H; Aryl), 7.31 (dd, ^3J(H,H)=7.4 Hz, ^4J(H,H)=2.0 Hz, 1H; Aryl), 7.41 (dt, ^3J(H,H)=7.4 Hz, ^4J(H,H)=2.0 Hz, 1H; Aryl), 7.71 (d, ^3J(H,H)=15.9, 1H; olefin), 7.82 (dd, ^3J(H,H)=7.4 Hz, ^4J(H,H)=2.0 Hz, 1H; Aryl), 7.95 (d, ^3J(H,H)=8.1, 1H; Leu N*H*), 8.10 (d, ^3J(H,H)=7.0, 1H; Ala N*H*), and 9.80 ppm (s, 1H; Aryl N*H*).

Preparation of (*E*)-3-(2-(*N*-acetyl-L-leucyl-L-alanyl)amido phenyl)acrylic acid (*E*-5)

(*E*)-ethyl 3-(2-(*N*-acetyl-L-leucyl-L-alanyl-)amido phenyl)acrylate (824.0 mg, 1.97 mmol) was suspended in ethanol (250 mL). 10.0 mL of 1.0 M sodium hydroxide aqueous solution (10.0 mmol) was added to obtain yellow solution. 100 mL of water was added and the solution was stirred for 3 days at room temperature. The reaction was traced by TLC method (ethyl acetate/hexane=2/1; v/v). The solution was concentrated to colorless oil. The oil was dissolved in 4% sodium bicarbonate aqueous solution, and washed with a little amount of ethyl acetate once. The aqueous layer was acidified by solid citric acid monohydride toward pH 4 to obtain white suspension. The suspension was extracted with ethylacetate, and washed with 2% hydrochloric acid aqueous solution, water and brine. Organic layer was the yellow suspension. The precipitate was filtered and dried under reduced pressure. The white powder was washed by ice cooled ethylacetate twice, and dried under reduced pressure again (1st. white powder, 379.0 mg, 49.4%). The filterates are combined and dried over anhydrous magnesium sulfate. Solvent was removed under reduced pressure to obtain yellow-white powder. The powder was

reprecipitated from diethylether/*n*-hexane, and washed by diethylether and ice-cooled ethylacetate. (2nd. white powder, 187.4 mg, 24.4%) m.p. 198-205 ^{o}C; (Found: C, 60.14; H, 6.97; N, 10.57. Calc. for $C_{20}H_{27}N_3O_5\cdot(H2O)_{0.35}$: C, 60.70; H, 7.05; N, 10.62 %); δ_H(270 MHz; DMSO-d_6) 0.86 (m, 6H; Leu δH), 1.36 (d, ^3J(H,H)= 7.1 Hz, 3H; Ala βH), 1.45 (m, 2H; Leu βH), 1.60 (m, 1H; Leu γH), 1.84 (s, 3H; Ac), 4.31 (m, 1H; Leu αH), 4.48 (m, 1H; Ala αH), 6.45 (d, ^3J(H,H)=15.9, 1H; olefin), 7.25 (dt, ^3J(H,H)=7.4 Hz, ^4J(H,H)=2.0 Hz, 1H; Aryl), 7.35 (dd, ^3J(H,H)=7.4 Hz, ^4J(H,H)=2.0 Hz, 1H; Aryl), 7.40 (dt, ^3J(H,H)=7.4 Hz, ^4J(H,H)=2.0 Hz, 1H; Aryl), 7.68 (d, ^3J(H,H)=15.9, 1H; olefin), 7.78 (dd, ^3J(H,H)=7.4 Hz, ^4J(H,H)=2.0 Hz, 1H; Aryl), 7.96 (d, ^3J(H,H)=8.1, 1H; Leu N*H*), 8.11 (d, ^3J(H,H)=7.0, 1H; Ala N*H*), 9.78 (s, 1H; Aryl N*H*) and 12.22 ppm (s, 1H; COO*H*).

UV-light irradiation technique for UV-vis and ^{1}H NMR spectrum measurement

Xe/Hg lamp (MUV-202U, Moritex Co.) was used for 313 nm UV-light irradiation. UV-light was filtered through 6784-t01.uv1 (Asahi tech.) to pick out the 313 nm emission line of Hg gas. The spectrum was measured before and after irradiation in NMR tube or UV cell. During irradiation and spectrum measurements, the sample was always kept desired temperature.

References

[1] R. Mimna, M. S. Camus, A. Schmid, G. Tuchscherer, H. A. Lashuel, M. Mutter, *Angew Chem. Int. Ed.* **2007**, *46*, 2681-2684.

[2] H. S. Mandal, H. B. Kraatz, *J. Am. Chem. Soc.* **2007**, *129*, 6356-6357.

[3] T. S. Haque, J. C. Little, S. H. Gellman, *J. Am. Chem. Soc*, **1994**, *116*, 4105-4106.

[4] T. S. Haque, J. C. Little, S. H. Gellman, *J. Am. Chem. Soc*, **1996**, *118*, 6975-6985.

[5] H. E. Stanger, S. H. Gellman, *J. Am. Chem. Soc*, **1998**, *120*, 4236-4237.

[6] G. J. Sharman, M. S. Searle, *J. Am. Chem. Soc*, **1998**, *120*, 4869-4870.

[7] F. Haung, W. M. Nau, *Angew. Chem. Int. Ed.* **2003**, *42*, 2269-3372.

[8] A. Onoda, H. Yamamoto, Y. Yamada, K. Lee, S. Adachi, T. Okamura, K. Yoshizawa-Kumagaye, K. Nakajima, T. Kawakami, S. Aimoto, N. Ueyama, *Biopolymers*, **2005**, *80* (2 and 3), 233-248.

[9] N. Ueyama, K. Takahashi, A. Onoda, T. Okamura, H. Yamamoto, *Macromol. Symp.*, **2003**, *204*, 287-294

[10] A. Onoda, H. Haruna, H. Yamamoto, K. Takahashi, H. Kozuki, T. Okamura, N. Ueyama, *Eur. J. Org. Chem.* **2005**, 641-645.

Summary and Conclusions

The present thesis deals with the synthesis and characterization of intramolcular NH··· O hydrogen bond switchable carboxylic acid and phenol derivatives. The aim of this thesis is to switch the chemical property of carboxylic acids or phenols, and examine the possibility of applying these functions to the oligopeptides.

Photoswitching devices

Novel photoswitching devices, which can control the distance between amide NH (hydrogen bond donor) and oxy anion moiety (hydrogen bond accepter) were synthesized. These distances were controlled using photochromic compounds, which contain *E*/*Z* isomerization of π-conjugated double bond moieties. OFF→ON and ON→OFF switching of intramolecular NH···O hydrogen bond toward carboxylate, using cinnamic acid framework, was described in chapter 3 and 4. Reversible switching of intramolecular NH···O hydrogen bond toward carboxylate achieved by *E* to *Z* photoisomerization and *Z* to *E* thermal isomerization of benzylideneaniline framework, was described in chapter 2. And the switching of intramolecular NH···O hydrogen bond toward phenolate derivative, achieved by photoisomerization of *ortho*-coumaric acid framework, was described in chapter 5. An intramolecular NH···O hydrogen bond was formed when the acids were deprotonated, and additionally when the hydrogen bond donor was closed to hydrogen accepter. The hydrogen bond formation was confirmed by the spectroscopic methods, such 1D and NOESY ^{1}H NMR spectra in solution, X-ray crystallography and solid FT-IR spectrum measurements in solid state. The hydrogen bond formation was also confirmed by kinetic method. It was revealed that the formation of intramolecular NH···O hydrogen bond in carboxylate retardants the *Z* to *E* thermal isomerization by stabilizing the *Z* carboxylate.

pK_a control by switching of intramolecular NH···O hydrogen bond

pK_a shift of carboxylic acid or phenol derivatives caused by the switching of intramolecular NH···O hydrogen bond, which is strongly related to the stabilization of the deprotonated anions, was described in chapter 3, 4 and 5. The author synthesized the compounds having cinnamic acid or *ortho*-coumaric acid frameworks, which photoproducts were thermally stable at room temperature, and isolated the isomers to

detect their acidities. The pK_a value was examined by potentiometric titration in aqueous micellar solution in chapter 2, ion exchange reactions in DMSO solution in chapter 2 and 3, and UV-vis titration in aqueous micellar solution in chapter 4. OFF→ON switching of intramolecular NH···O hydrogen bond in carboxylate lowers the pK_a value of corresponding carboxylic acid, and ON→OFF switching of hydrogen bond increases the pK_a value. That means intramolecular NH···O hydrogen bond formation in carboxylate encourages the deprotonation process of carboxylic acid, and the interruption discourages the deprotonation oppositely. This acidity trend was applicable not only to carboxylate but also to the phenol derivatives. The pK_a value of phenol compound was lowered in *Z* isomer, which forms the intramolecular NH···O hydrogen bond in phenolate. The pH value was also controlled by photoirradiation in OFF→ON type compounds with the pK_a value, which was described in chapter 3.

Artificial photocycle of phenol and phenolate, derived by the switching of an intramolecular NH···O hydrogen bond

In chapter 5, the author designed the artificial photocycle contains the protonation and deprotonation process of phenol derivatives, which modeling the PYP photocycle. The designed compound was consist of *ortho*-coumaric acid moiety having an extended π-conjugation in phenolate, thus the red shift of the absorption maximum was observed. Because of the difference of the absorption wavelength, phenol and phenolate have different *E*/*Z* ratio whereas same wavelength light irradiation. 313 nm UV light irradiation generate *Z* form in phenol and generate *E* form in phenolate, preferentially. The pK_a value of the phenol compound was lowered in *Z* compound by stabilizing the *Z* phenolate with formation of an intramolecular NH···O hydrogen bond. The *E*/*Z* ratio difference in phenol and phenolate, and the decrease of pK_a value in *Z* phenol compound, achieves the artificial photocycle containing protonation and deprotonation process, constructed like PYP photocycle.

Intramolecular hydrogen bond switching of oligopeptide

Linear to turn conformation change of oligopeptide, which induced photoinduced OFF→ON switching device of intramolecular NH···O hydrogen bond in C-terminal, was described in chapter 6. The conformation of peptide was controlled by multiple stimulations, not only deprotonation process but also photoisomerization of cinnamic acid framework, that is photo- and proton-driven conformation control. Multiple hydrogen bonds between the amide NH of oligopeptide and carboxylate oxygen were photoswitched by *E*/*Z* photoisomerization of cinnamate framework. The dipeptide

(Ac-Leu-Ala-) introduced compound does not form carboxylic acid in neither *E* nor *Z* isomers, forms one intramolecular NH···O hydrogen bond in *E* carboxylate between Leu NH and carboxyl oxygen, and forms three intramolecular NH···O hydrogen bonds in *Z* carboxylate. Elongation of peptide moiety stabilizes the turn conformation of *Z* carboxylate by forming three intramolecular NH···O hydrogen bonds.

In conclusion, the author establishes the photoswitching of intramolecular NH···O hydrogen bond by using *E*/*Z* isomerization of π-conjugated double bond, and elucidated that the switching of distance between amide NH and oxy-anion controls the chemical properties of carboxylic acid and phenol derivatives as follows; acidity of corresponding acids, photoreaction efficiency of phenol derivatives, thermal isomerization rate control of benzilideneaniline moiety. Native proteins switch the hydrogen bond toward carboxylate or phenolate by dramatic conformation changes to control the activity of oxy-anion. The author achieved to control the chemical properties of carboxylate and phenolate by minimal conformation change of photochromic compound. This finding is important not only as the model of native enzymatic reaction, but also as the construction of artificial enzymatic reaction by small molecules.

The author applied this photoswitching device of intramolecular NH···O hydrogen bond toward the C-terminal of oligopeptide and demonstrated the photo- and proton-driven conformation change of peptide moiety. In carboxylic acid, both *E* and *Z* isomers have no interaction and forms linear conformation, in carboxylate, *E* compound can form turn conformation by forming one intramolecular NH···O hydrogen bond, and *Z* compound was strongly constrained to the turn conformation by forming three NH···O hydrogen bonds. The switching of intramolecular NH···O hydrogen bond of terminal amino acids indicate the possibility of photocontrol of second dimension structure of longer peptide, such as α-helix to random coil conversion.

List of Publications

Chapter 2

1. Photoinduced switching of intramolecular hydrogen bond between amide NH and carboxyl oxygen
   T. Matsuhira, H. Yamamoto, A. Onoda, T. Okamura, and N. Ueyama, *Org. Biomol. Chem.* **2006**, *4*, 1338-1342.

Chapter 3

2. Manipulation of an intramolecular NH···O hydrogen bond by photoswitching between stable *E*/*Z* isomers of the cinnamate framework
   T. Matsuhira, H. Yamamoto, T. Okamura, and N. Ueyama, *Org. Biomol. Chem.* in press (DOI: 10.1039/b19960k)

Chapter 4

3. Acidity control by ON/OFF switching of an intramolecular NH···O hydrogen bond by *E*/*Z* photoisomerization of the cinnamate framework
   T. Matsuhira, H. Yamamoto, T. Okamura, and N. Ueyama, submitting for publication

Chapter 5

4. The artificial photocycle containing protonation and deprotonation process of phenol derivative
   T. Matsuhira, H. Yamamoto, T. Okamura, and N. Ueyama, submitted to *Org. Biomol. Chem.*

Chapter 6

5. Photo- and proton-driven conformation change of oligopeptide by switching of multiple intramolecular NH···O hydrogen bonds
   T. Matsuhira, H. Yamamoto, T. Okamura, and N. Ueyama, submitting for publication